

NASA Contractor Report 181609

COMPARISON OF TWO TRANSONIC NOISE PREDICTION FORMULATIONS USING THE AIRCRAFT NOISE PREDICTION PROGRAM

Peter L. Spence

PLANNING RESEARCH CORPORATION
Aerospace Technologies Division
Hampton, Virginia

Contract NAS1-18000
December 1987

**(NASA-CR-181609) COMPARISON OF TWO
TRANSONIC NOISE PREDICTION FORMULATIONS
USING THE AIRCRAFT NOISE PREDICTION PROGRAM
(Planning Research Corp.) 86 p CSCL 20A**

N88-20095

Unclass

G3/71 0133251



National Aeronautics and
Space Administration

Langley Research Center
Hampton, Virginia 23665

CONTENTS

1.	Summary	3
2.	Symbols and Abbreviations	4
3.	Introduction.	6
4.	Description of Software	7
5.	Study Cases	9
	Cases 1 and 2	9
	Case 3	10
	Case 4	10
6.	Results - Aerodynamic Loading Calculations.	12
	Steady - Cases 1, 2, and 4	12
	Unsteady - Case 3.	13
7.	Results - Acoustic Calculations	15
	Case 1	15
	Case 2	16
	Case 3	17
	Case 4	18
8.	Execution of Formulation 3 with ANOPP	19
9.	Conclusions	23
10.	Acknowledgements.	24
11.	References	25
12.	Tables	26
13.	Figures	32
14.	Appendix	A1

SUMMARY

This paper addresses recently completed work on using Farassat's Formulation 3 (ref. 1) noise prediction code with the Aircraft Noise Prediction Program (ANOPP) (ref. 2). Software was written to link aerodynamic loading generated by the Propeller Loading (PLD) module within ANOPP with Formulation 3.

Formulation 3 is actually comprised of two formulations. One predicts propeller noise under subsonic conditions (Formulation 1-a) and the other (Formulation 3) makes transonic and supersonic noise predictions. The purpose of this study was to link Formulation 3 with ANOPP and compare results of Formulation 3 with ANOPP's existing noise prediction modules, Subsonic Propeller Noise (SPN) and Transonic Propeller Noise (TPN). Four case studies were investigated. The first two cases involve flyover studies using an SR-3 propeller. The SR-3 blade is loaded under subsonic conditions in the first case and loaded under transonic conditions in the second case. The third case shows results of using Formulation 3 to make a noise prediction of a blade under unsteady loading. In the fourth case, an example is given on using the output of Formulation 3 as input to ANOPP's Fuselage Surface Scattering (FSS) module.

Results of the comparison studies show excellent agreement between Formulatin 1-a and SPN. Differences between the TPN and Formulation 3 comparison in Case 2 are strictly numerical and can be explained by the way in which the time derivative is calculated in Formulation 3.

Also included is a section on how to execute Formulation 3 with ANOPP.

PRECEDING PAGE BLANK NOT FILMED

SYMBOLS AND ABBREVIATIONS

C	Complex pressure
c_p	Power coefficient
c_T	Thrust coefficient
J	Advance ratio
M_T	Tip Mach number
M_∞	Inflow Mach number
P	Loading pressure normal to blade surface
t	Time
$\beta_{.75}$	Blade twist at 75% span
ϵ	$1 \pm \epsilon$ defines transonic region ($\epsilon = .05$ for this report)
η	Blade coordinate vector
η_p	Propeller efficiency
ξ_1	Spanwise coordinate of blade
ξ_2	Chordwise coordinate of blade
ρ	Air density [slugs/ft ³]
σ	Loading pressure tangent to blade surface
ψ	Azimuth angle in propeller disk
Ω	Rotational speed of propeller [rpm]
ANOPP	Aircraft Noise Prediction Program Modules within ANOPP
BLM	Boundary Layer Module
FSS	Fuselage Surface Scattering
PLD	Propeller Loading
PRP	Propeller Performance
RBA	Rotating Blade Aerodynamics
RBS	Rotating Blade Shape

SPN	Subsonic Propeller Noise
TPN	Transonic Propeller Noise
BPF	Blade Passing Frequency
FFT	Fast Fourier Transform
OASPL	Overall Sound Pressure Level
rpm	revolutions per minute
SPL	Sound Pressure Level

INTRODUCTION

Because of the advent of advanced propeller blades which are highly swept and very thin, a more accurate means of predicting their noise is important. Farassat's new noise prediction code, Formulation 3 (ref. 1), has been developed for such propellers. Formulation 3 is actually comprised of two formulations. Formulation 1-a is used for subsonic predictions and Formulation 3 is used for transonic and supersonic predictions. Both formulations use a panel method to segment the entire blade into individual cells. During execution a decision is made internally as to which formulation is used to compute the noise for an individual cell. The total noise is then generated by combining the noise calculated for each panel at the observer position.

The formulations which exist in ANOPP's SPN and TPN are earlier formulations of the Ffowcs Williams-Hawkins equation (ref. 3). Formulation 3 is an improvement over these earlier versions, and, therefore, it was desirable to implement Formulation 3 with ANOPP.

To execute Formulation 3, software was written to interface output of the aerodynamic loading tables generated by ANOPP with Formulation 3. Also, software was implemented into Formulation 3 to create output tables analogous to the output tables generated by SPN and TPN. These tables supply the predicted noise levels.

DESCRIPTION OF SOFTWARE

The software that links Formulation 3 with ANOPP consists of two subroutines. ETASUB describes the blade shape and FUNPRES describes the loading pressure distribution on the blade. These subroutines are illustrated in the section on executing Formulation 3 with ANOPP.

This type of noise prediction must be made in two steps (refer to figure 1). The first step involves executing ANOPP modules (RBS, RBA, BLM, PRP, PLD) which will generate loading pressures across the desired propeller blade under specified operating conditions. The second step involves using PLD tables which describe the loading on the blade, as input to the Formulation 3 code. Also needed as input at this point are the blade coordinates previously used as input to RBS. ETASUB reads the blade coordinate information while FUNPRES reads the PLD tables. Some redundancy exists at this point since both RBS and ETASUB curve fit the blade surface. Formulation 3 requires second derivatives in both span and chord directions as well as cross derivatives. Since RBS only curve fits in the chord direction, additional curve fitting had to be implemented. Initial attempts to curve fit RBS output data resulted in a rounded trailing edge. This rounded trailing edge is believed to be a result of RBS fitting the top and bottom of the blade together with one curve fit in a least squares sense while specifying the condition that the trailing edges must meet. This fit resulted in large chordwise curvatures at the trailing edge which in turn made the resulting noise prediction too high. Curve fitting the blade coordinates input to RBS in two pieces, a top and bottom section, resulted in sharper leading and trailing edges and smaller curvatures calculated from second derivatives in Formulation 3. However, RBS must be kept to build the proper ANOPP tables to execute the remaining modules which create the PLD tables.

FUNPRES reads the untabled form of the PLD (LOADS) data base structure from PLD. For the loading pressure distribution, Formulation 3 requires the loading pressure and its first derivative in both span and chord and also time if the loading is unsteady.

For both the blade shape and loading pressure curve fits, a fifth order spline fit in a least squares sense was used.

In order to match ANOPP blade coordinates for both shape and pressure loading, the chordwise grid variable in Formulation 3 had to be changed. Like the chordwise coordinate in ANOPP, ξ_2 was redefined in Formulation 3 to be zero at the trailing edge, increase along the top to π at the leading edge and continue along the bottom to 2π at the trailing edge (figure 2).

STUDY CASES

CASES 1 and 2

In each of these case studies, the type of propeller and the operating conditions used are summed up in Tables 1 and 2. The first two comparisons were made using an 8 bladed SR-3 propeller of 9 ft. diameter. The tests were made to simulate a flyover analysis of the SR-3 propeller at an altitude of 32000 ft. At this altitude the air density (ρ) was taken to be .000825 slugs/ft³, and an ambient speed of sound of 986 ft/sec was used. The noise calculated for this comparison was measured with respect to an observer located 45 ft. directly beneath the plane of the propeller. In both the subsonic and transonic comparison the rotational speed of the blade was 1650 rpm.

The transonic case used an inflow Mach number of .72, and the blade twist at 75 percent span was 58 deg. To create a subsonic example, the inflow Mach number was reduced to .4, and to improve the propeller efficiency the blade twist at 75 percent span was changed to 48 deg.

These two flyover cases were each run for the respective comparisons to calculate the acoustic pressure signal for one revolution of the propeller. The acoustic pressure was then Fourier analyzed to obtain the harmonics of the blade passing frequency (BPF). Because the formulations in SPN and TPN use a fast Fourier transform (FFT), the number of time points used in the acoustic signature were chosen be the result of 2 raised to an integer power. Since 1024 time points provided more time resolution than was required, 512 time points were used in making the comparisons.

CASE 3

The third case involves a noise prediction on a propeller under unsteady loading. The unsteady loading in this case is due to a SR-2 propeller in a pusher configuration, figure 3. Here the pylon in front of the SR-2 propeller is modeled by a NACA 0012 wing of constant chord length. This configuration is patterned after the experiment by Block (ref. 4). For this example, the SR-2 propeller consisted of four blades and had a 16.1 inch diameter. As a result of the pylon placed in front of the propeller, each blade encountered a momentum deficit as it passed the pylon induced wake. Thus the wake creates unsteady loading pressure on the propeller blades. The uniform inflow Mach number is .108 and the rotational speed of the propeller is 11400 rpm. Since this is subsonic, the Formulation 1-a is executed. The speed of sound used was 1111 ft/sec, and ρ was .00263 slugs/ft³.

The observer was located axially 44.8 inches in front of the propeller disk and circumferentially 35 inches 30 deg from the pylon looking upstream.

In this unsteady case the subroutine FUNPRES numerically differentiates the loading pressure for each spatial grid point generated by Formulation 1-a or Formulation 3 with respect to the circumferential angle, ψ , in the propeller disk. Once this derivative, $\partial P / \partial \psi$, is calculated, $\partial P / \partial t$ is obtained by the chain rule and spline fit across the entire blade. This is illustrated in the next section on Aerodynamic Loading.

CASE 4

This case illustrates the use of Formulation 3 results as the input to another ANOPP module. Specifically the Fuselage Surface Scattering (FSS) module is used here. FSS computes the complex acoustic pressure and sound

pressure levels incident on an infinite circular cylinder (representing a fuselage) taking into account boundary layer effects.

The running conditions used in Case 2 are again used (Tables 1 and 2). This time, however, there were 32 observer locations (figure 4). All locations were 6.334 ft. to one side of the propeller and equally spaced ranging from 10.976 ft. aft to 10.29 ft. forward of the propeller. The fuselage radius was 4 ft., and a boundary layer thickness of 4 inches was assumed.

FSS was executed using the output of TPN and again executed using the output generated by Formulation 3. The loading was the same as for Case 2 and is described in more detail in the next section.

RESULTS

AERODYNAMIC LOADING CALCULATIONS

STEADY - CASES 1, 2, and 4

In order to make a noise prediction using Formulation 1-a (subsonic) or Formulation 3 (transonic to supersonic) a description of the loading stresses on the propeller blade is required (figure 1). Executing the ANOPP module PLD provides these normal (P) and tangential (σ) loads, figure 2. Although the shearing stress due to skin friction is considered small with respect to the normal pressure, both loads are included using Formulation 1-a. The Formulation 3 prediction only uses the loading pressure normal to the blade, however, the first spanwise derivative ($\partial P / \partial \xi_1$) and chordwise derivative ($\partial P / \partial \xi_2$) are also required. Since these derivatives are not provided by PLD, they are calculated in FUNPRES.

Along with having to provide Formulation 3 with spatial derivatives of pressure, both prediction formulations use a panel method which generates a grid different from the ANOPP grid defining the pressure distribution. To describe the ANOPP pressure distribution, which interpolates a pressure value for any point on the blade and calculates its spatial derivatives at that point, a two dimensional fifth order spline is used.

To illustrate how close the spline fits the data, figures are included comparing the spline curve with the data provided by PLD. Figure 5 is a contour of the loading pressure data generated by PLD for the top surface of the SR3 blade under the subsonic conditions described in Case 1. The resulting spline fit of that data is contoured in figure 6. Similarly, figures 7 and 8 show the same information in a three dimensional projection. In the same fashion, the bottom pressure data and spline fit are plotted in figures 9 through 12.

Although these plots illustrate the spline fit in two dimensions, a direct comparison of the spline fit of the subsonic loading pressure data is given in figure 13. Here, the chordwise curve fits are compared with the data at ten spanwise stations. The location of the breakpoints used in the spline calculation are displayed as diamonds on the chordwise axes. As can be seen, the breakpoints are stacked towards the leading edge since the chordwise pressure gradients are greater there. Breakpoints are distributed evenly in the spanwise direction.

Plots are also included showing the spline fits used in the loading pressure of the transonic case. As above, the spline fits are shown in figures 14 through 18. Figures 14, 15, 16, and 17 show the two dimensional curve fits across the top and bottom of the SR-3 blade. A direct comparison of the data is illustrated in figure 18. Since the spline fits the data very well, the resulting spatial derivatives computed from the polynomial describing the curve will be accurate.

UNSTEADY - CASE 3

A further complexity in describing the loading pressure is encountered when the noise prediction is to be made using unsteady loading. Here, $\partial P/\partial t$ on the blade surface is nonzero. PLD is capable of providing the loading distribution on the blade as a function of azimuth angles (ψ) in the propeller disk. For this case, a second order accurate, three point centered difference scheme (ref. 5) is used to obtain $\partial P/\partial t$ from $\partial P/\partial \psi$. This is shown in figure 19. Once $\partial P/\partial t (\xi_1, \xi_2, \psi)$ has been determined, it is curve fit with the same spline as the pressure distribution.

For the unsteady case described previously, comparisons between the loading pressure computed in PLD and the spline fits of that data are shown in figures 20 through 29. These figures are presented like the previous figures,

however, here figures 20 through 24 describe the loading pressure distribution outside the wake region ($\psi = 0$ deg.), while the remaining figures 25 through 29 show the curve fit of pressure data at the center of the wake.

As with the steady case, the spline fits the data very well. It is important to emphasize here that the same curve fit was used to generate the pressure distributions of the two steady cases and the unsteady case. These three cases were operating under different conditions with different blades and the spline fit was very good in each case. Also, for the subsonic case (Formulation 1-a) the tangential stresses supplied by PLD are curve fit in the same manner as the normal loading pressure.

RESULTS

ACOUSTIC CALCULATIONS

CASE 1

The blade performance results for all cases are tabulated in Table 2. As explained in the Discussion section, the first part of this prediction required executing ANOPP to obtain the aerodynamic loading pressure. The loading was illustrated in the previous section. The thrust coefficient was determined to be 0.907, and the power coefficient was 2.224. The advance ratio was 1.594, and the propeller efficiency was 0.65.

The results of the noise predictions are shown in figures 30 and 31 with the pressure spectra listed in Table 3. The agreement is considered good. Figure 30 shows the acoustic pressure history for one period of the blade passing frequency (BPF) generated by the propeller as detected by the observer 45 ft. below the propeller. The thickness noise, illustrated in figure 30(a), shows good agreement between the two methods. Comparing results found between Formulation 1-a and SPN concerning the loading noise, figure 30(b), it can be seen that the two are slightly out of phase but the shape of the signals appear the same. The total noise generated is shown in figure 30(c). Only the thickness and loading noise is computed numerically. Total noise is the sum of computed thickness and loading noise. Therefore, any differences in the results of the thickness and loading noise between the two computational methods is propagated to the total noise results.

The overall sound pressure level (OASPL) determined by SPN was 114.23 dB and by Formulation 1-a was 115.42 dB. Formulation 1-a is essentially the same as SPN except for the numerical integration used. Thus, the differences in sound pressure levels (SPL) between SPN and Formulation 1-a are probably due

to the curve fitting of the blade shape and of the pressure loading. ANOPP does linear interpolation in describing the pressure distribution across the blade while FUNPRES and ETASUB evaluate the blade shape and pressure distribution using a fifth order spline.

The acoustic pressure signals of figure 30 were Fourier analyzed and plotted in figure 31. The primary and secondary harmonics of the thickness noise and loading noise, figures 31(a), 31(b), and Table 3, are almost identical. Slight differences in pressure signals can be seen in the higher harmonics of figure 31.

CASE 2

In executing ANOPP to determine loading pressure on the blade, a thrust coefficient of 0.853 was found. The power coefficient was 3.397, the advance ratio was 2.868, and the propeller efficiency was 0.72. Formulation 3 internally distributes the computational panels according to what portion of the blade is under subsonic and what portion is under supersonic running conditions. With the operating conditions listed in Table 2 for Case 2, the panels of the transonic grid were placed over 21 percent of the blade's tip area and the panels of the subsonic grid were placed inboard over the remaining 79 percent of the blade. This transition is based on where the resultant of the inflow Mach number and the tip Mach number approaches $(1 - \epsilon)$ where $\epsilon = .05$ for all cases in this report.

As was done for Case 1, thickness, loading, and total acoustic pressure signatures at the same observer position as Case 1 were plotted for one period of the BPF, figure 32. Also, resulting harmonics of the BPF were plotted in figure 33 and listed in Table 4. The OASPL for TPN was 124.31 dB and for Formulation 3 was 128.26 dB.

Since Formulation 3 moves the time derivative inside the integral of the Ffowcs Williams-Hawkins equation (ref. 3), the time derivative is performed analytically. The formulation in TPN computes the time derivative numerically outside the integral. Because of this, Formulation 3 finds sharper peaks in the time history of the acoustic pressure as shown in the thickness noise in figure 32(a). This in turn results in larger values of SPL at the higher harmonics shown in figure 33(a).

Spatial pressure derivatives are required for Formulation 3 and not for TPN. This is believed to account for the slight difference in loading spectra in figure 32(b) and Table 4. Chordwise derivatives are large at the leading edge especially using the discrete pressure data from PLD.

A transonic prediction was made using the Formulation 3 code not altered to link with ANOPP. The parameters used for Case 2 were used here but the loading was different. The results of the thickness noise is included in Table 5. Discrepancies here are probably due to slight differences in the respective blade shape descriptions.

CASE 3

Generating the unsteady loading for this case resulted in a power coefficient of 0.221, a thrust coefficient of 0.272, a propeller efficiency of 0.58, and an advance ratio of 0.471. The acoustic pressure signature and the harmonics of the BPF calculated for 1000 time points are plotted in figure 34.

As stated previously, the sharp peaks of the pressure signature cause larger SPL's at higher frequencies. This also results in much larger OASPL than a steady case. The OASPL for this case was 124.72 dB. In addition sharp peaks found in the acoustic pressure signature are also due to the analytical prediction considering the observer to be a point. In experiments, the average acoustic pressure over the surface of the microphone is measured. This tends to dampen some of the sharp peaks found analytically.

CASE 4

The sound pressure levels (SPL) computed on the 4 ft. radius fuselage are plotted in figures 35 and 36. As may be observed, results are very similar. The predominate difference is found directly beneath the propeller where Formulation 3 computed higher peak values in the SPL, figure 37. The larger SPL values computed by Formulation 3 resulted in higher values of SPL on the fuselage near the propeller.

EXECUTION OF FORMULATION 3 WITH ANOPP

As stated in the discussion, this prediction must be made in two steps. The first step requires using ANOPP to generate loading pressure by executing PLD and saving the untabled form of the data structure PLD (LOADS). What is primarily discussed here is the second step, noise prediction. Unless stated otherwise, all files referred to in this section are on account (UN = 836357C).

To illustrate this noise prediction, an example file, RUNFM3, containing job control language is listed here.

1. /JOB
2. RUNFM3,T32000.
3. USER,<USER INFO>
4. CHARGE,<CHARGE INFO>
5. DELIVER.<DELIVER INFO>
6. GET,EXFM3/UN=836357C.
7. BEGIN,FM3,EXFM3,F1,F2,F3,F4,F5,F6.
8. EXIT.
9. /EOR
10. /READ NAMLIST
11. /EOR
12. /READ ETASUB
13. /EOF

The parameters F1, F2, F3, F4, F5, and F6 (line 7) represent the files defined below.

F1 - Blade coordinates file [INPUT]

F2 - Untabled PLD (LOADS) file [INPUT]

F3 - Total blade pressure history file [OUTPUT]

F4 - Single blade pressure history file [OUTPUT]

F5 - SPN (FFT) file in ANOPP job format (used in executing FSS) [OUTPUT]

F6 - DAYFILE [OUTPUT]

Subroutines ETASUB and FUNPRES are stored on file ETASUB (line 12).

Three input files are needed for the prediction, the namelist file (line 10), the blade coordinates file, F1 (line 7), and the loading pressure file from ANOPP, F2 (line 7). The namelist file contains the descriptive input of the noise prediction and is made up of three namelist groups.

1. PHYSICAL

BTIP - distance from hub to tip [feet (meters)]
BINNER - distance from hub to root [feet (meters)]
VF - forward velocity [feet/second (meters/second)]
OMEGA - rotational velocity [radians/second]
CO - speed of sound [feet/second (meters/second)]
RHOO - density of air [slugs/feet³ (kilograms/meter³)]
NB - number of blades
NOBS - number of observer positions
STEADY - logical variable. TRUE → steady loading
 FALSE → unsteady loading
IENGLH - units switch. 1 = English units
 0 = SI units
THETAR - original blade twist at 3/4 span minus desired
 blade twist at 3/4 span [degrees]

2. GRID

NT - number of time points for one blade signature
NS - number of spectral levels to be computed
N1SUB - number of equally spaced spanwise intervals for the
 subsonic portion of the blade
N1SUP - number of equally spaced spanwise intervals for the
 supersonic portion of the blade
N2SUB - number of equally spaced chordwise intervals for
 the supersonic portion of the blade
N2SUP - number of equally spaced chordwise intervals for
 the supersonic portion of the blade
N1S - number of equally spaced spanwise points for a
 Formulation 3 cell

N2S - number of equally spaced chordwise points for a
Formulation 3 cell

EPSILON - if for some point on a panel the condition
 $1 - M_r < EPSILON$ is met, then Formulation 3
is used to compute the acoustic pressure for
that panel

IGAUSS - order of Gaussian Quadrature used to compute
Formulation 1A integrals

3. OBSERV

OBS(I,J) - i-th component of the j-th observer position
 $I = 1,2,3 \quad J = 1, \dots, NOBS.$

The namelist file SR3NAMT was used to execute the SR-3 transonic prediction in Case 2 and can be used as an example. It is recommended that the variables in GRID other than NT and NS be kept the same as the values in SR3NAMT.

The blade coordinates file is simply an input deck of coordinates used for RBS with the dollar signs removed and two lines added at the top of the file. The top line needs to be the value used as B (blade radius) in the RBS input and the second line must have the number of spanwise stations included in the deck. An example of this file can be found on DATSR3 (SR-3 blade coordinates).

The untabled loading pressure file is direct output from an ANOPP run. SR3LDS2 is an example containing the loading used in the SR-3 transonic prediction.

When executing different blades and different loadings the dimensions of the arrays used in ETASUB and FUNPRES may need to be changed. Included as an appendix are copies of the subroutines showing values in PARAMETER statements

which are not constant. In ETASUB, the variable NX1DM in the PARAMETER statement on line 6 must be set to the number of spanwise stations. The variable NDTDM on the same line must equal the largest value of chordwise coordinates on the top or bottom of the airfoil in the input deck of blade coordinates.

In FUNPRES, the variables NX1DM, NX2DM, NPSDM, and NXI2T in the PARAMETER statement on line 7 must be set before execution. NX1DM must be the number of spanwise stations while NX2DM must be set to the number of chordwise stations of the loading pressure file. In FUNPRES and XINTRP (a subroutine called by FUNPRES to do linear interpolations) NPSDM must be equal to the number of azimuthal values (ψ positions) on the loading pressure file. NPSDM appears in the PARAMETER statement on line 4 of XINTRP. For steady runs this value is one. Lastly, the variable NXI2T (line 7 of FUNPRES) must be set equal to the number of chordwise grid points along the top of the airfoil set in the ANOPP run.

The output files, F3, F4, and F5 (line 7) are replaced onto the account which the job is run. F3 and F4 can be used as input to graphics routines. The output file F5 can be inserted into an ANOPP job stream used in executing the Fuselage Surface Scattering (FSS) module.

CONCLUSIONS

Work has been completed on interfacing the Formulation 3 noise prediction code with ANOPP. For the example problems investigated here, good agreement was found in comparing Formulation 1-a with SPN for the same input conditions. Discrepancies here were probably due to differences in the curve fits and interpolation procedures between Formulation 1-a and SPN.

In comparing Formulation 3 with TPN in the transonic flyover reported as Case 2, discrepancies were due to the implementation of the time derivative in the two formulations. Formulation 3 determines sharper peaks in its acoustic pressure signature which result in a larger OASPL than the TPN result.

Results were reported on executing Formulation 3 under unsteady loading. Additionally, results of using output of Formulation 3 as input to an ANOPP module (FSS) were provided.

A section was included which detailed how to make a Formulation 3 noise prediction using ANOPP generated input.

ACKNOWLEDGEMENTS

It needs to be mentioned that the spline software used in this study was written by Mark Dunn of PRC. Also the author wishes to thank Mark Dunn and Mohammad Takallu of PRC and Patricia Block of NASA Langley Research Center for their helpful discussions involving this work.

REFERENCES

1. Farrasat, F., Prediction of Advanced Propeller Noise in the Time Domain, AIAA Journal, 24 (4), pp. 578-584, April, 1986.
2. Zorumski, W. E., and Weir, D. S. (editors), NASA Technical Memorandum 83199 Part 3, Aircraft Noise Prediction Program Theoretical Manual -- Propeller Aerodynamics and Noise, June, 1986.
3. Ffowcs Williams, J. E., and Hawkings, D. L., Sound Generation by Turbulence and Surfaces in Arbitrary Motion, Philosophical Transactions of the Royal Society of London, Vol. A264, pp. 321-342, 1969.
4. Block, P. J. W., Pusher Propeller Noise Directivity and Trends, AIAA 86-1929, July, 1986.
5. Anderson, D. A., Tannehill, J. C., and Pletcher, R. H., Computational Fluids Mechanics and Heat Transfer, pp. 54, 1984.

TABLE 1: PROPELLERS USED IN THE CASE STUDIES

	Propeller	Number of Blades	Blade Diameter [ft]
CASES I, II, IV	SR3	8	9.0
CASE III	SR2	4	1.3417

TABLE 2: OPERATING CONDITIONS AND OASPL

	M_∞	M_T	ρ [slug $\frac{s}{ft^3}$]	$\beta_{.75}$ [deg]	Ω [rpm]	J	c_T	c_P	η_P	SPN OSDPL [dB]	FORM.3 OASPL [dB]
CASE 1	0.40	0.79	0.000825	48.0	1650	1.59	0.907	2.22	0.65	114.23	115.42
CASE 2	0.72	0.79	0.000825	58.0	1650	2.87	0.853	3.40	0.72	124.31	128.26
CASE 3	0.108	0.72	0.00243	24.0	11400	0.471	0.272	0.221	0.58	---	124.72 dB
CASE 4	0.72	0.79	0.000825	58.0	1650	2.87	0.853	3.40	0.72	124.31	128.26

TABLE 3: PRESSURE SPECTRA OF NOISE COMPONENTS
 SUBSONIC RESULTS; (a) SPN
 (b) Subsonic portion
 of Formulation 3

(a)

NUMBER	---- HARMONIC ---- FREQUENCY (Hz)	THICKNESS NOISE (dB)	LOADING NOISE (dB)	OVERALL NOISE (dB)
1	220.00	103.65	113.52	113.85
2	440.00	98.52	102.10	102.91
3	660.00	93.29	92.91	93.26
4	880.00	86.93	86.23	81.82
5	1100.00	79.65	82.43	76.27
6	1320.00	74.18	78.17	76.21
7	1540.00	71.90	72.62	73.48
8	1760.00	69.21	66.23	68.63
9	1980.00	65.10	61.09	61.76
10	2200.00	59.88	58.08	54.37
11	2420.00	54.90	54.84	52.24
12	2640.00	51.63	50.42	50.94
13	2860.00	48.81	45.01	47.69
14	3080.00	45.09	39.87	42.56
15	3300.00	40.40	36.33	36.26
16	3520.00	35.58	33.14	32.14

(b)

NUMBER	---- HARMONIC ---- FREQUENCY (Hz)	THICKNESS NOISE (dB)	LOADING NOISE (dB)	OVERALL NOISE (dB)
1	220.02	103.81	114.03	114.93
2	440.03	99.31	101.92	104.98
3	660.05	94.89	90.53	96.98
4	880.06	89.41	80.99	87.64
5	1100.08	82.76	80.69	76.99
6	1320.09	76.70	78.42	77.92
7	1540.11	74.16	73.77	77.59
8	1760.13	72.01	66.72	74.50
9	1980.14	68.37	56.45	69.16
10	2200.16	63.18	53.12	61.65
11	2420.17	57.47	54.07	57.04
12	2640.19	54.14	51.83	57.25
13	2860.21	52.24	47.29	55.64
14	3080.22	49.36	40.44	51.97
15	3300.24	45.16	29.55	46.46
16	3520.25	40.43	13.05	40.10

TABLE 4: PRESSURE SPECTRA OF NOISE COMPONENTS
 TRANSONIC RESULTS; (a) TPN
 (b) Formulation 3

(a)

---- HARMONIC -----		THICKNESS	LOADING	OVERALL
NUMBER	FREQUENCY (Hz)	NOISE (dB)	NOISE (dB)	NOISE (dB)
1	220.00	121.27	117.97	123.02
2	440.00	119.22	115.26	115.02
3	660.00	114.72	111.46	111.72
4	880.00	111.55	105.30	110.23
5	1100.00	110.29	102.20	108.66
6	1320.00	106.42	98.07	104.79
7	1540.00	101.17	93.42	99.79
8	1760.00	97.48	88.48	96.30
9	1980.00	92.52	83.37	90.21
10	2200.00	87.94	79.23	84.13
11	2420.00	77.28	74.67	76.49
12	2640.00	88.64	81.60	86.03
13	2860.00	91.37	81.12	90.68
14	3080.00	91.14	80.85	88.91
15	3300.00	93.17	80.28	91.43
16	3520.00	92.27	80.07	90.34

(b)

---- HARMONIC -----		THICKNESS	LOADING	OVERALL
NUMBER	FREQUENCY (Hz)	NOISE (dB)	NOISE (dB)	NOISE (dB)
1	220.02	121.75	120.60	126.31
2	440.03	120.46	111.86	118.39
3	660.05	117.03	110.79	115.76
4	880.06	113.43	105.33	113.89
5	1100.08	113.02	101.92	113.51
6	1320.09	110.35	99.82	111.05
7	1540.11	107.87	97.80	109.63
8	1760.13	109.07	94.46	110.28
9	1980.14	108.89	92.52	109.66
10	2200.16	107.11	93.51	108.47
11	2420.17	108.34	91.85	109.55
12	2640.19	108.02	85.19	108.55
13	2860.21	105.07	71.26	105.24
14	3080.22	104.54	76.61	104.88
15	3300.24	104.19	74.80	104.41
16	3520.25	101.80	66.38	101.65

TABLE 5: PRESSURE SPECTRA OF NOISE COMPONENTS
 THICKNESS NOISE COMPARISON
 (a) Formulation 3 linked with ANOPP
 (b) Formulation 3 stand alone

NUMBER	----- HARMONIC ----- FREQUENCY (Hz)	(a) THICKNESS NOISE (dB)	(b) THICKNESS NOISE (dB)
1	220.02	121.75	121.36
2	440.03	120.46	119.99
3	660.05	117.03	116.94
4	880.06	113.43	113.40
5	1100.08	113.02	111.82
6	1320.09	110.35	110.08
7	1540.11	107.87	107.60
8	1760.13	109.07	107.28
9	1980.14	108.89	108.36
10	2200.16	107.11	108.12
11	2420.17	108.34	106.39
12	2640.19	108.02	105.68
13	2860.21	105.07	104.79
14	3080.22	104.54	103.11
15	3300.24	104.19	102.37
16	3520.25	101.80	103.53

TABLE 6: PRESSURE SPECTRA OF NOISE COMPONENTS
SUBSONIC RESULTS OF UNSTEADY CASE

---- HARMONIC ----		THICKNESS	LOADING	OVERALL
NUMBER	FREQUENCY (Hz)	NOISE (dB)	NOISE (dB)	NOISE (dB)
1	760.00	87.43	107.93	107.65
2	1519.99	68.59	109.18	109.26
3	2279.99	48.45	111.65	111.65
4	3039.99	27.45	112.61	112.61
5	3799.98	5.73	112.41	112.41
6	4559.98	-16.75	111.00	111.00
7	5319.98	-40.45	107.94	107.94
8	6079.97	-60.96	101.40	101.40
9	6839.97	-69.13	88.89	88.89
10	7599.97	-70.63	103.73	103.73
11	8359.96	-71.53	108.12	108.12
12	9119.96	-72.23	109.98	109.98
13	9879.96	-72.74	110.37	110.37
14	10639.95	-73.12	109.51	109.51
15	11399.95	-73.41	107.25	107.25
16	12159.95	-73.62	103.00	103.00
17	12919.94	-73.78	97.10	97.10
18	13679.94	-73.91	100.44	100.44
19	14439.94	-74.00	104.41	104.41
20	15199.93	-74.08	105.94	105.94
21	15959.93	-74.13	105.57	105.57
22	16719.93	-74.18	103.03	103.03
23	17479.92	-74.22	95.96	95.96
24	18239.92	-74.25	93.39	93.39

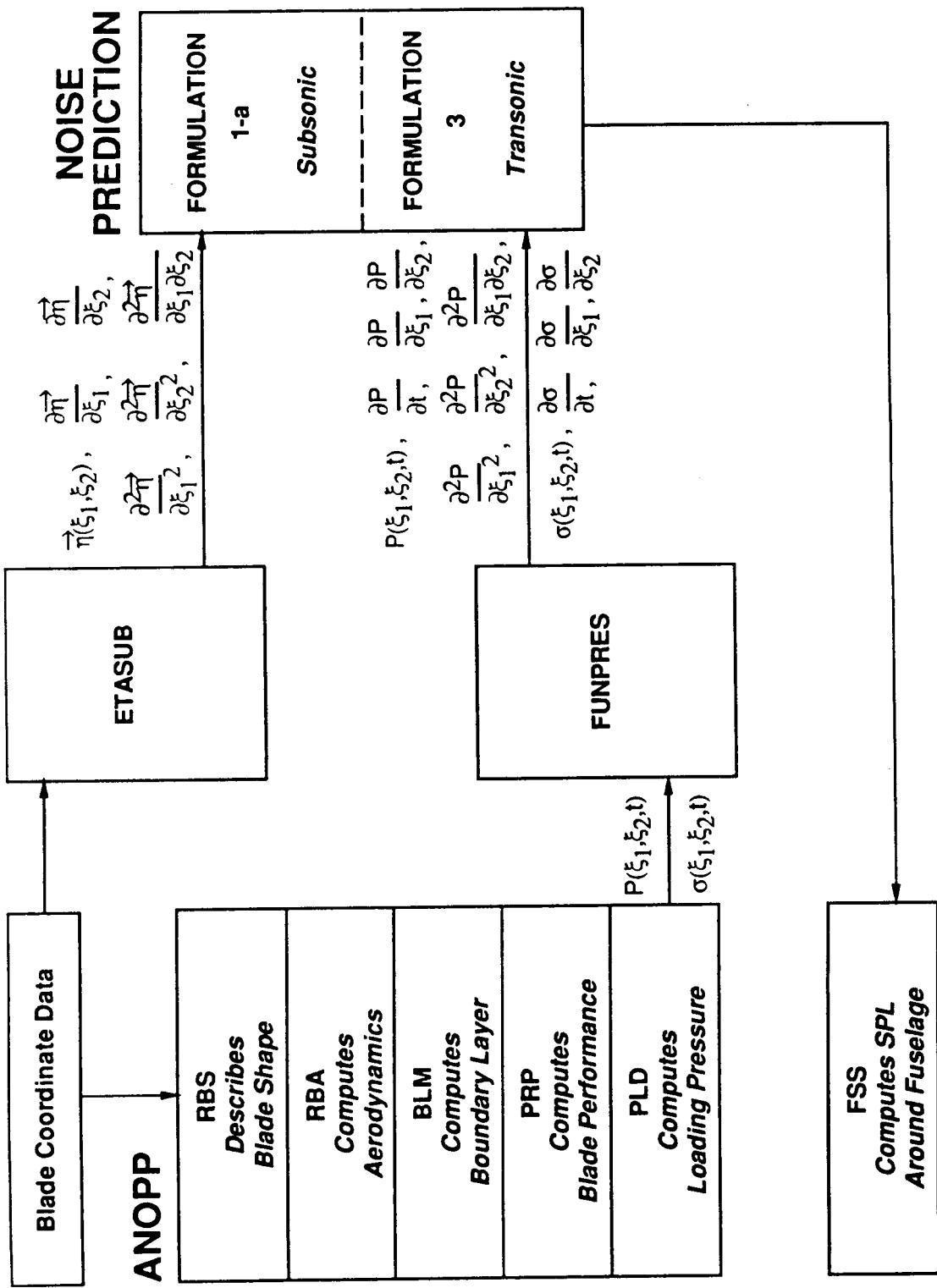


Figure 1. Flow chart showing steps in using Formulation 3 with ANOPP to make a noise prediction.

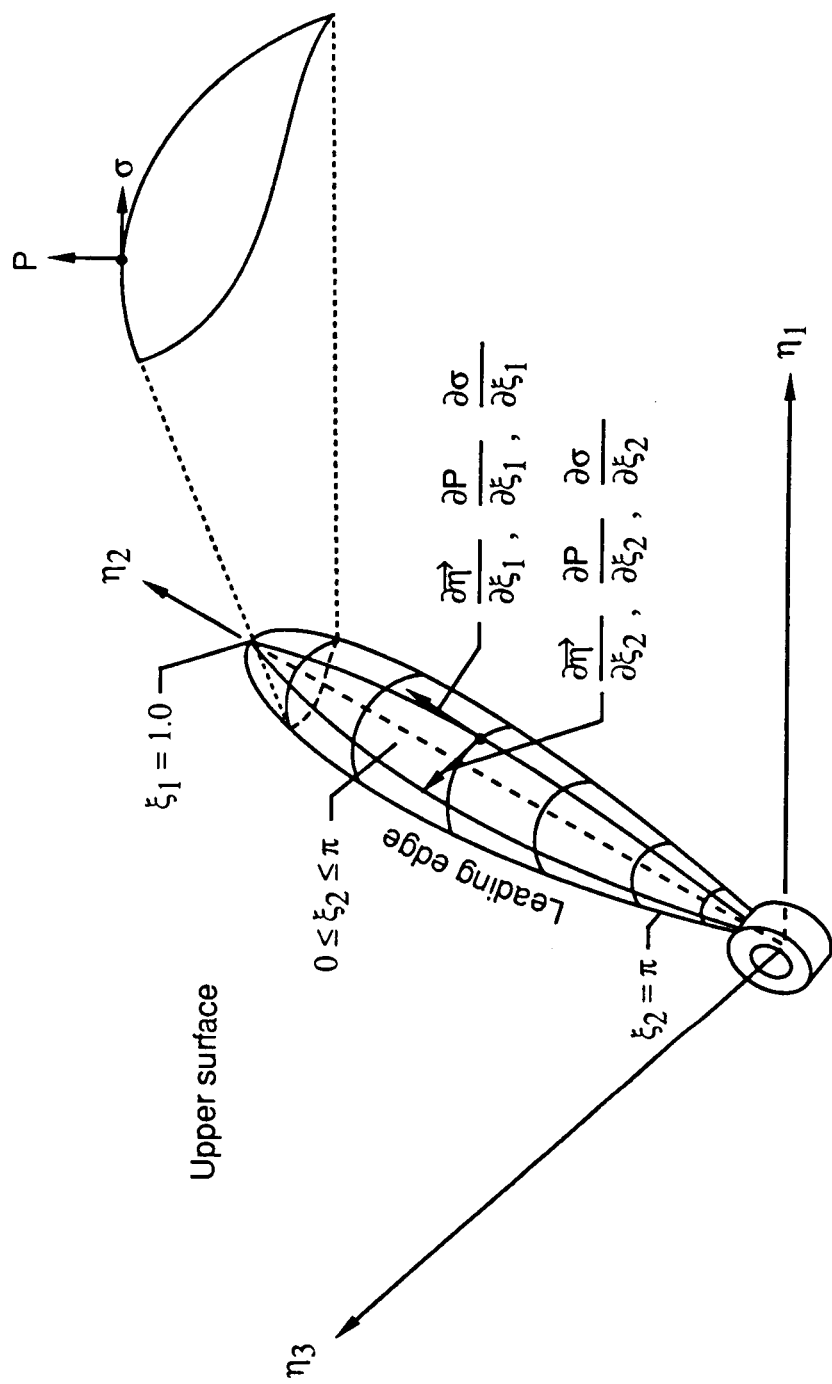


Figure 2. Blade surface coordinate system.

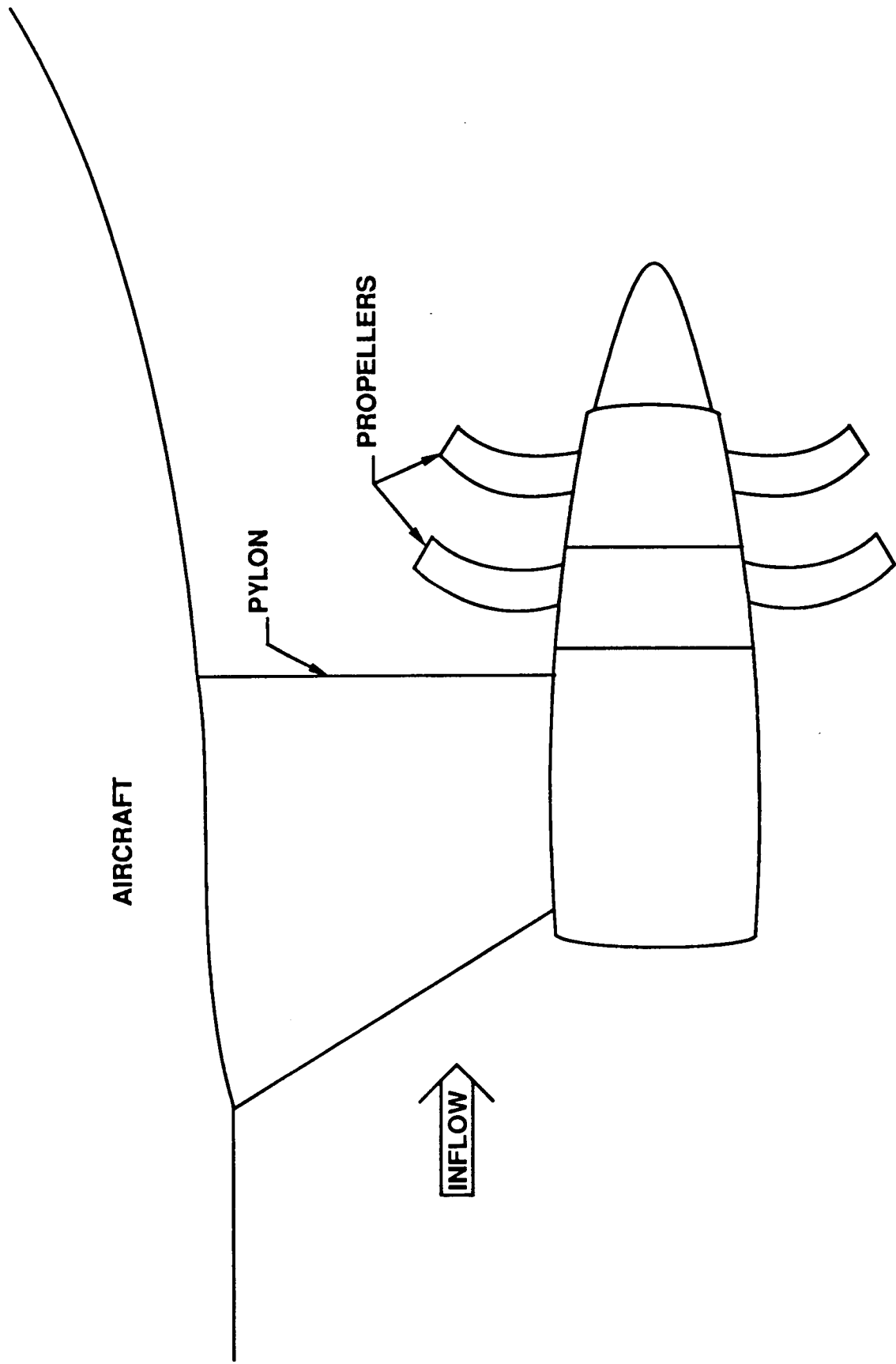


Figure 3. Configuration of a pusher propeller on an aircraft.

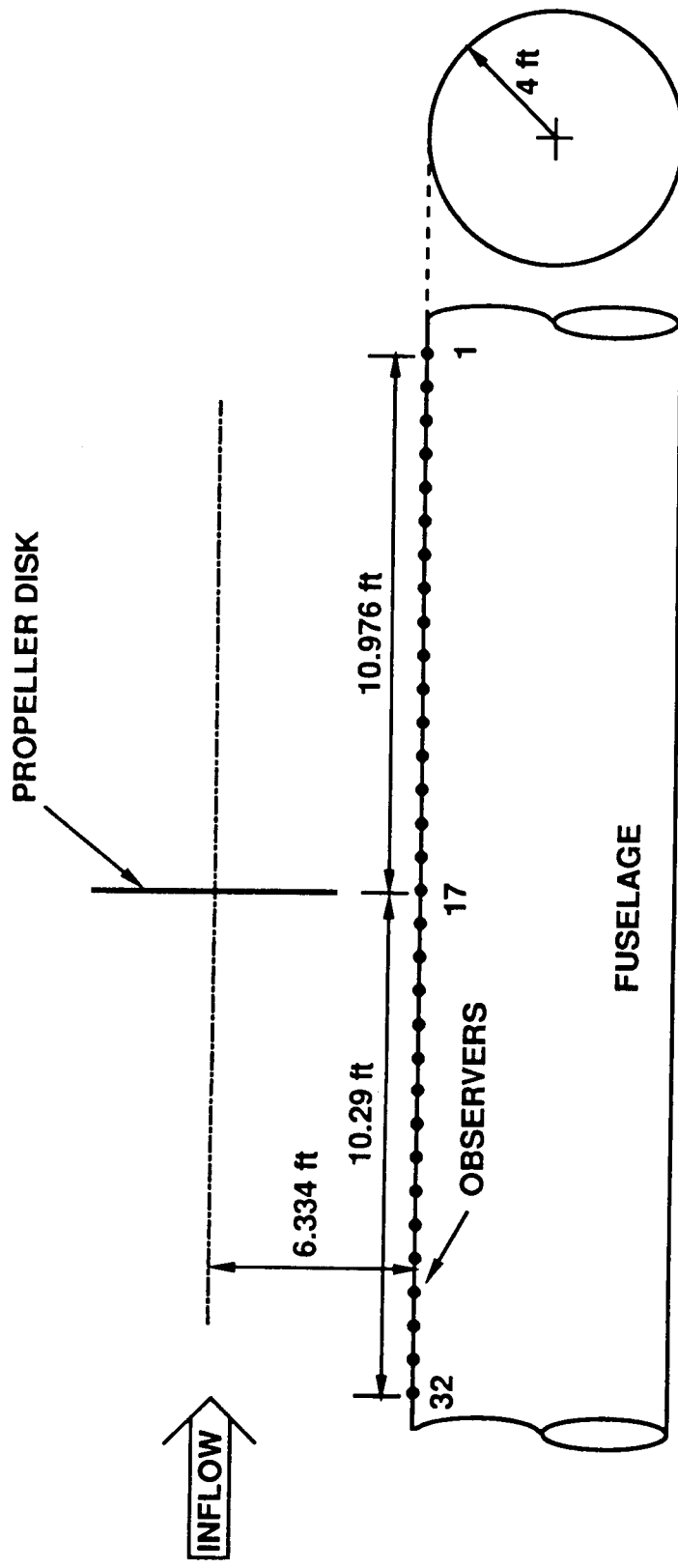


Figure 4. Illustration of observer locations for Case 4 configuration. Drawing not to scale.

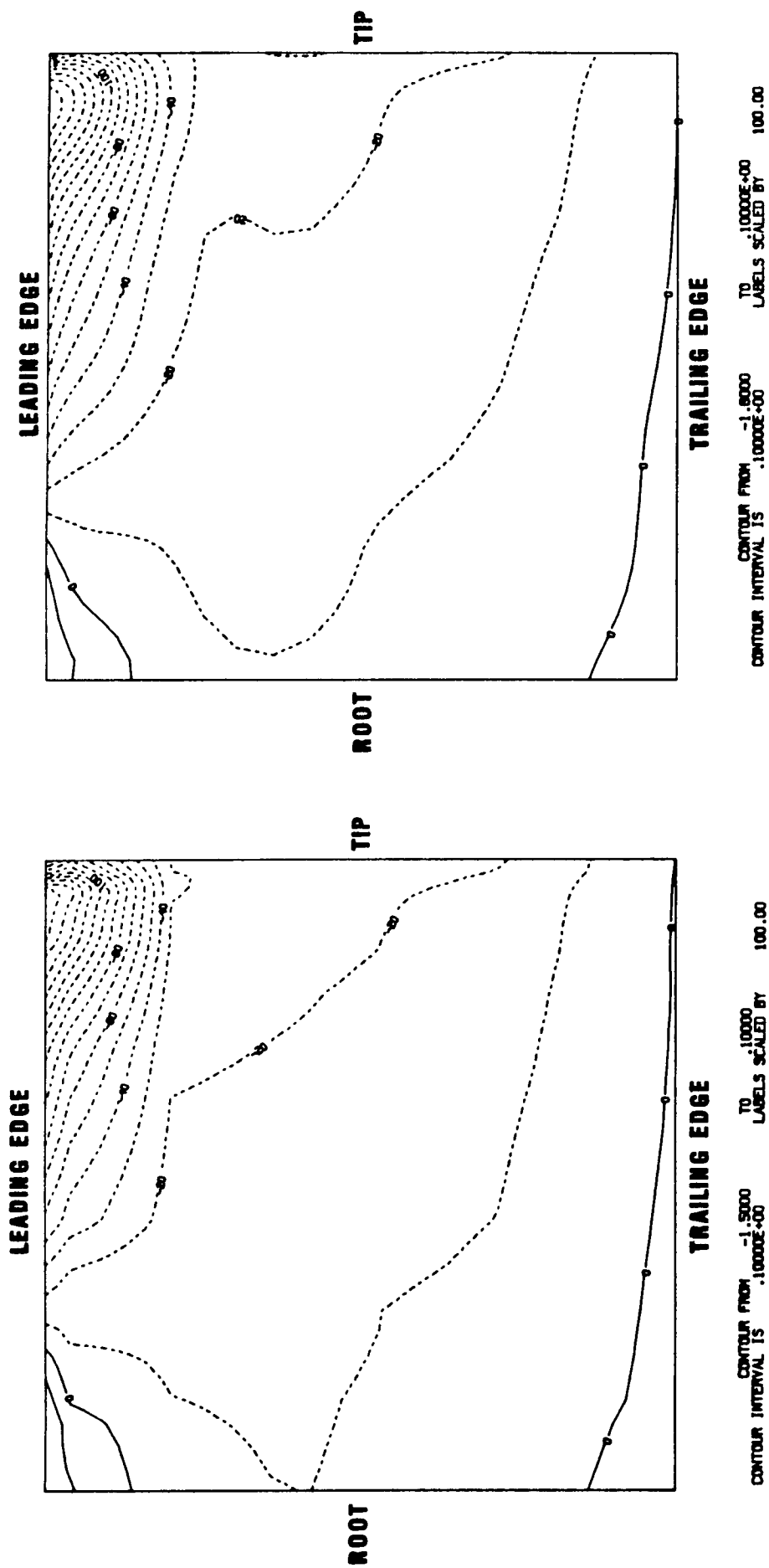


Figure 5. Loading pressure contours of the subsonic data on the top surface of the SR-3 blade. Case 1.

Figure 6. Contours of the loading pressure generated by the spline fit of the subsonic data on the top surface of the SR-3 blade. Case 1.

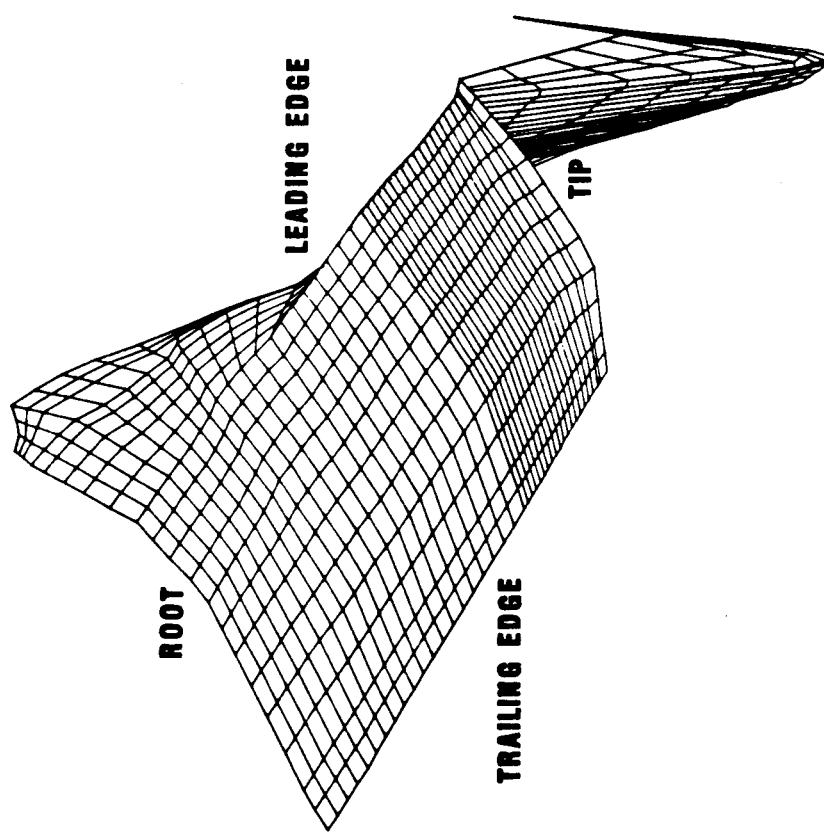
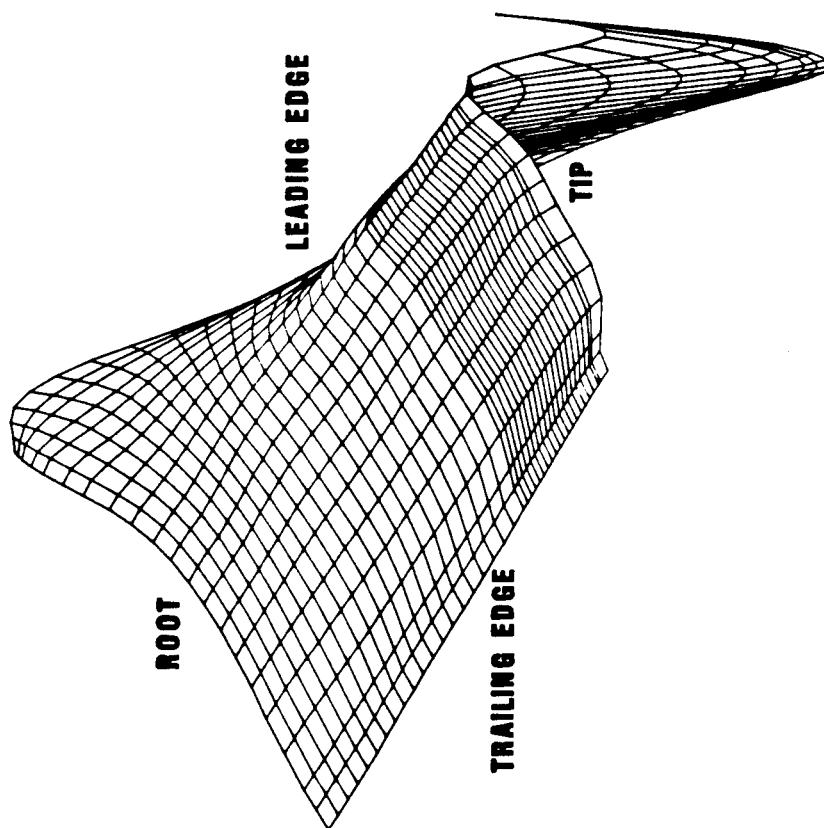


Figure 7. Three dimensional projection of the subsonic loading pressure data on the top surface of the SR-3 blade. Case 1.

Figure 8. Three dimensional projection of the spline fit of the transonic loading pressure data on the top surface of the SR-3 blade. Case 1.

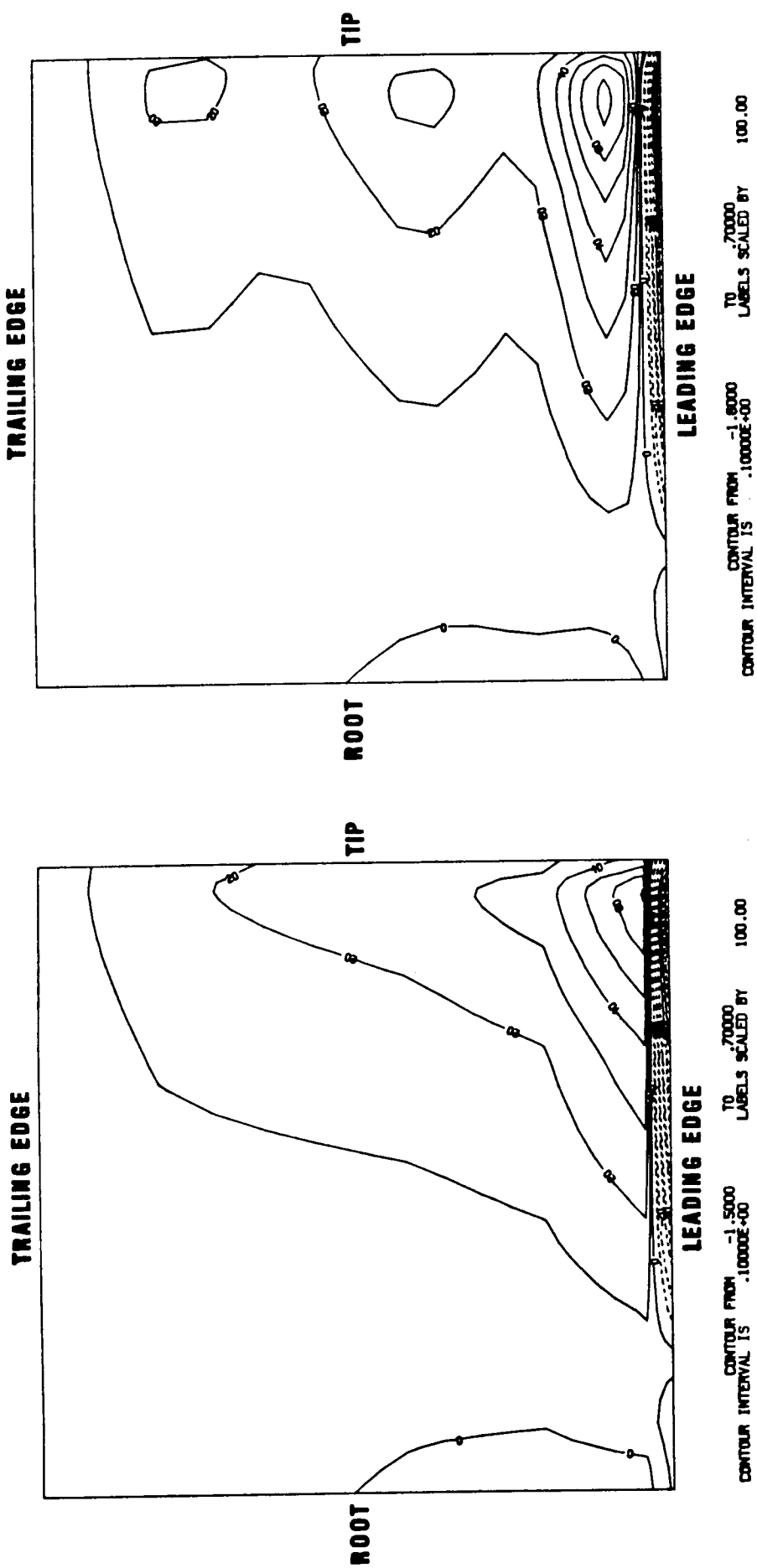


Figure 9. Loading pressure contours of the subsonic data on the bottom surface of the SR-3 blade. Case 1.

Figure 10. Contours of the loading pressure generated by the spline fit of the subsonic data on the bottom surface of the SR-3 blade. Case 1.

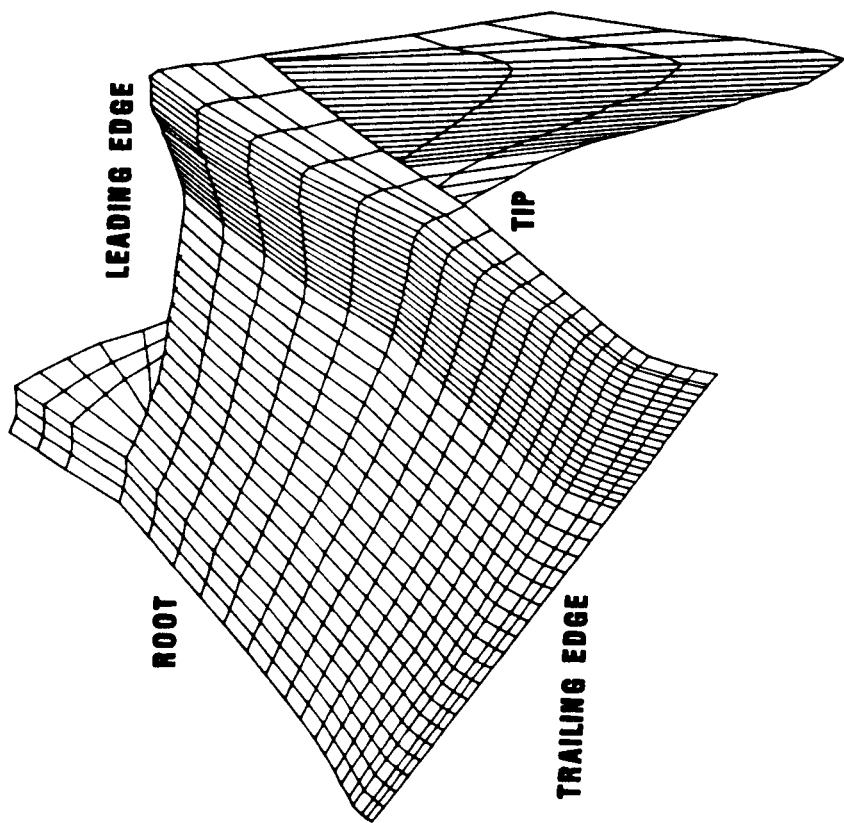
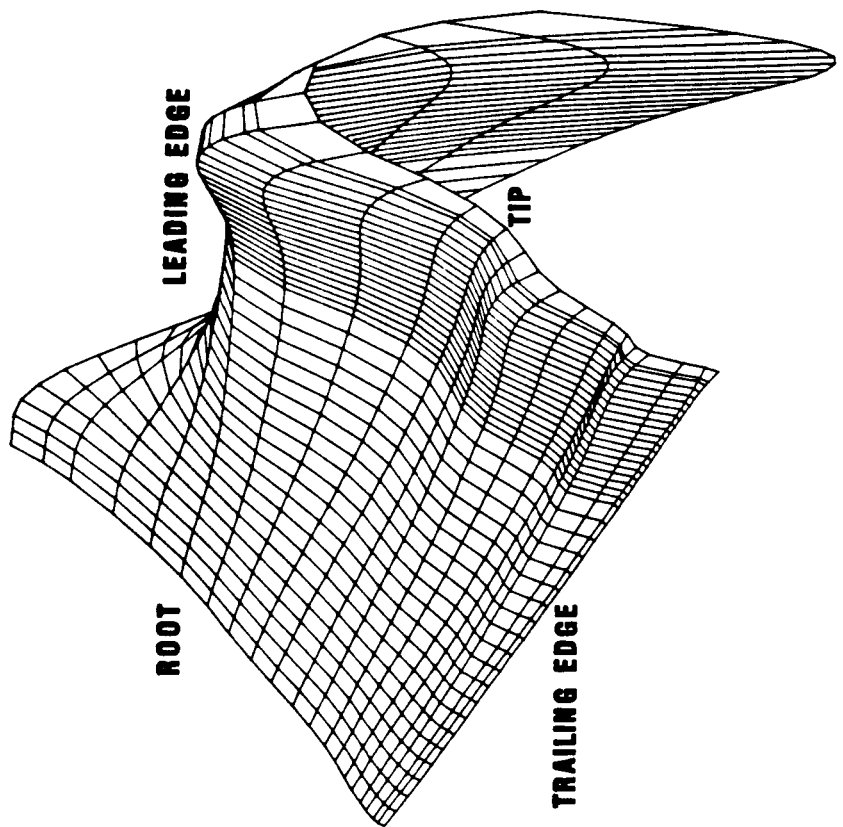


Figure 11. Three dimensional projection of the subsonic loading pressure data on the bottom surface of the SR-3 blade. Case 1.

Figure 12. Three dimensional projection of the spline fit of the transonic loading pressure data on the bottom surface of the SR-3 blade. Case 1.

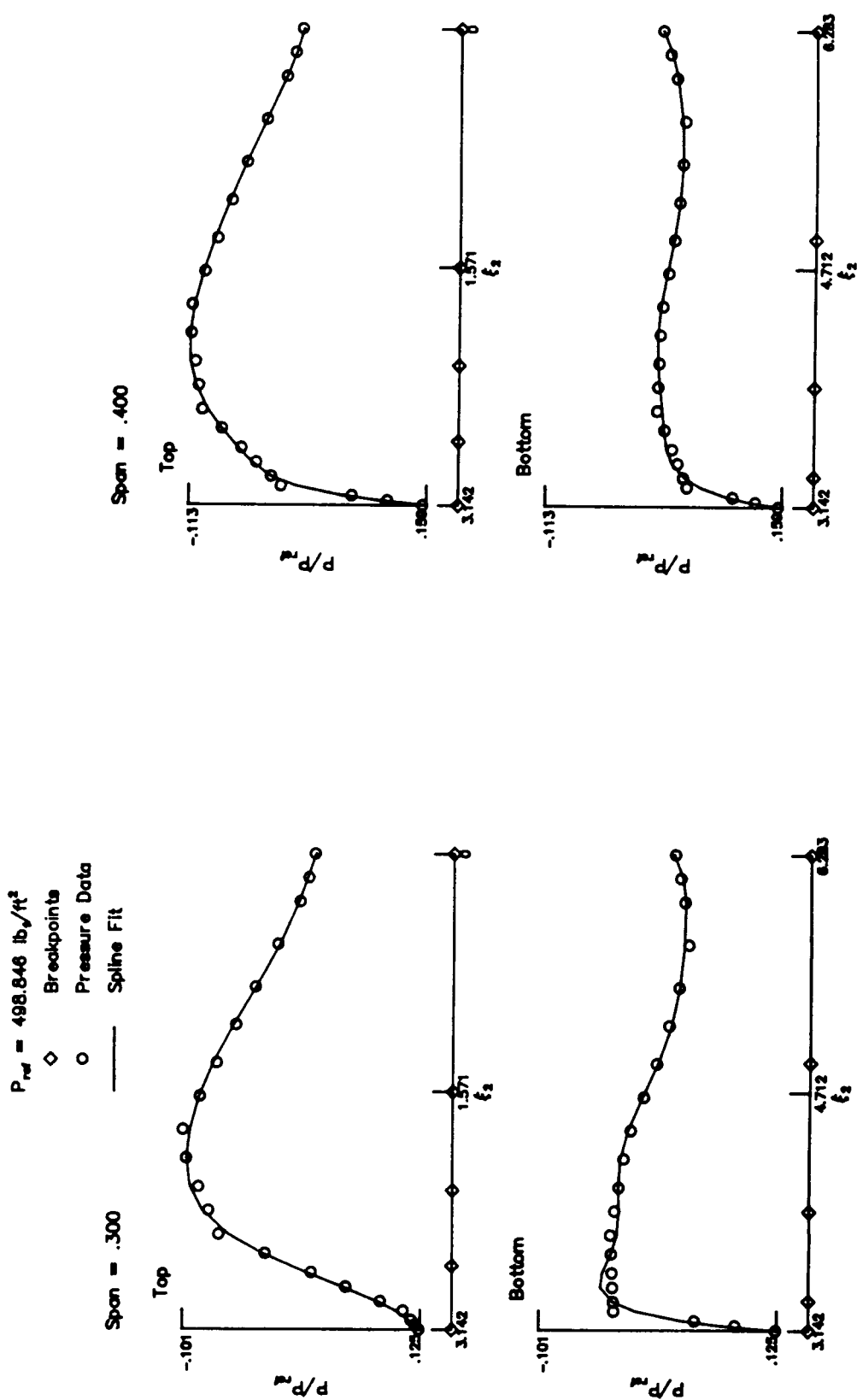


Figure 13. Span sections of the SR-3 blade comparing the subsonic loading pressure data with the spline fit. Case 1.

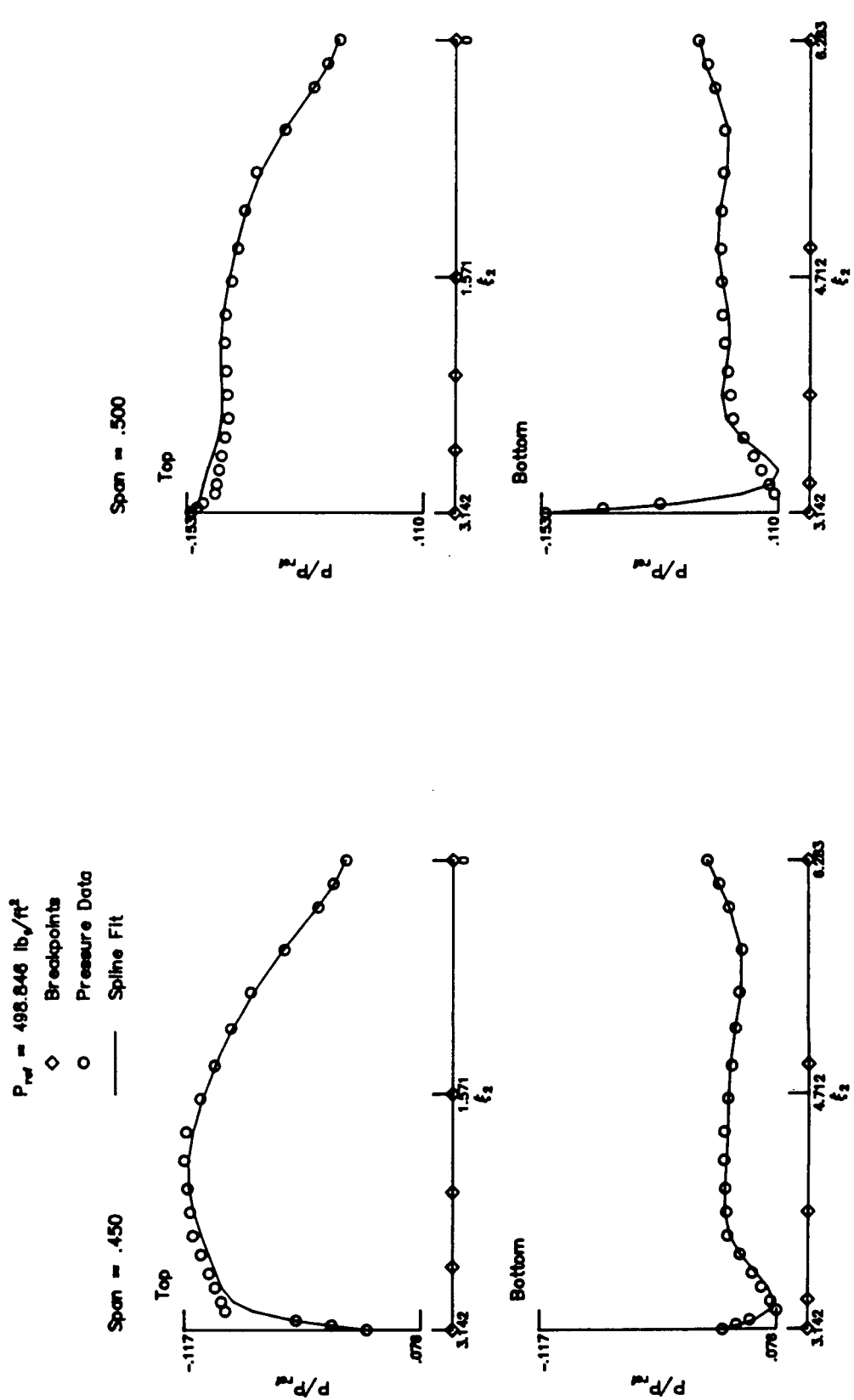


Figure 13. Continued.

Figure 13. Continued.

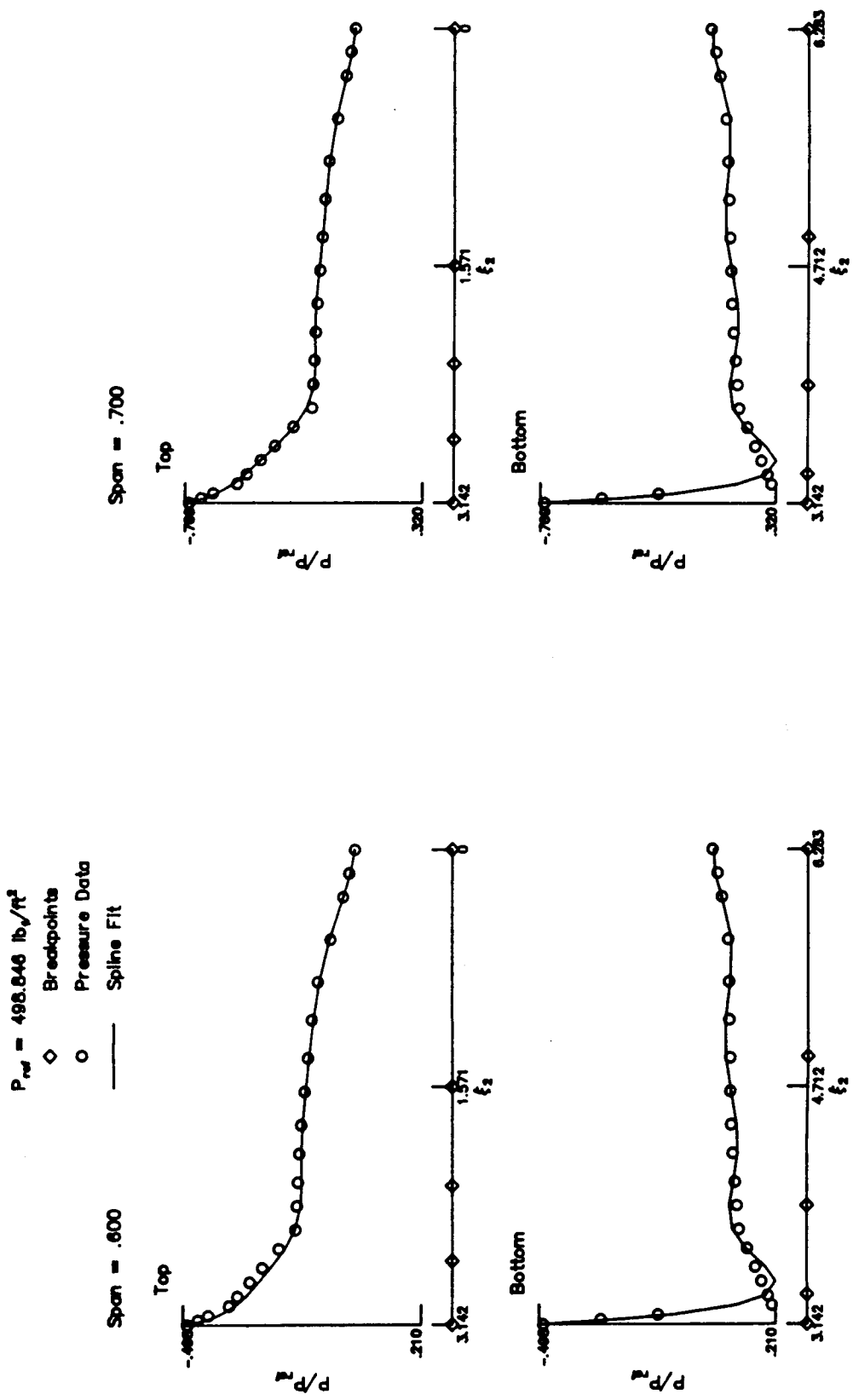


Figure 13. Continued.

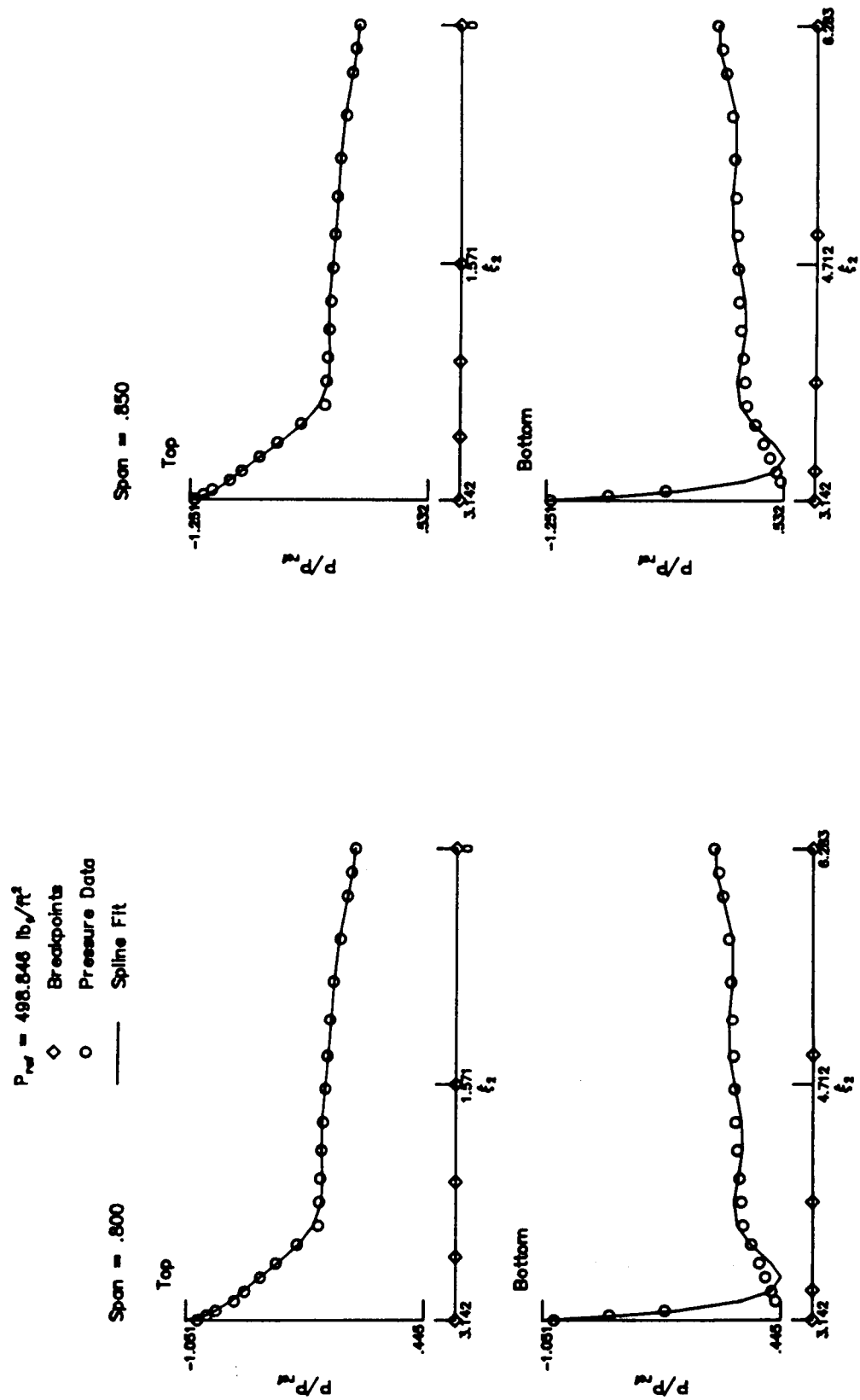
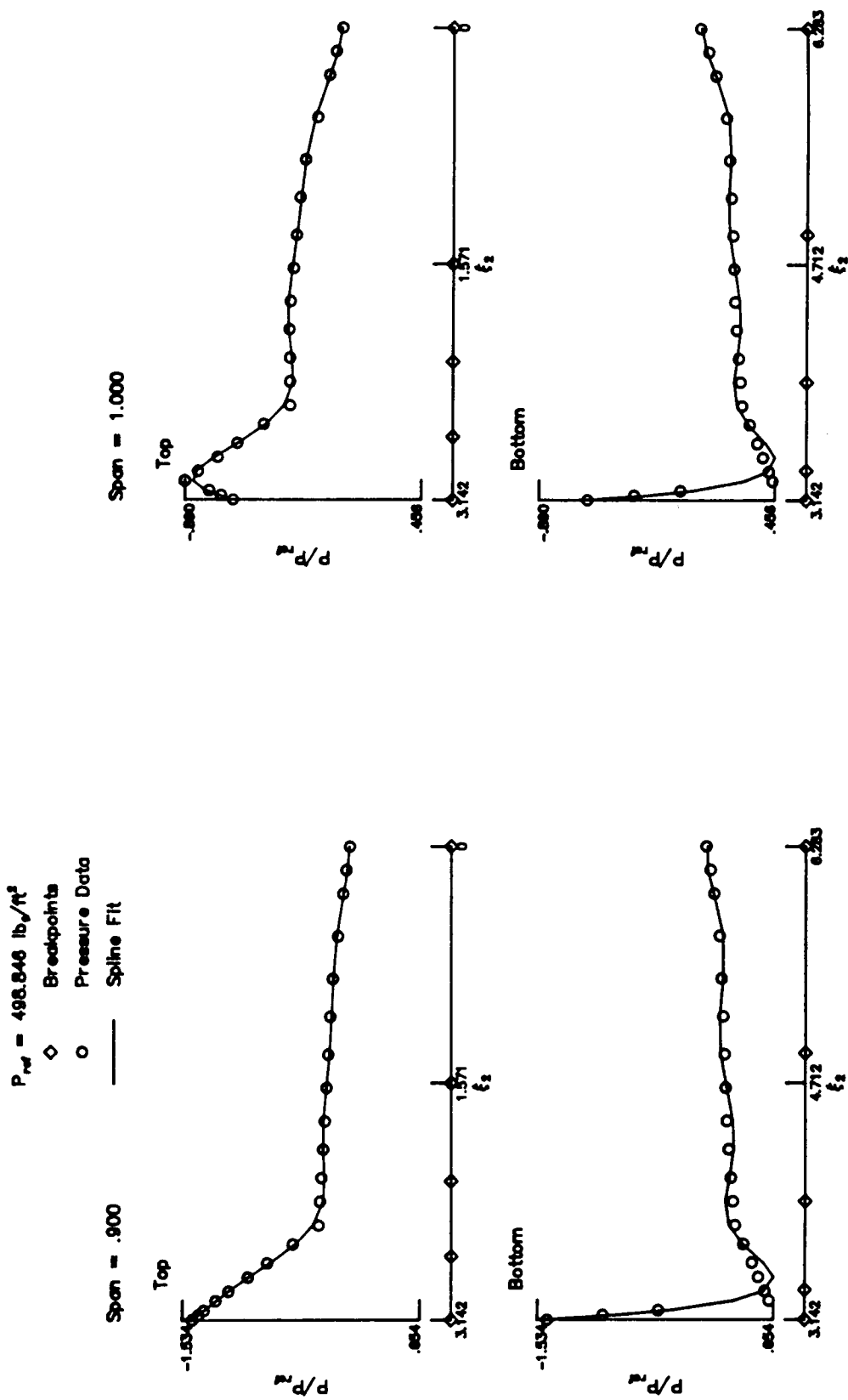


Figure 13. Continued.



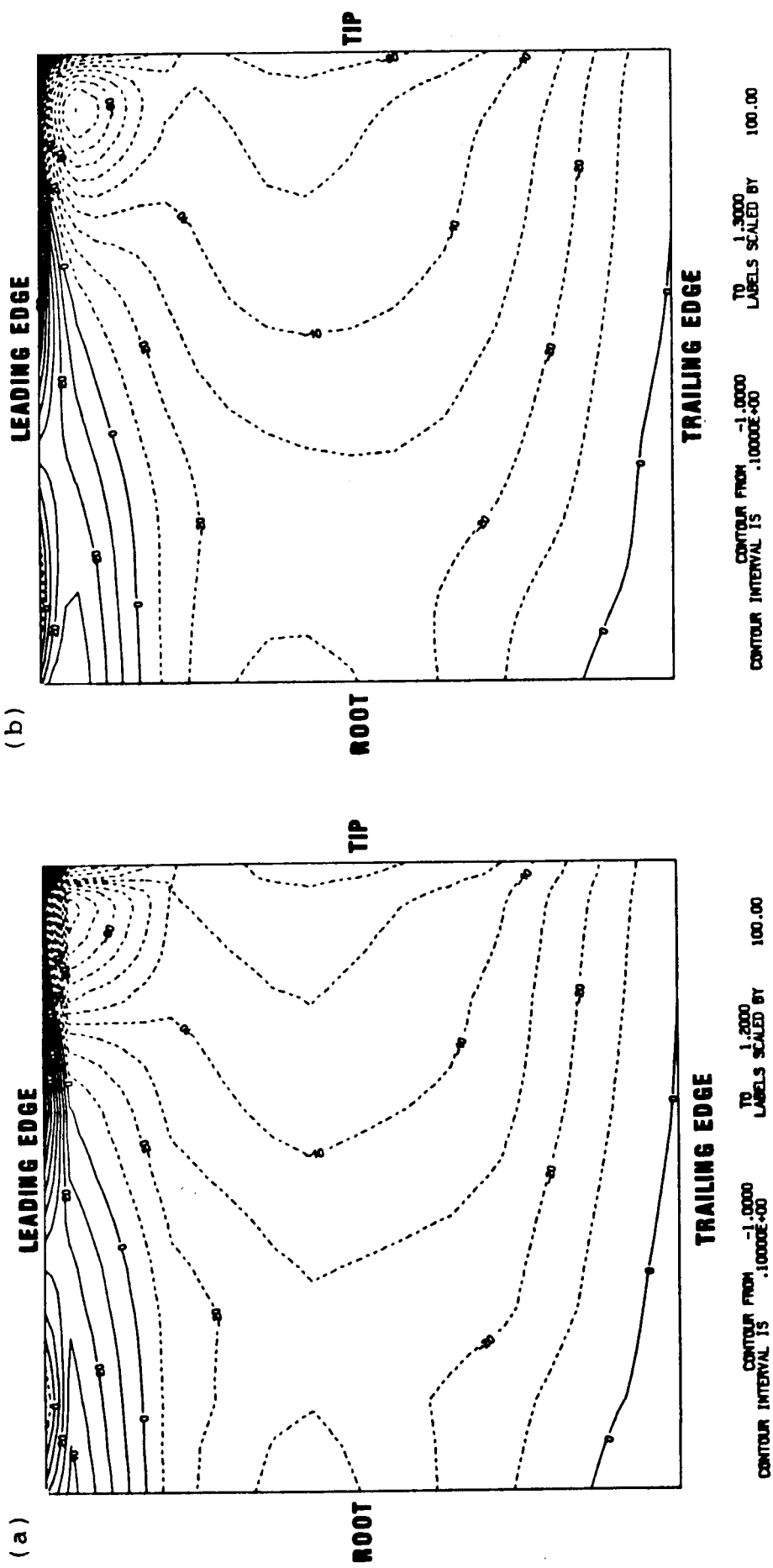


Figure 14. (a) Loading pressure contours of the transonic data on the top surface of the SR-3 blade. Case 2.
 (b) Contours of the loading pressure generated by the spline fit of the transonic data on the top surface of the SR-3 blade. Case 2.

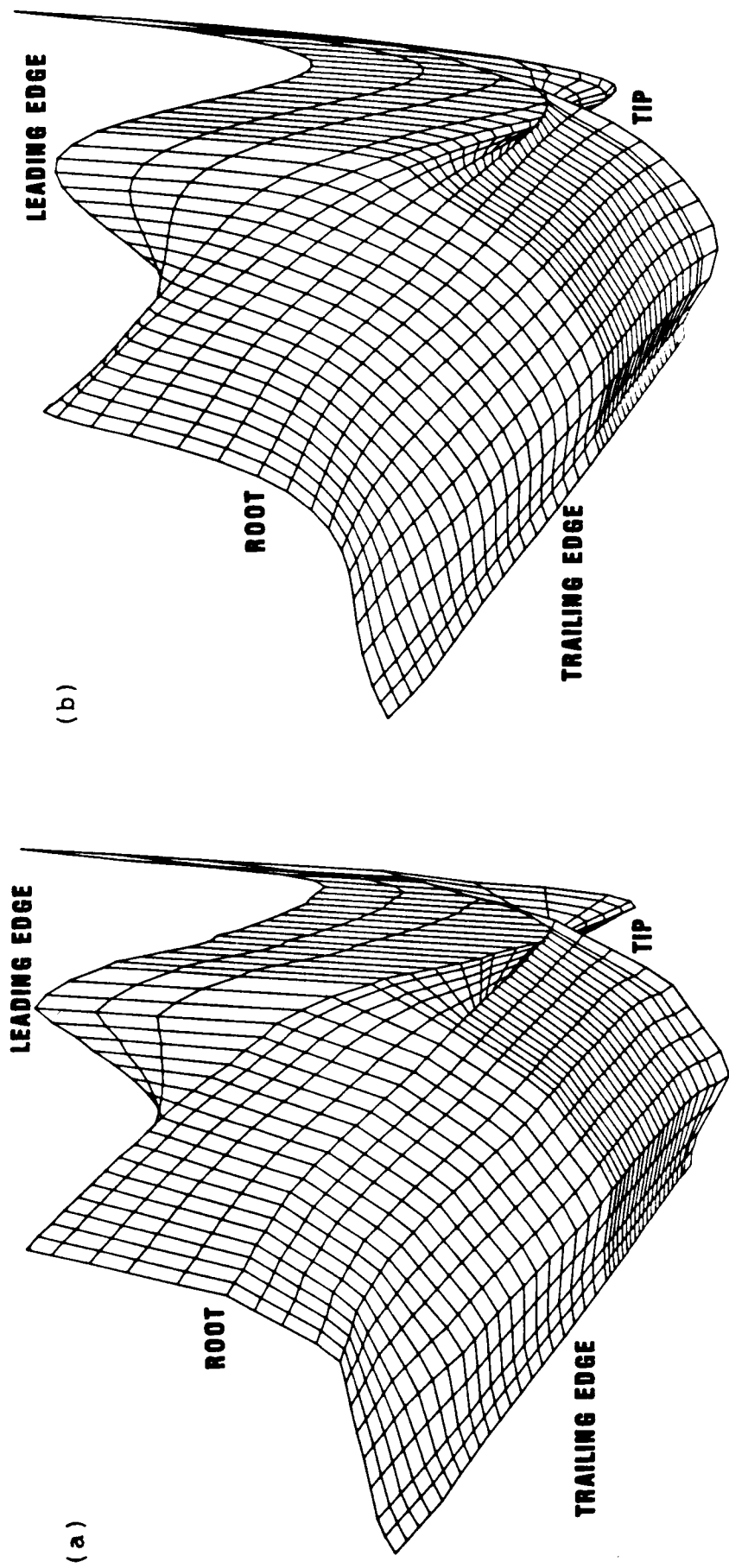


Figure 15. (a) Three dimensional projection of the transonic loading pressure data on the top surface of the SR-3 blade. Case 2.
 (b) Three dimensional projection of the spline fit of the transonic loading pressure data on the top surface of the SR-3 blade. Case 2.

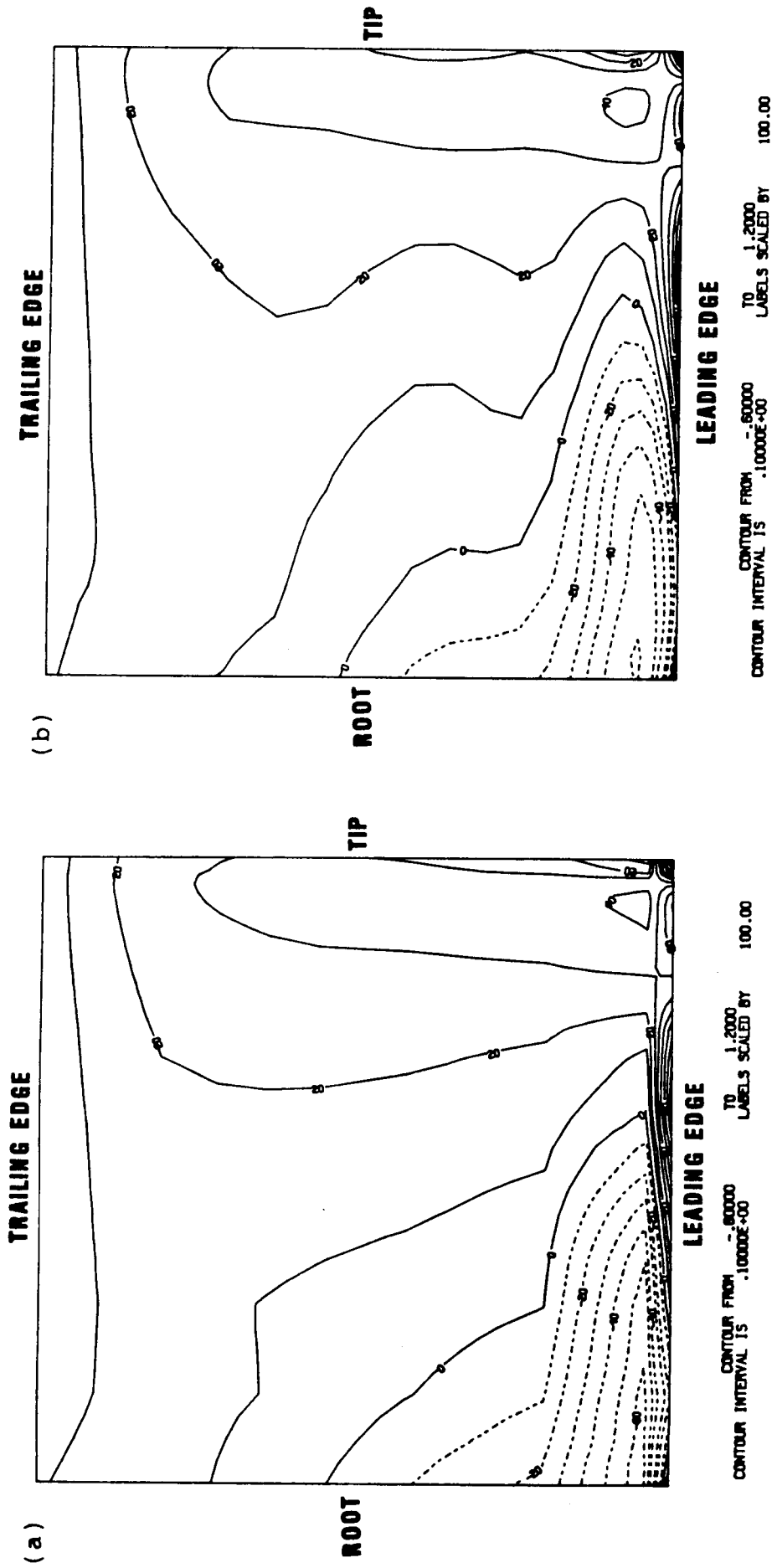


Figure 16. (a) Loading Pressure contours of the transonic data on the bottom surface of the SR-3 blade. Case 2.

(b) Contours of the loading pressure generated by the spline fit of the transonic data on the bottom surface of the SR-3 blade. Case 2.

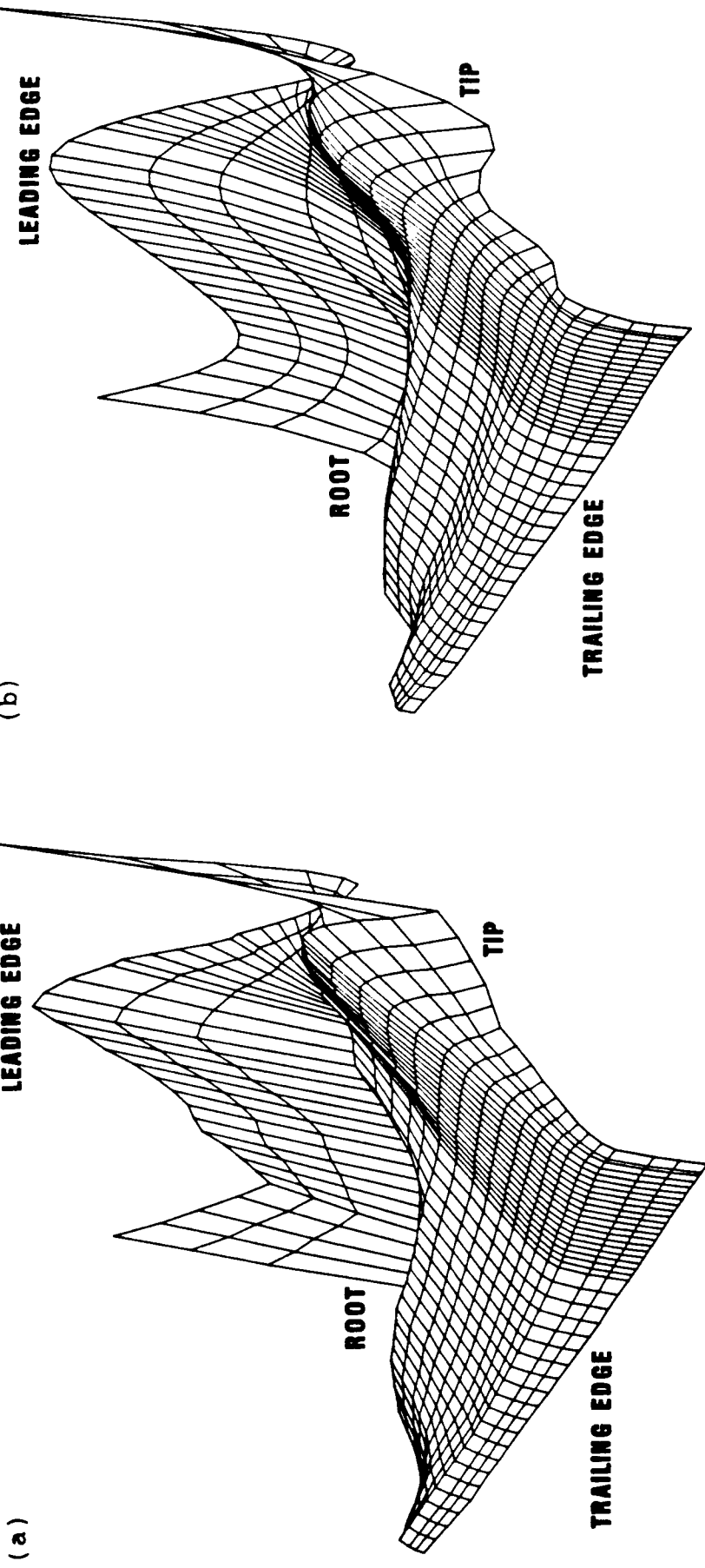


Figure 17. (a) Three dimensional projection of the transonic loading pressure data on the bottom surface of the SR-3 blade. Case 2.
 (b) Three dimensional projection of the spline fit of the transonic loading pressure data on the bottom surface of the SR-3 blade. Case 2.

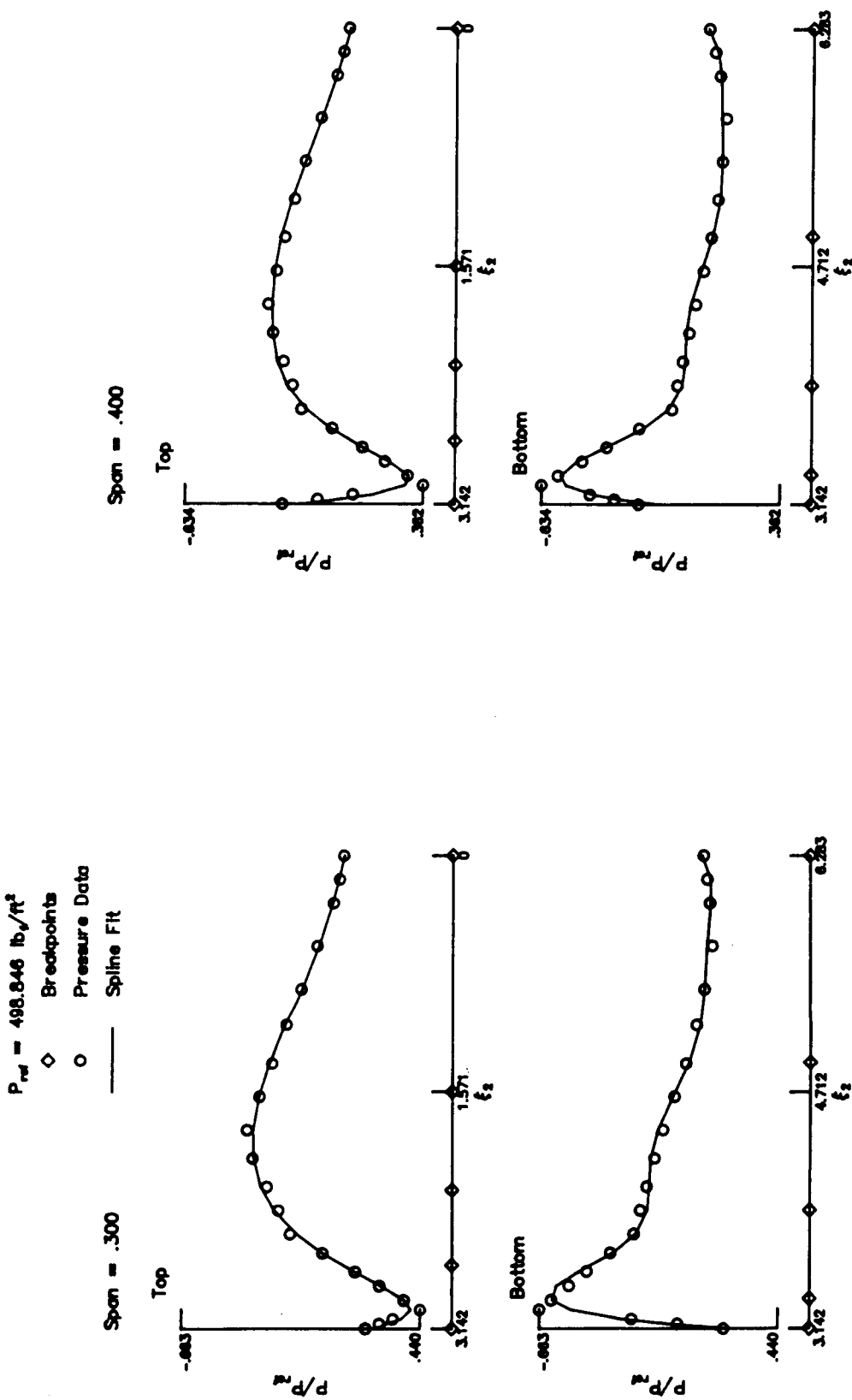


Figure 18. Span sections of the SR-3 blade comparing the transonic loading pressure data with the spline fit. Case 2.

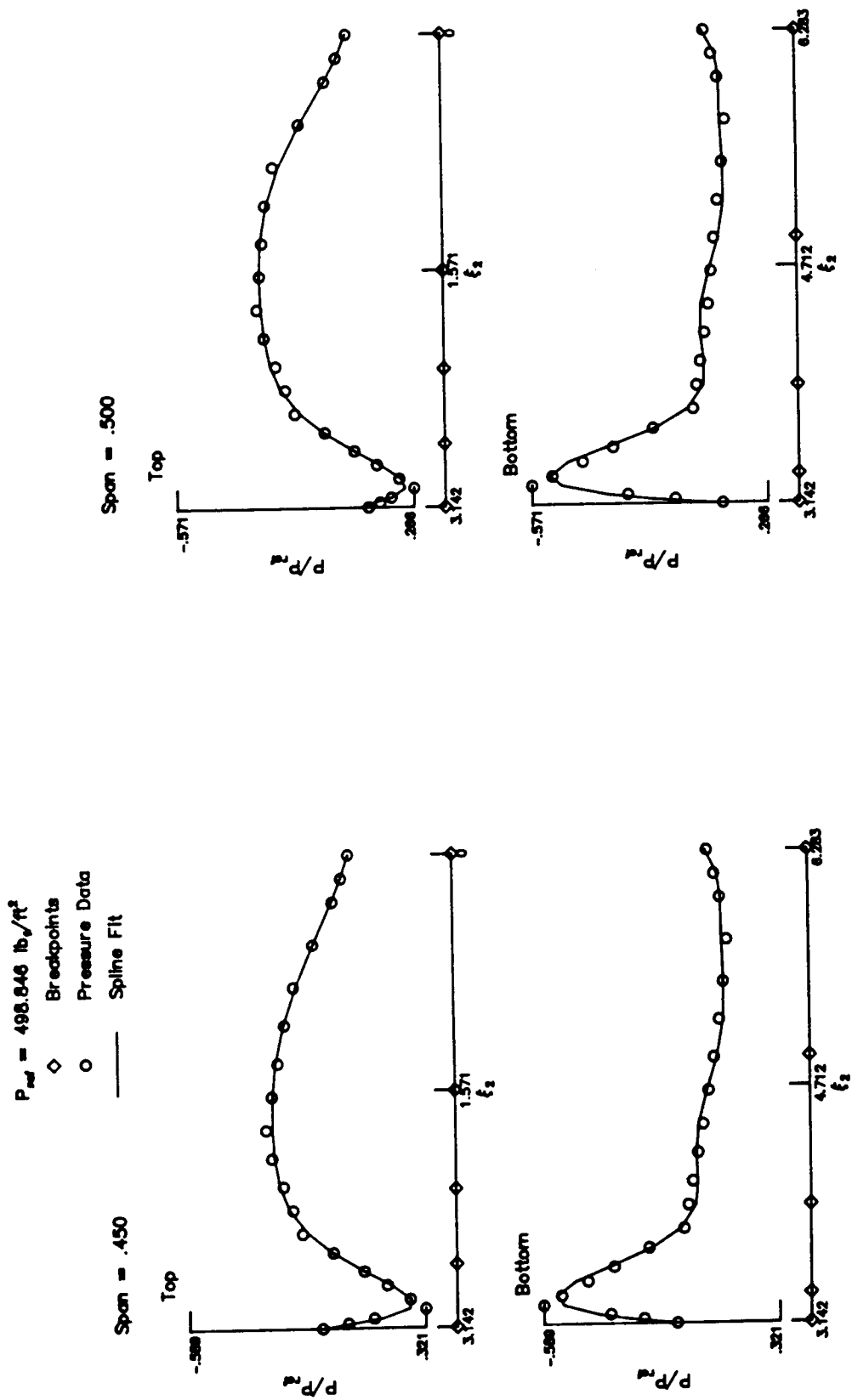


Figure 18. Continued.

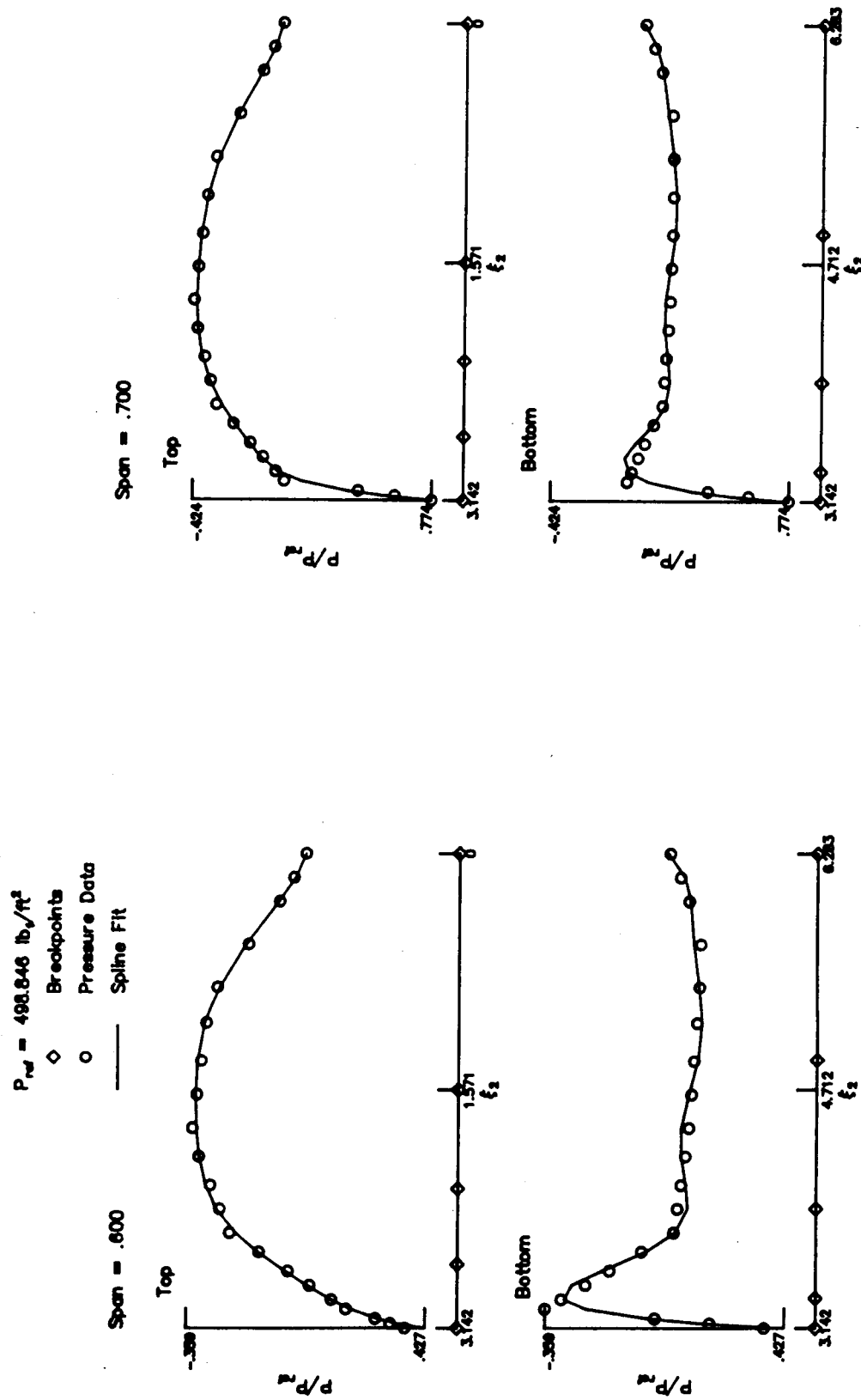


Figure 18. Continued.

Figure 18. Continued.

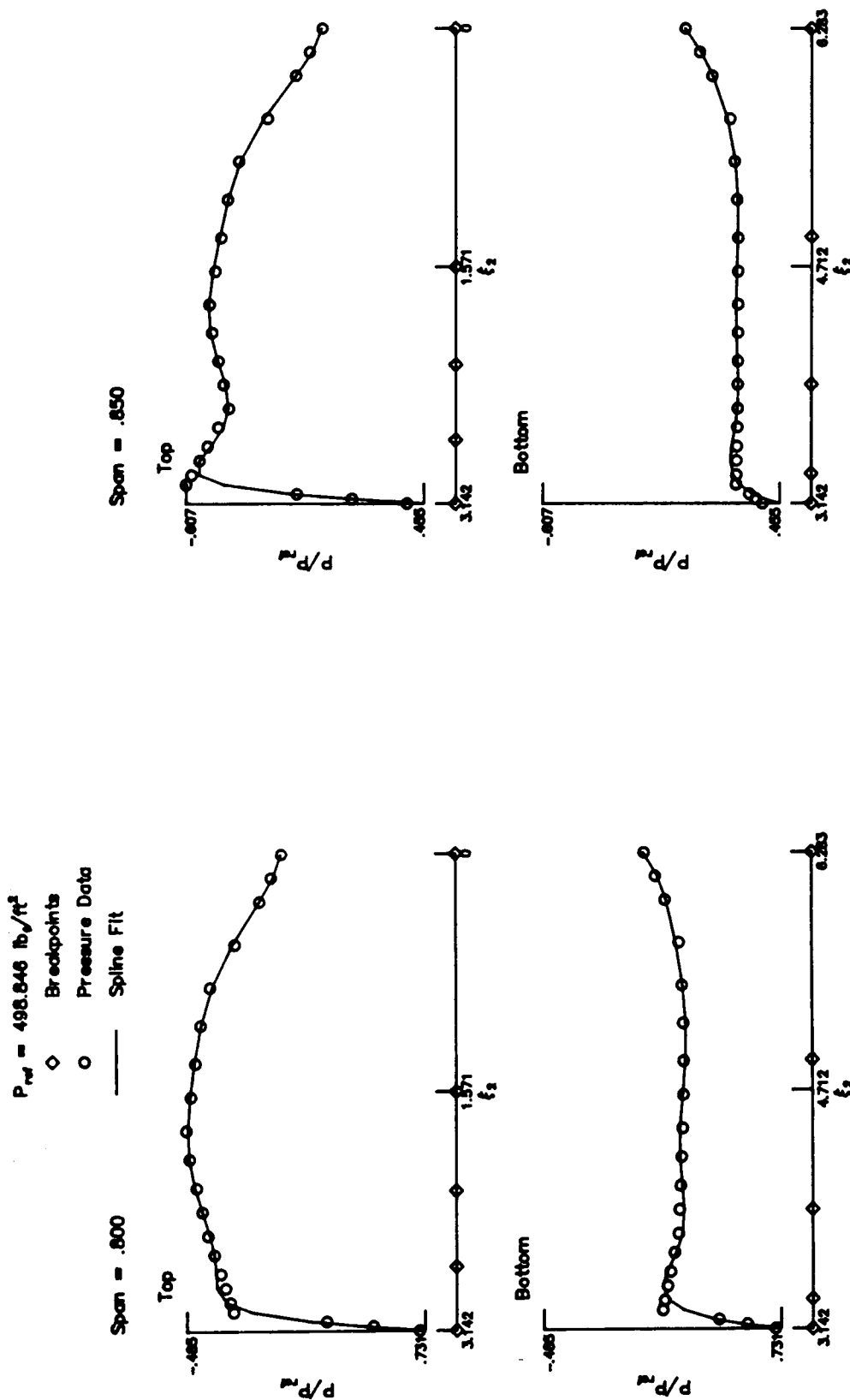
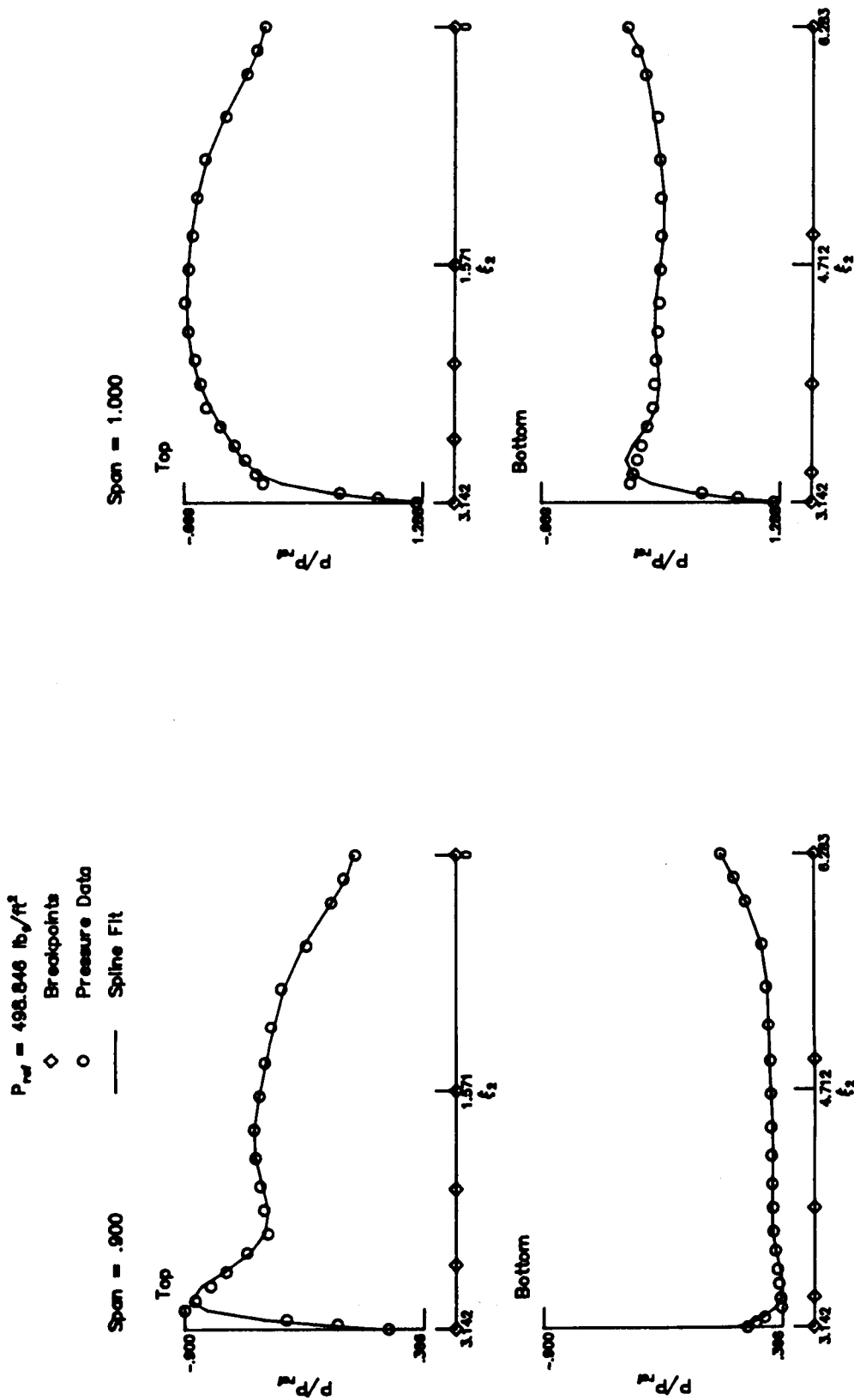
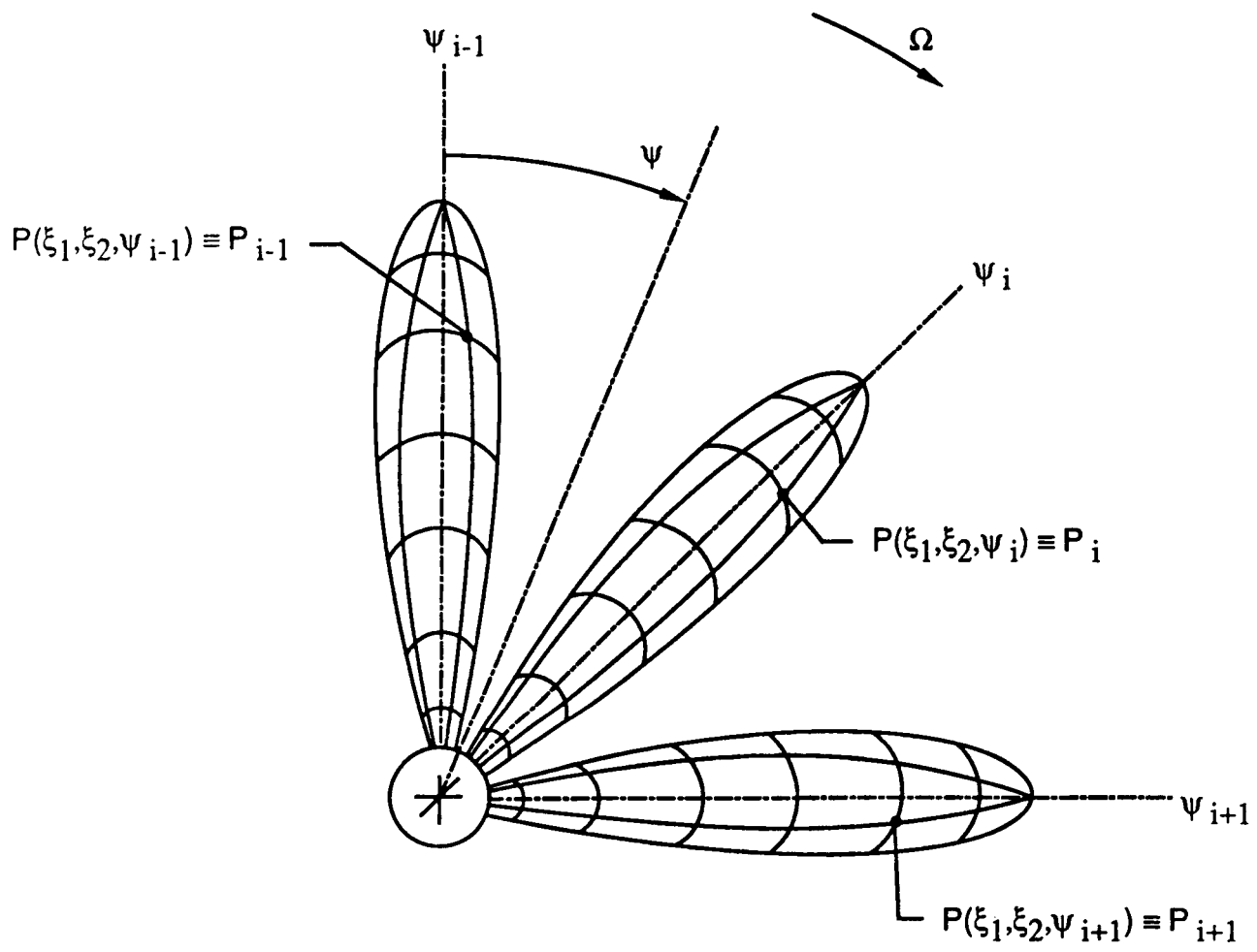


Figure 18. Continued.





$$\Delta t_+ = (\psi_{i+1} - \psi_i) / \Omega$$

$$\Delta t_- = (\psi_i - \psi_{i-1}) / \Omega$$

$$\alpha = \frac{\Delta t_+}{\Delta t_-}$$

$$\left. \frac{\Delta P}{\Delta t} \right|_i = (P_{i+1} + (\alpha^2 - 1)P_i - \alpha^2 P_{i-1}) / ((\alpha^2 + \alpha)\Delta t_-)$$

Figure 19. Numerical formulation for determining the time derivative of the loading pressure.

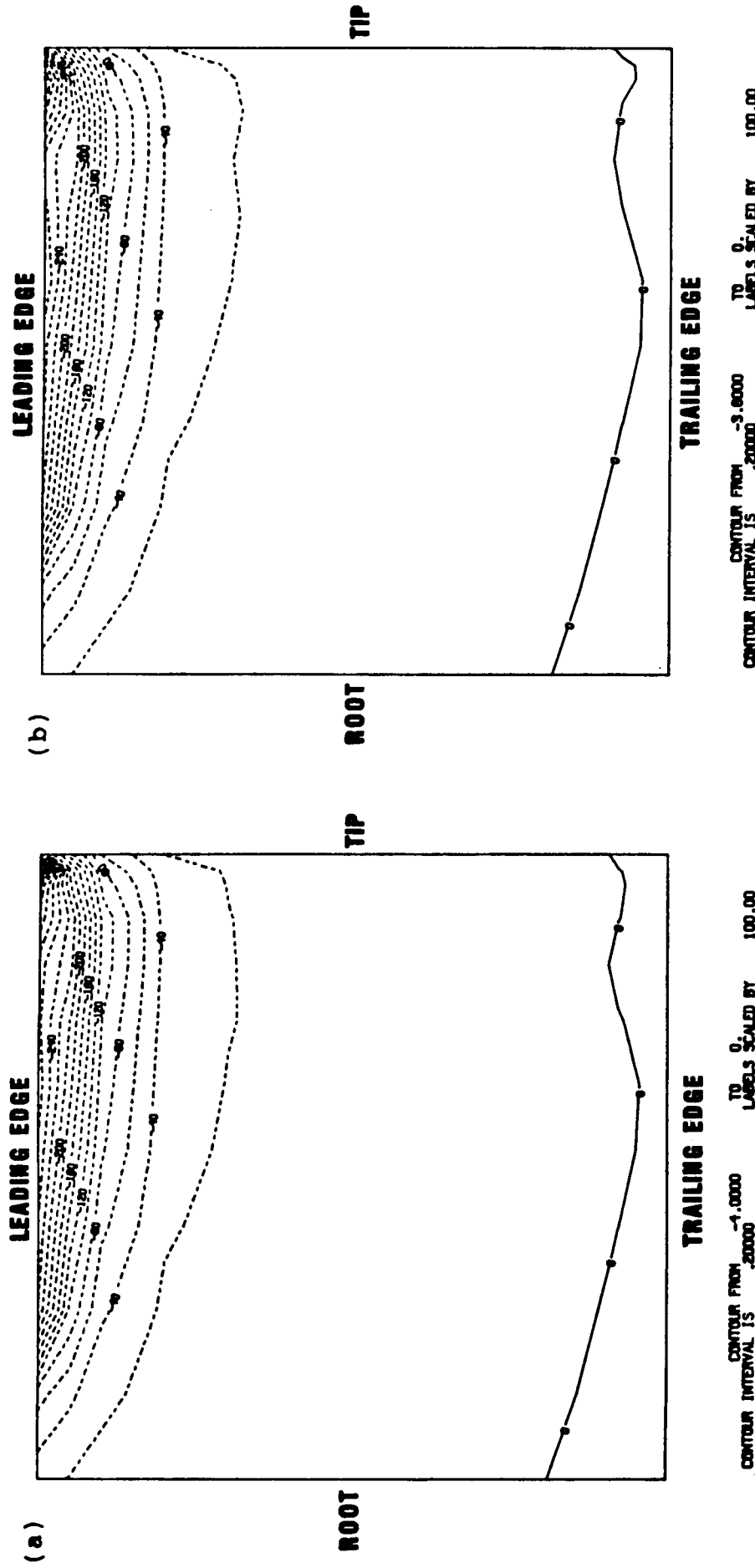


Figure 20. (a) Loading pressure contours of the unsteady data outside of the wake on the top surface of the SR-2 blade. Case 3.
 (b) Contours of the loading pressure generated by the spline fit of the unsteady data outside of the wake on the top surface of the SR-2 blade. Case 3.

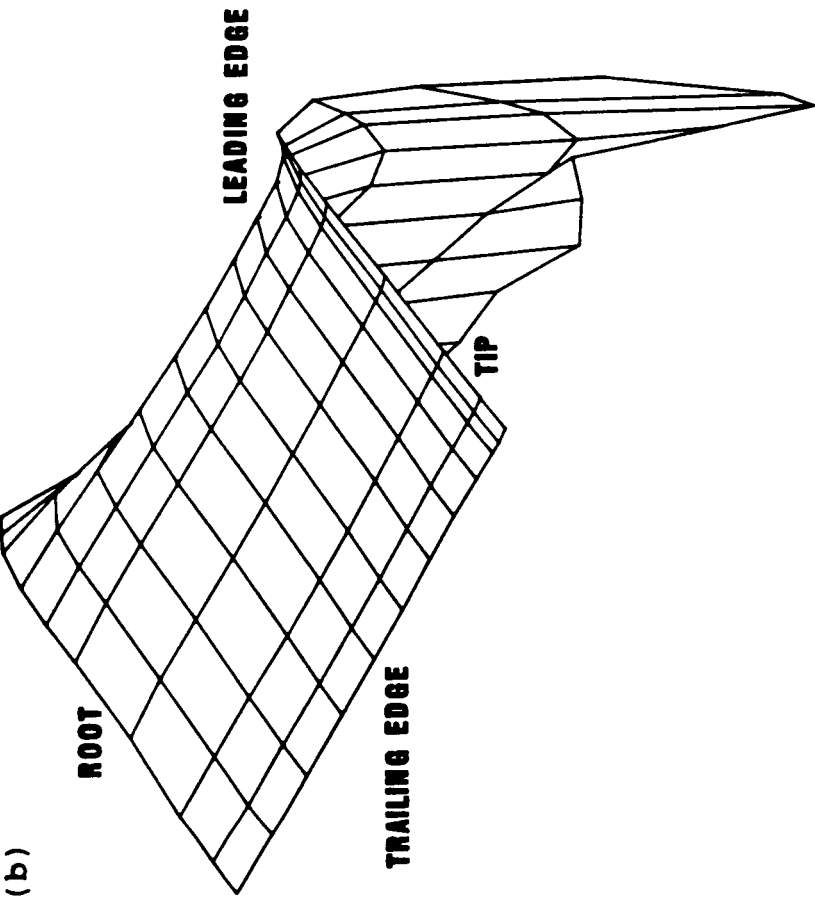
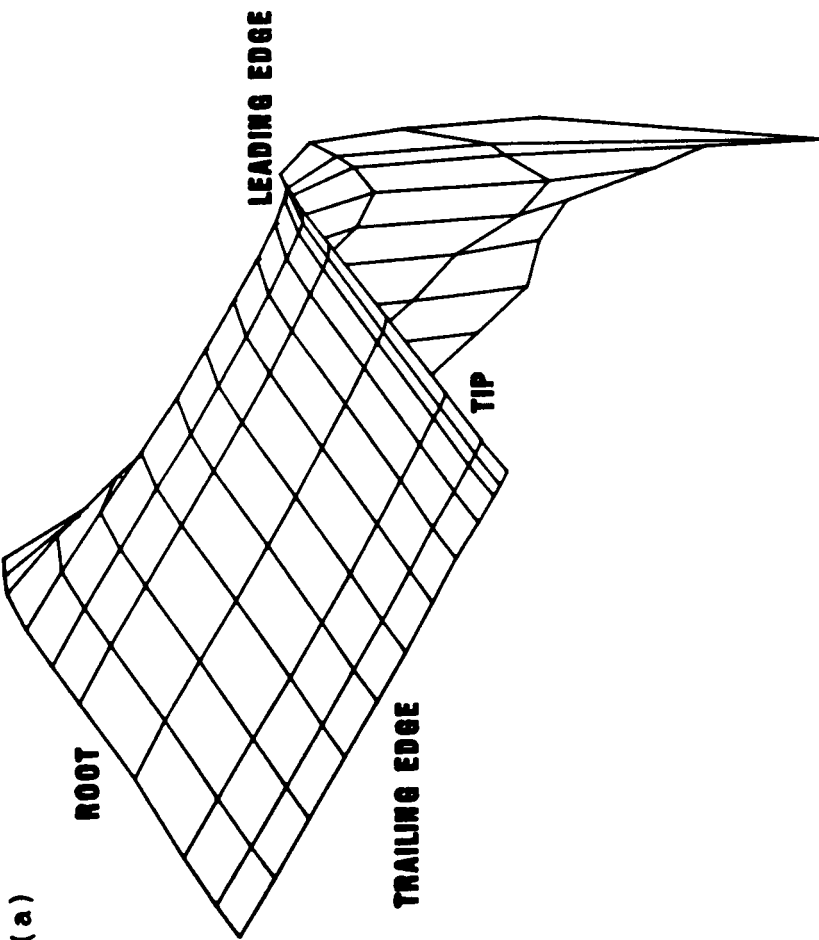


Figure 21. (a) Three dimensional projection of the unsteady loading pressure data outside of the wake on the top surface of the SR-2 blade. Case 3.

(b) Three dimensional projection of the spline fit of the unsteady loading pressure data outside of the wake on the top surface of the SR-2 blade. Case 3.

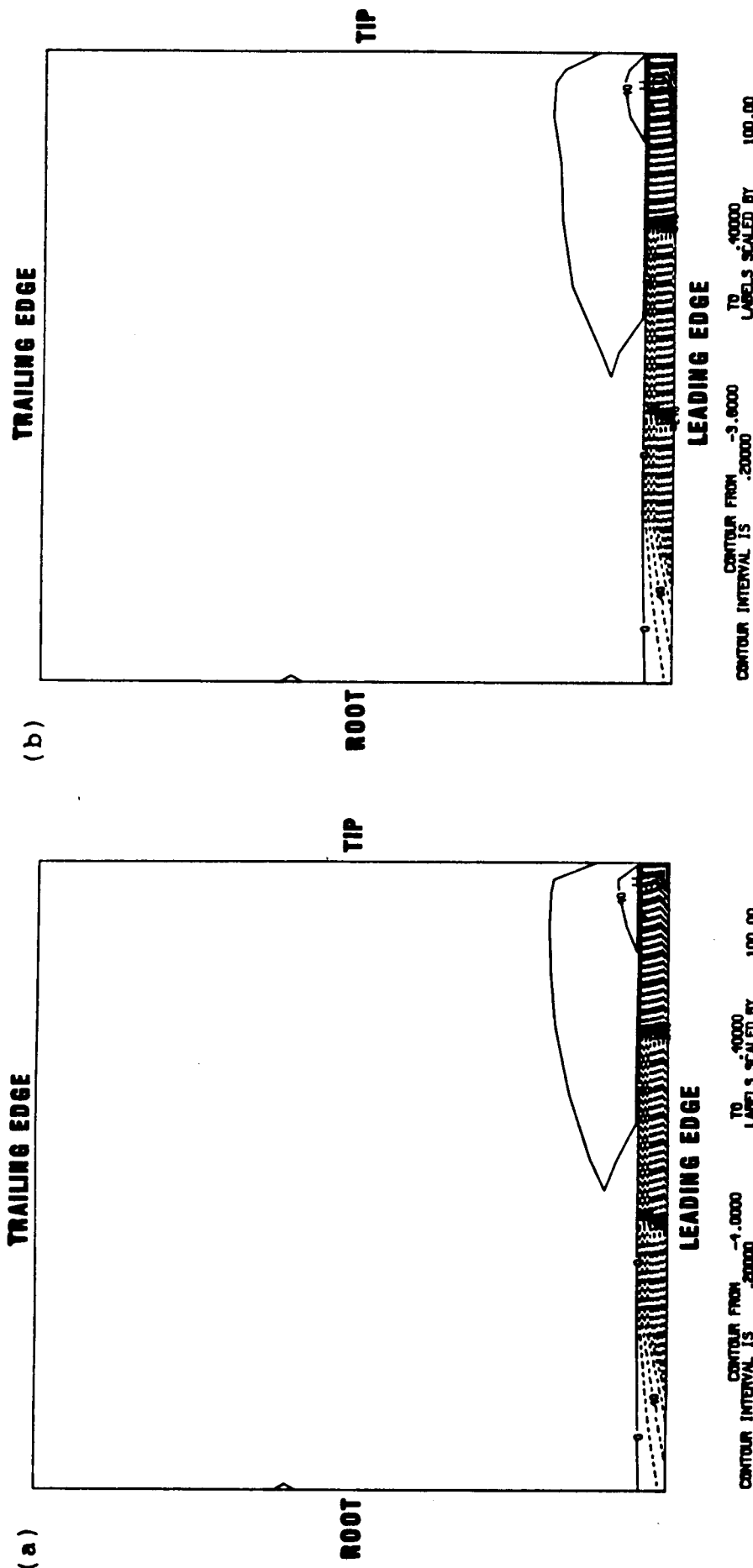


Figure 22. (a) Loading pressure contours of the unsteady data outside of the wake on the bottom surface of the SR-2 blade. Case 3.
 (b) Contours of the loading pressure generated by the spline fit of the unsteady data outside of the wake on the bottom surface of the SR-2 blade. Case 3.

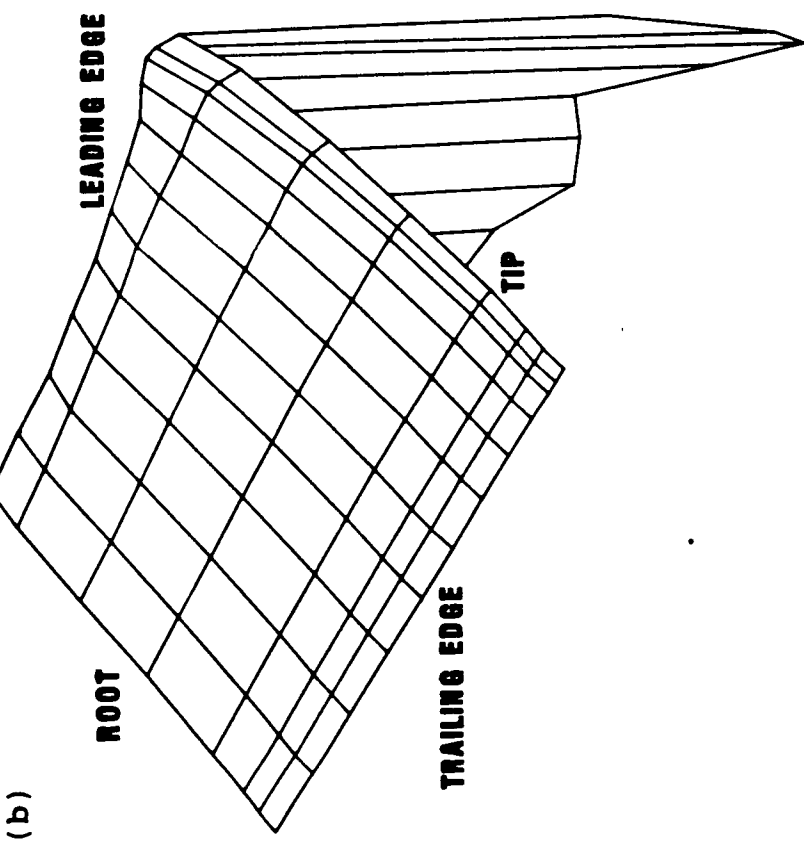
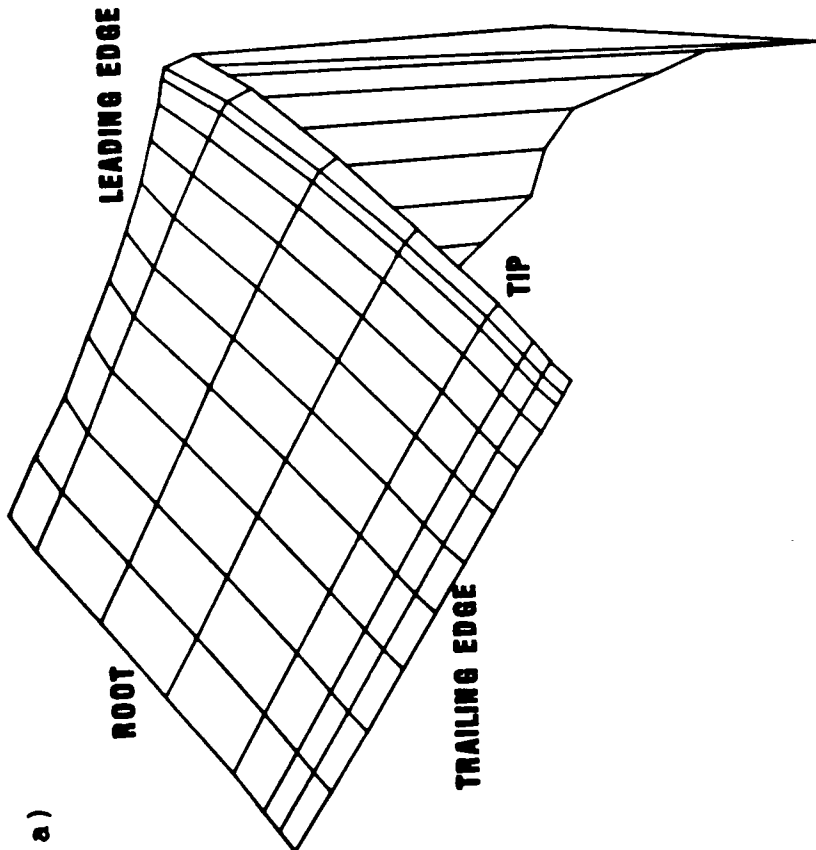


Figure 23. (a) Three dimensional projection of the unsteady loading pressure data outside of the wake on the bottom surface of the SR-2 blade. Case 3.
 (b) Three dimensional projection of the spline fit of the unsteady loading pressure data outside of the wake on the bottom surface of the SR-2 blade. Case 3.

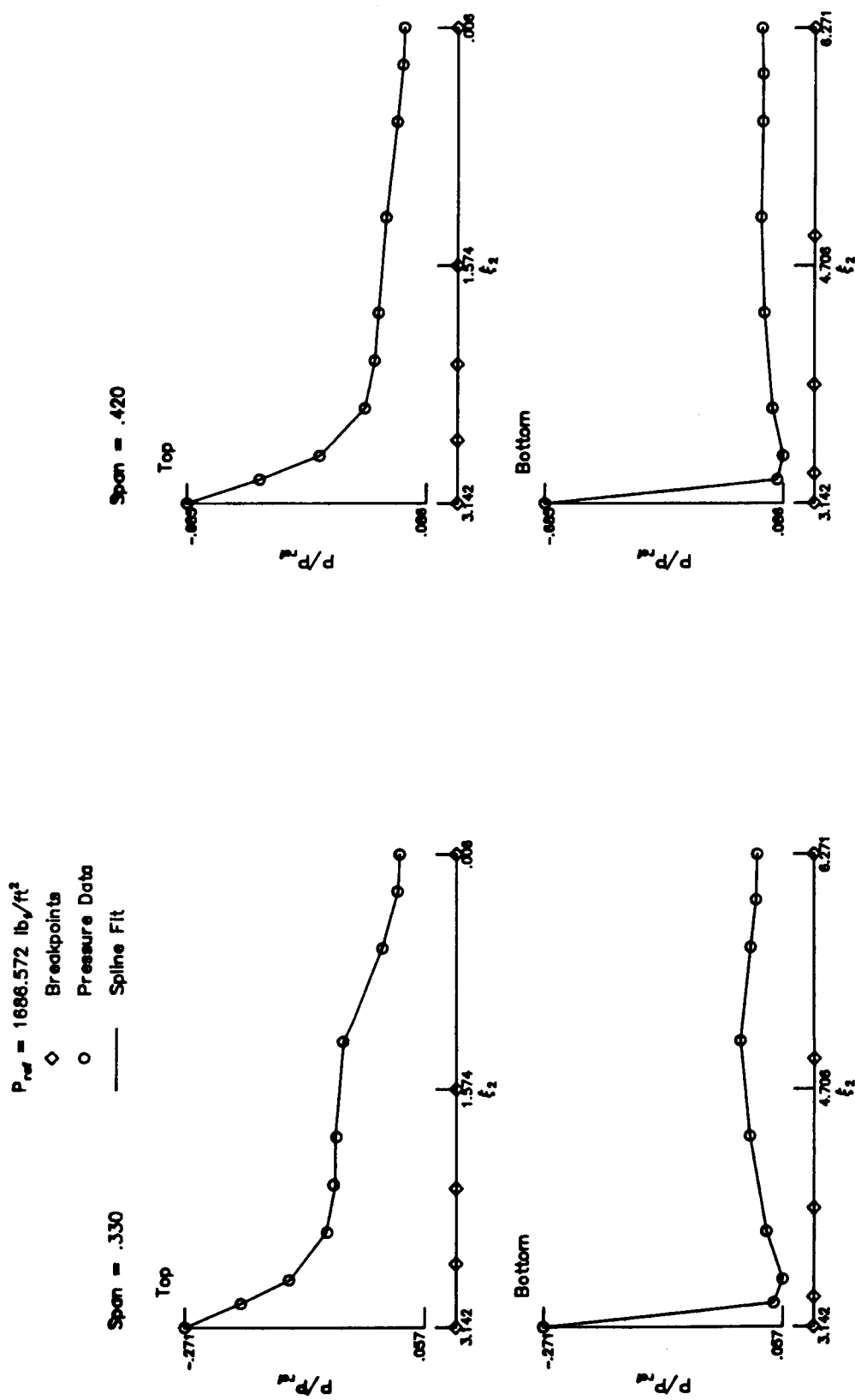
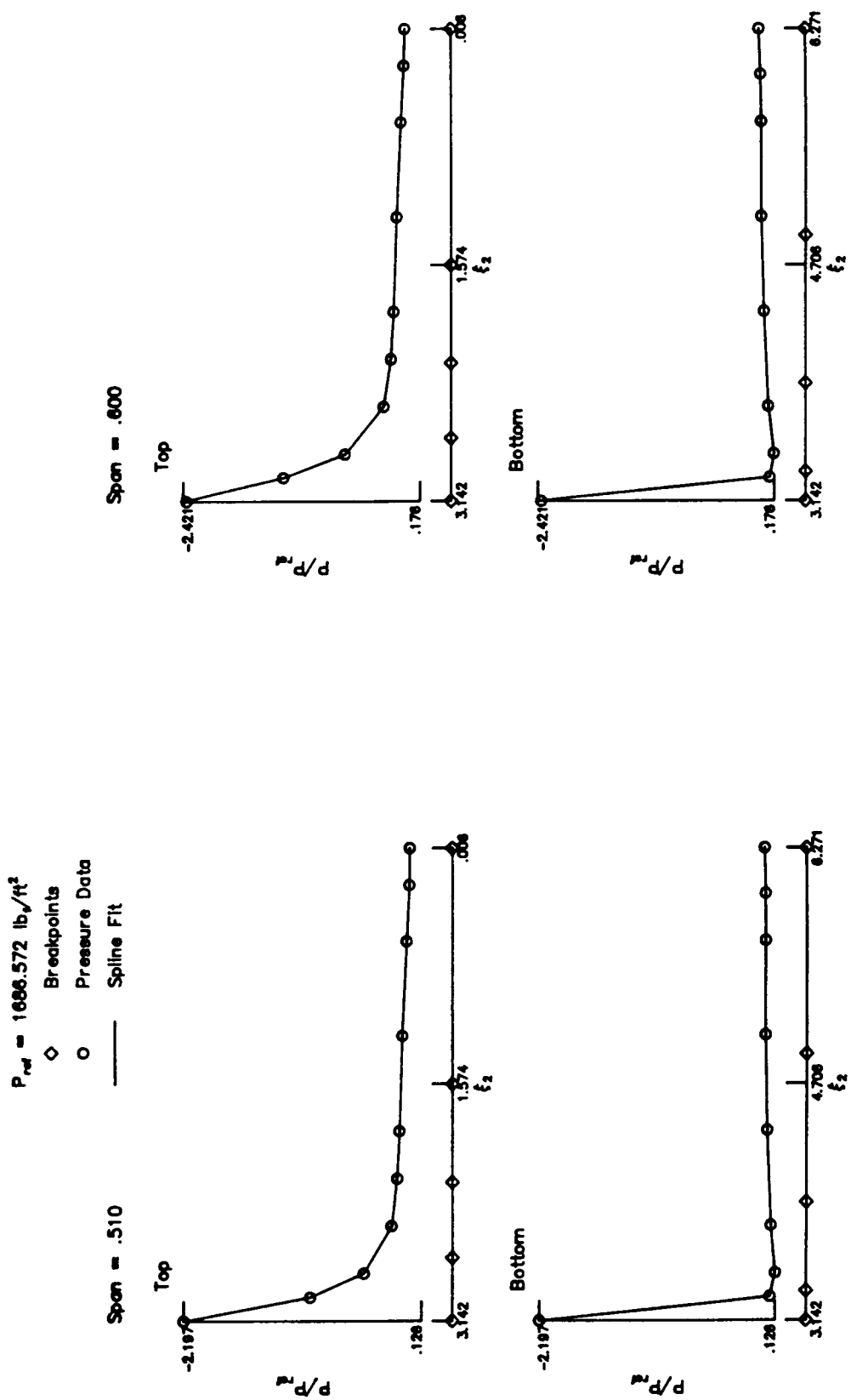


Figure 24. Span sections of the SR-2 blade comparing the unsteady loading pressure data outside of the wake with the spline fit. Case 3.

Figure 24. Continued.



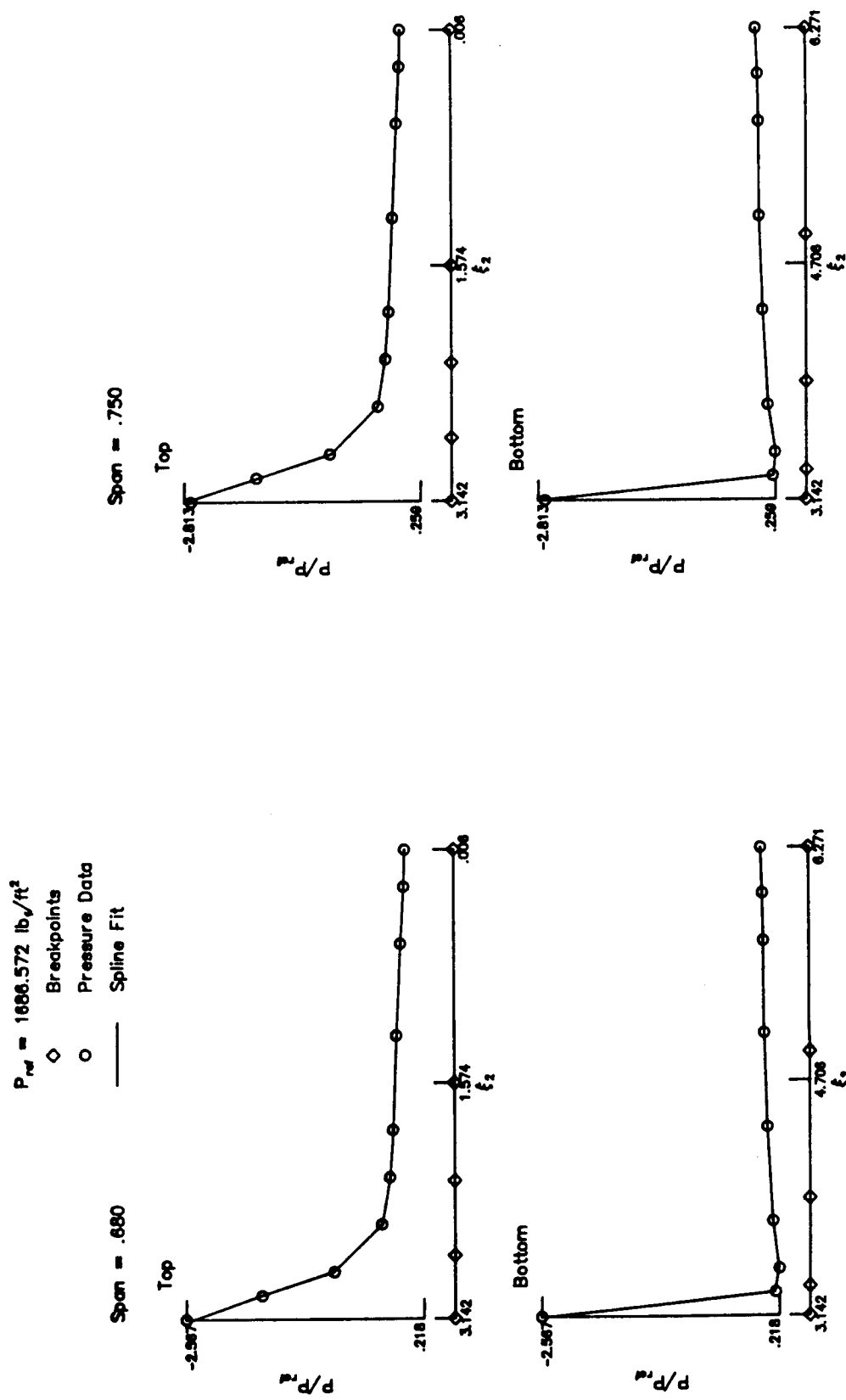


Figure 24. Continued.

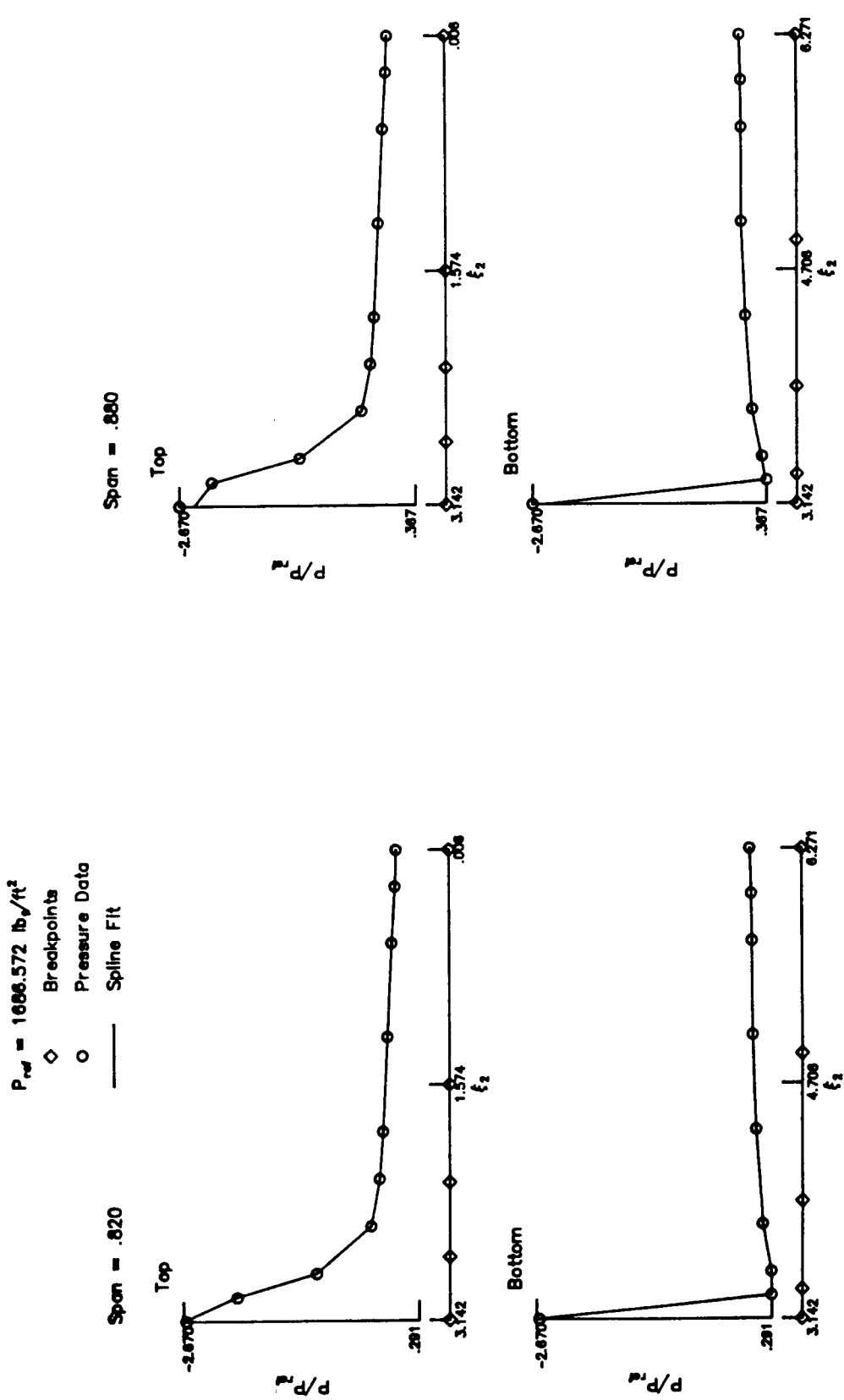
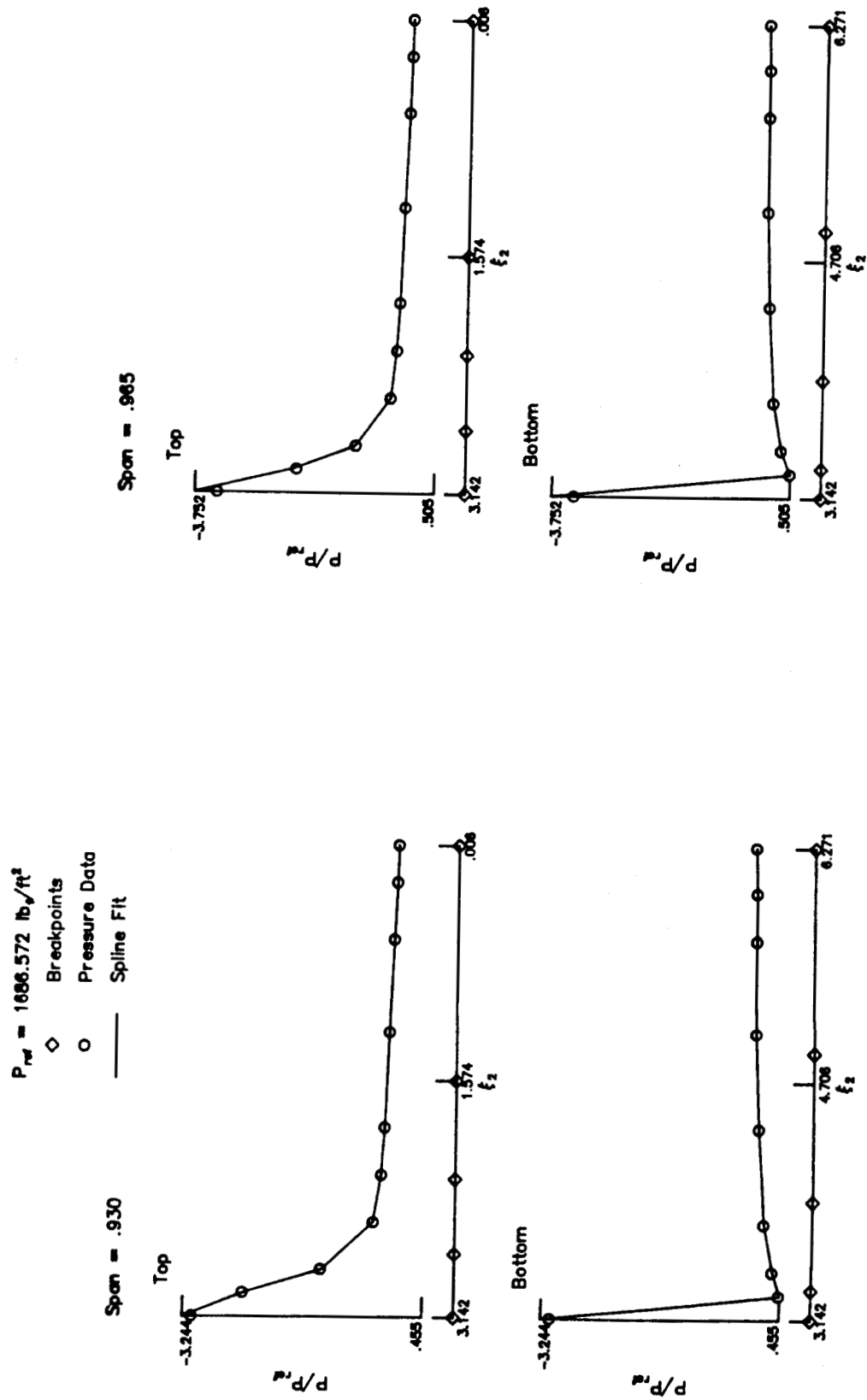


Figure 24. Continued.

Figure 24. Continued.



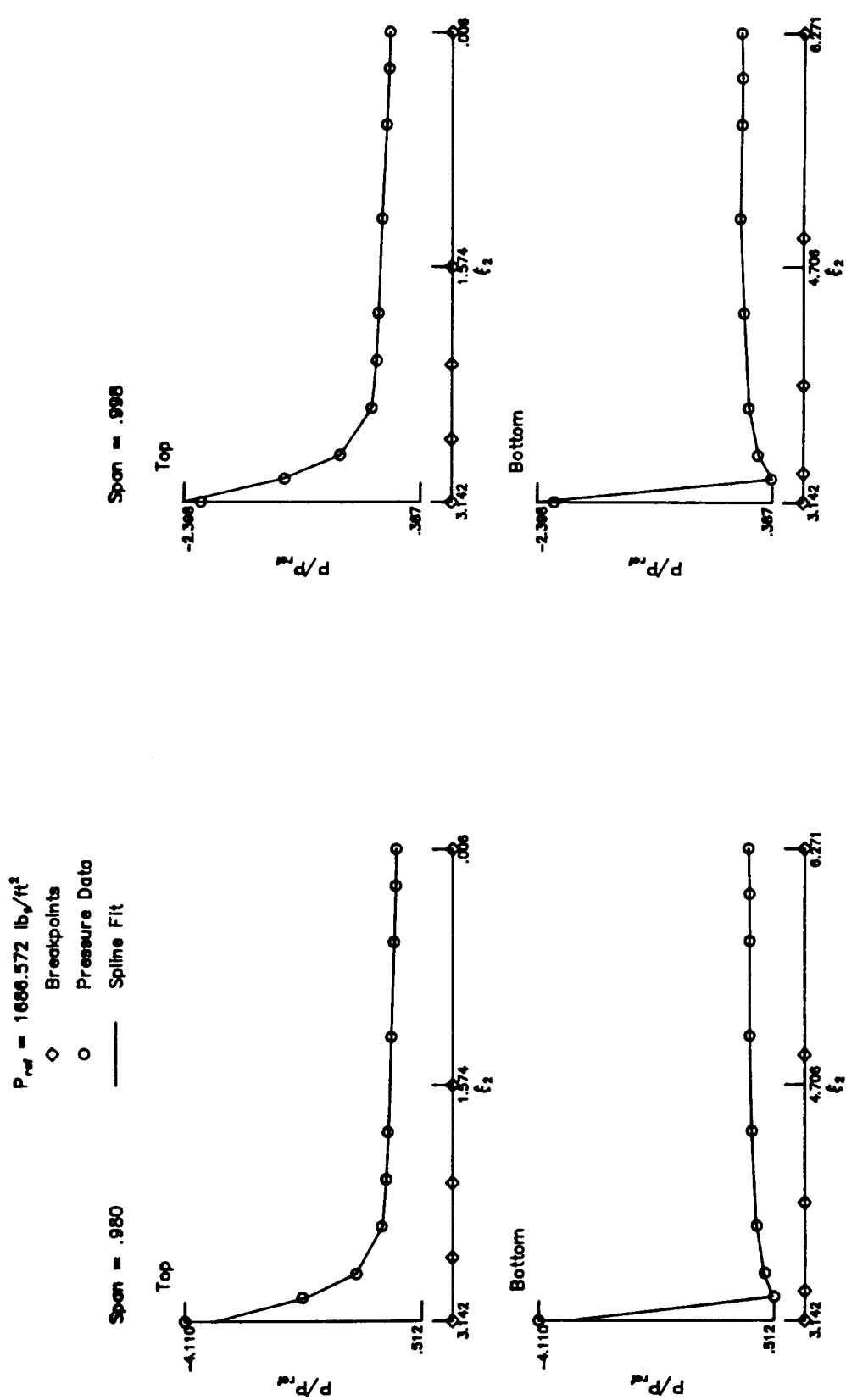


Figure 24. Continued.

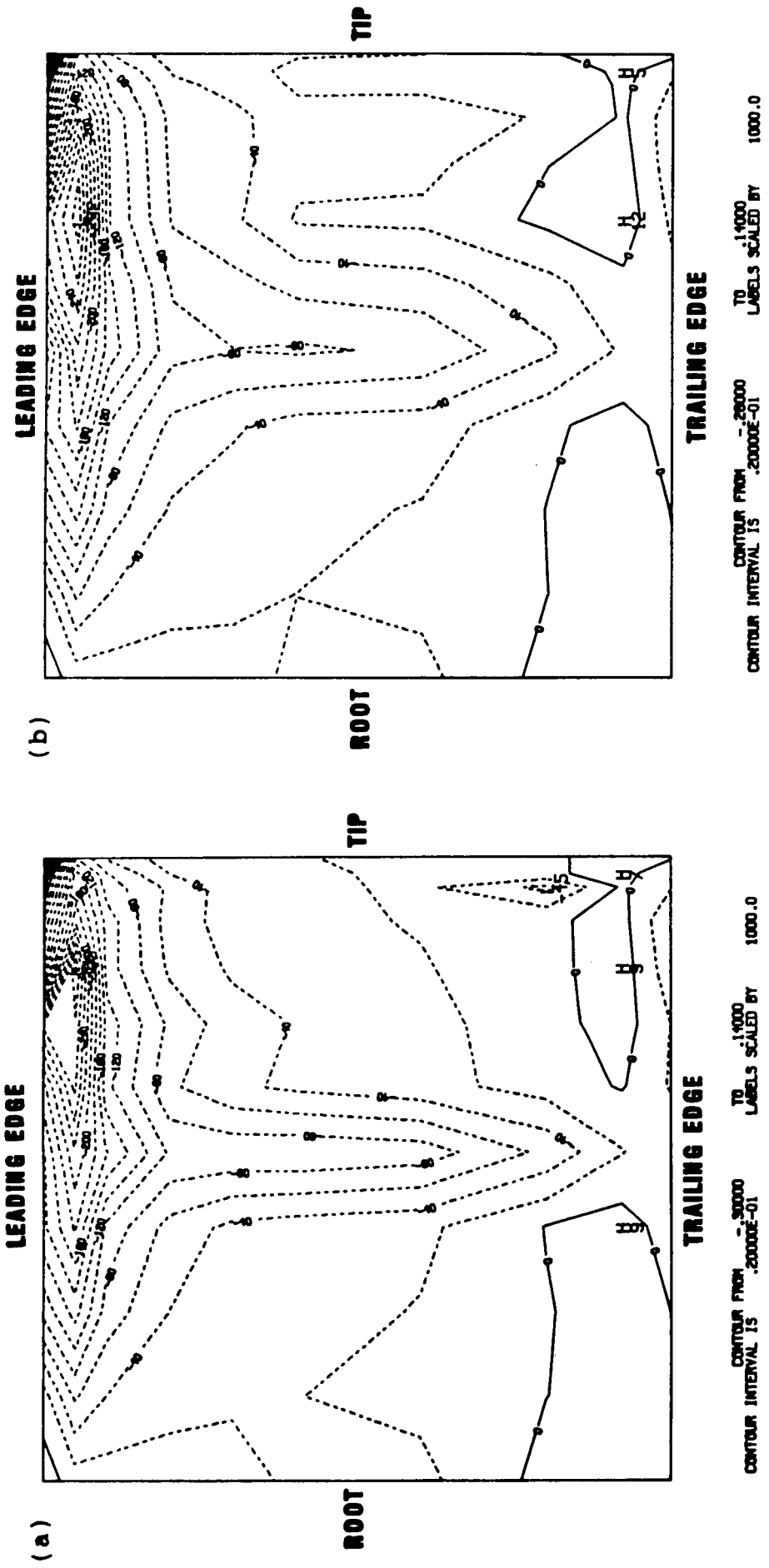
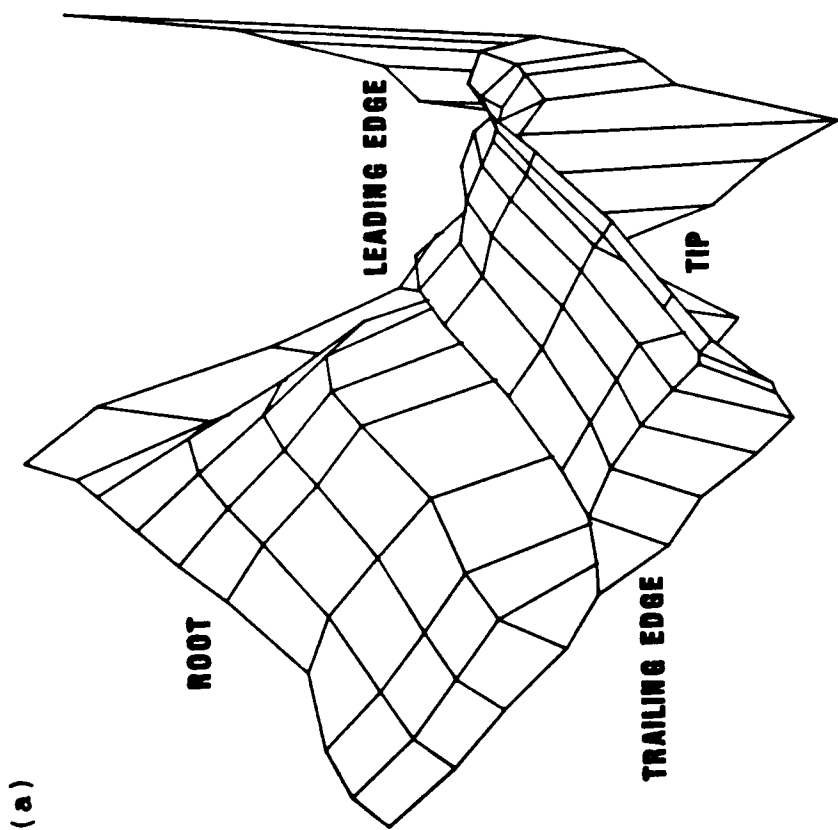


Figure 25. (a) Loading pressure contours of the unsteady data at the center of the wake on the top surface of the SR-2 blade. Case 3.
 (b) Contours of the loading pressure generated by the spline fit of the unsteady data at the center of the wake on the top surface of the SR-2 blade. Case 3.



(b)

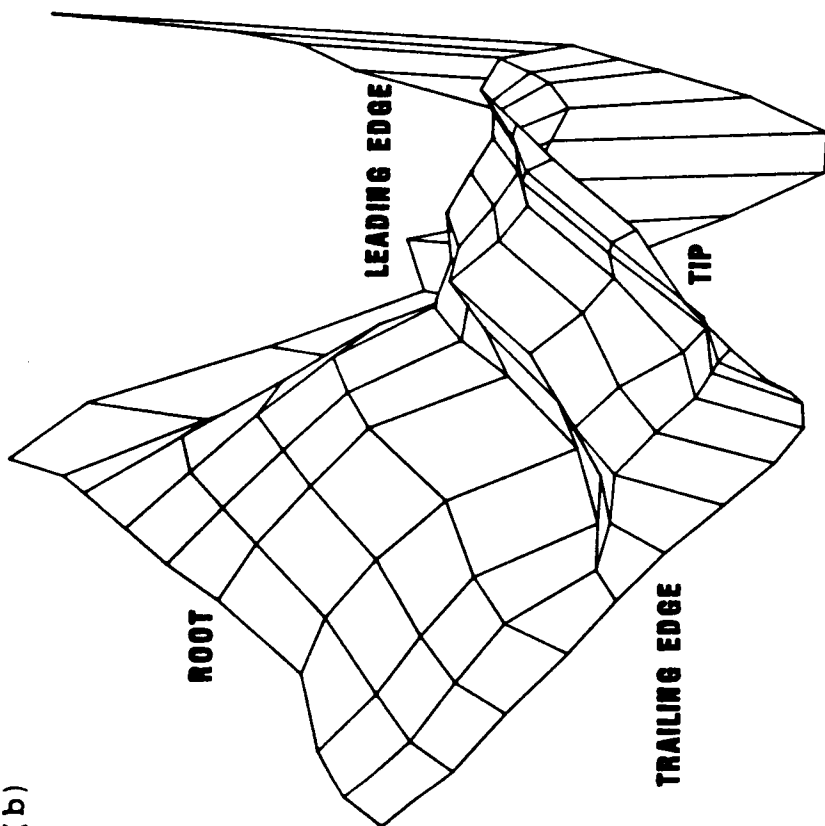


Figure 26. (a) Three dimensional projection of the unsteady loading pressure data at the center of the wake on the top surface of the SR-2 blade. Case 3.

(b) Three dimensional projection of the spline fit of the unsteady loading pressure data at the center of the wake on the top surface of the SR-2 blade. Case 3.

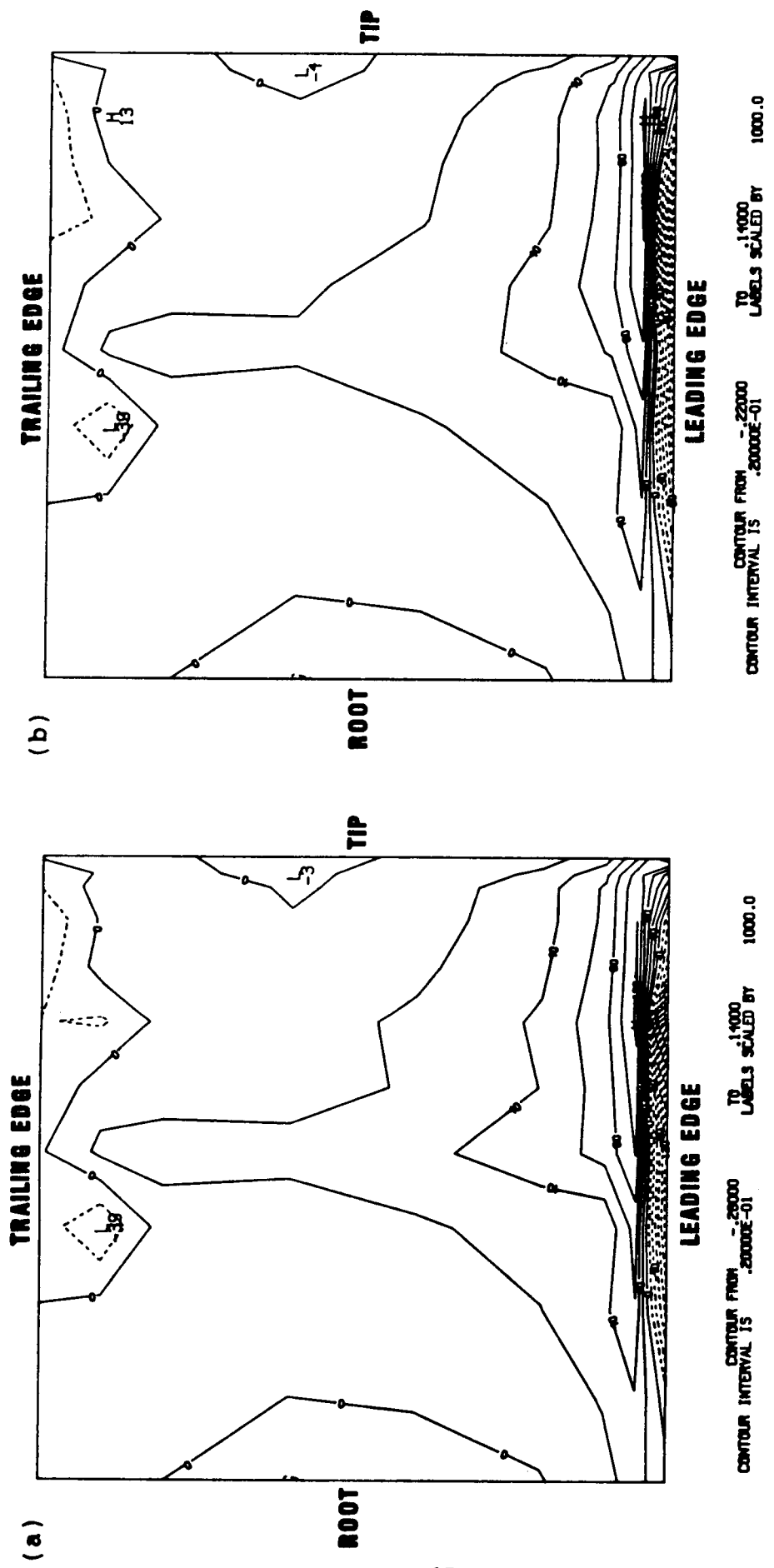


Figure 27. (a) Loading pressure contours of the unsteady data at the center the wake on the bottom surface of the SR-2 blade. Case 3.
 (b) Contours of the loading pressure generated by the spline fit of the unsteady data at the center of the wake on the bottom surface of the SR-2 blade. Case 3.

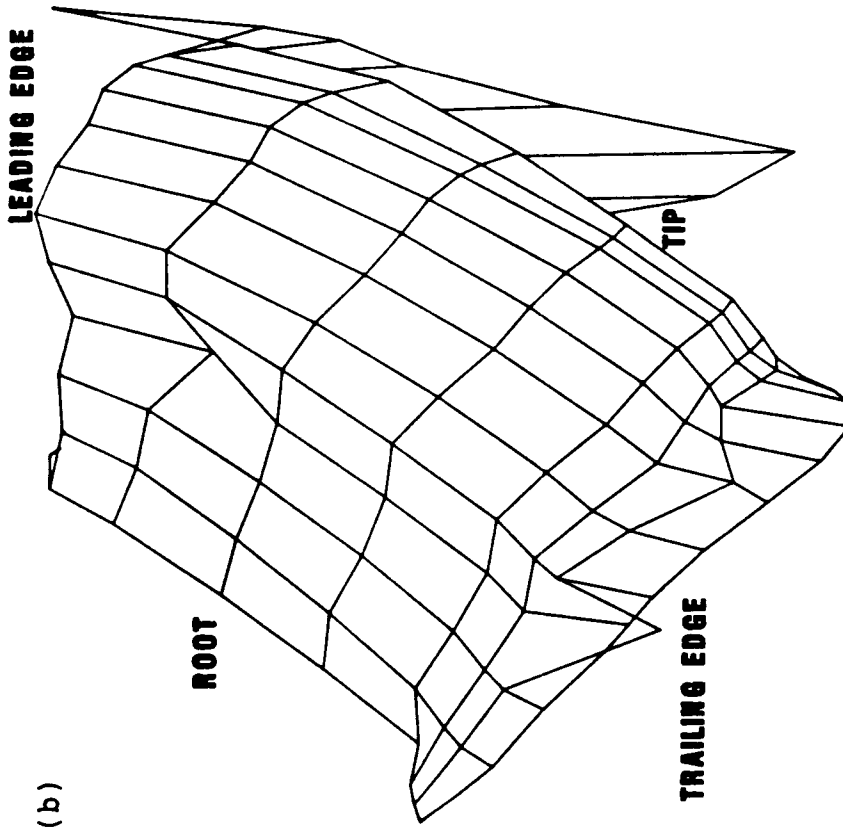
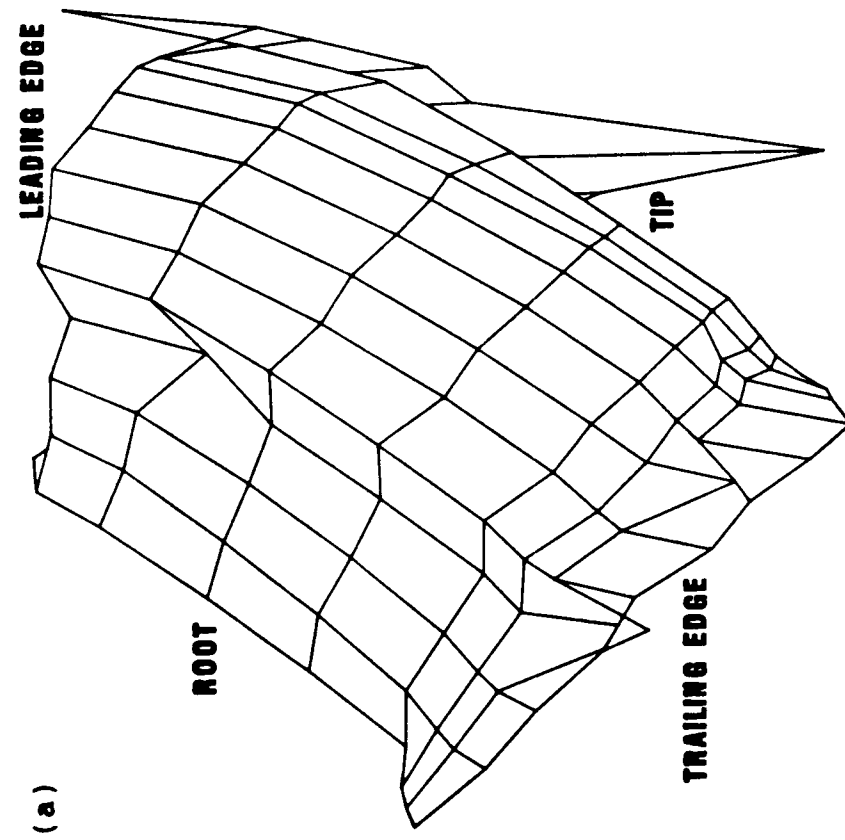


Figure 28. (a) Three dimensional projection of the unsteady loading pressure data at the center of the wake on the bottom surface of the SR-2 blade. Case 3.
 (b) Three dimensional projection of the spline fit of the unsteady loading pressure data at the center of the wake on the bottom surface of the SR-2 blade. Case 3.

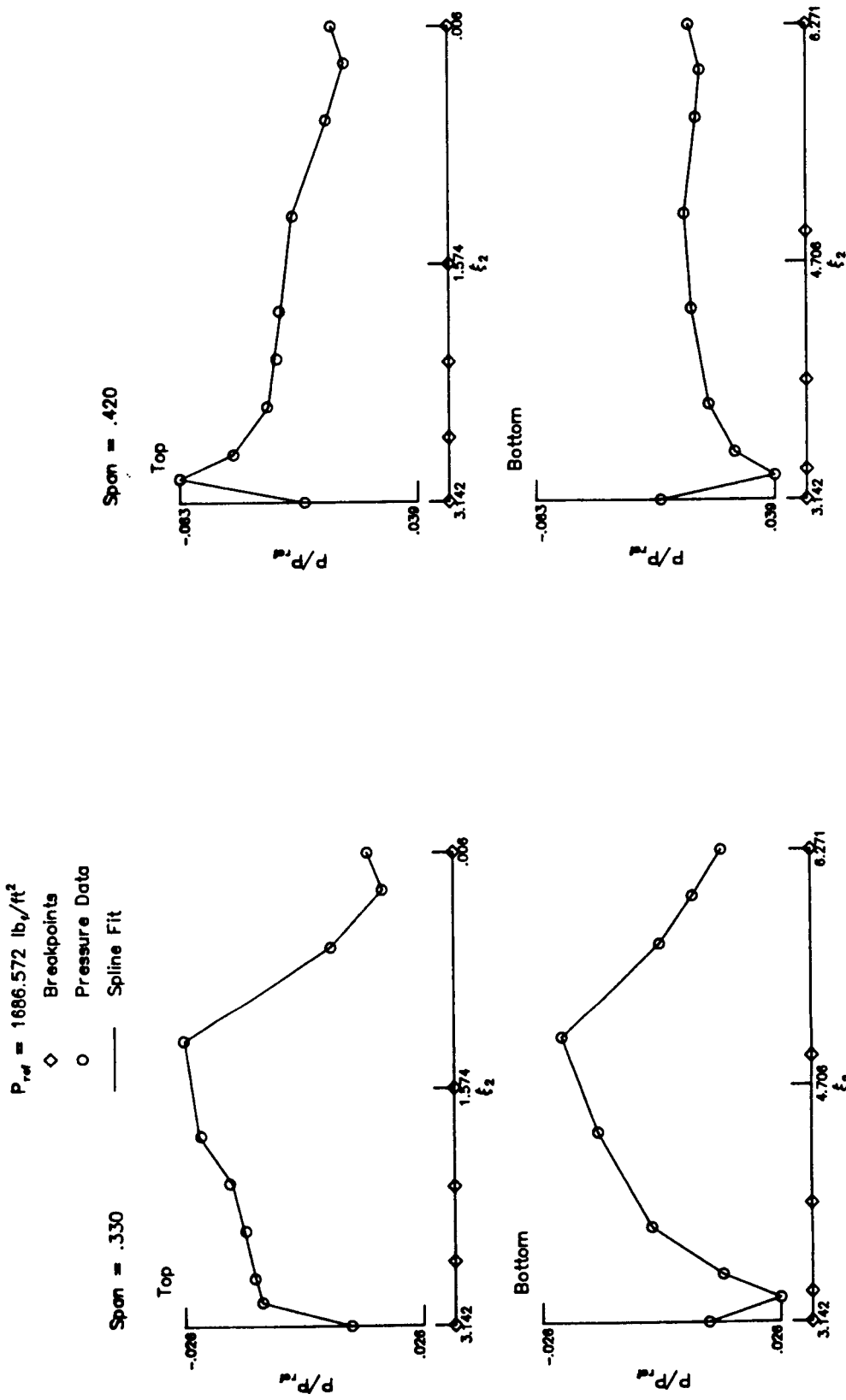
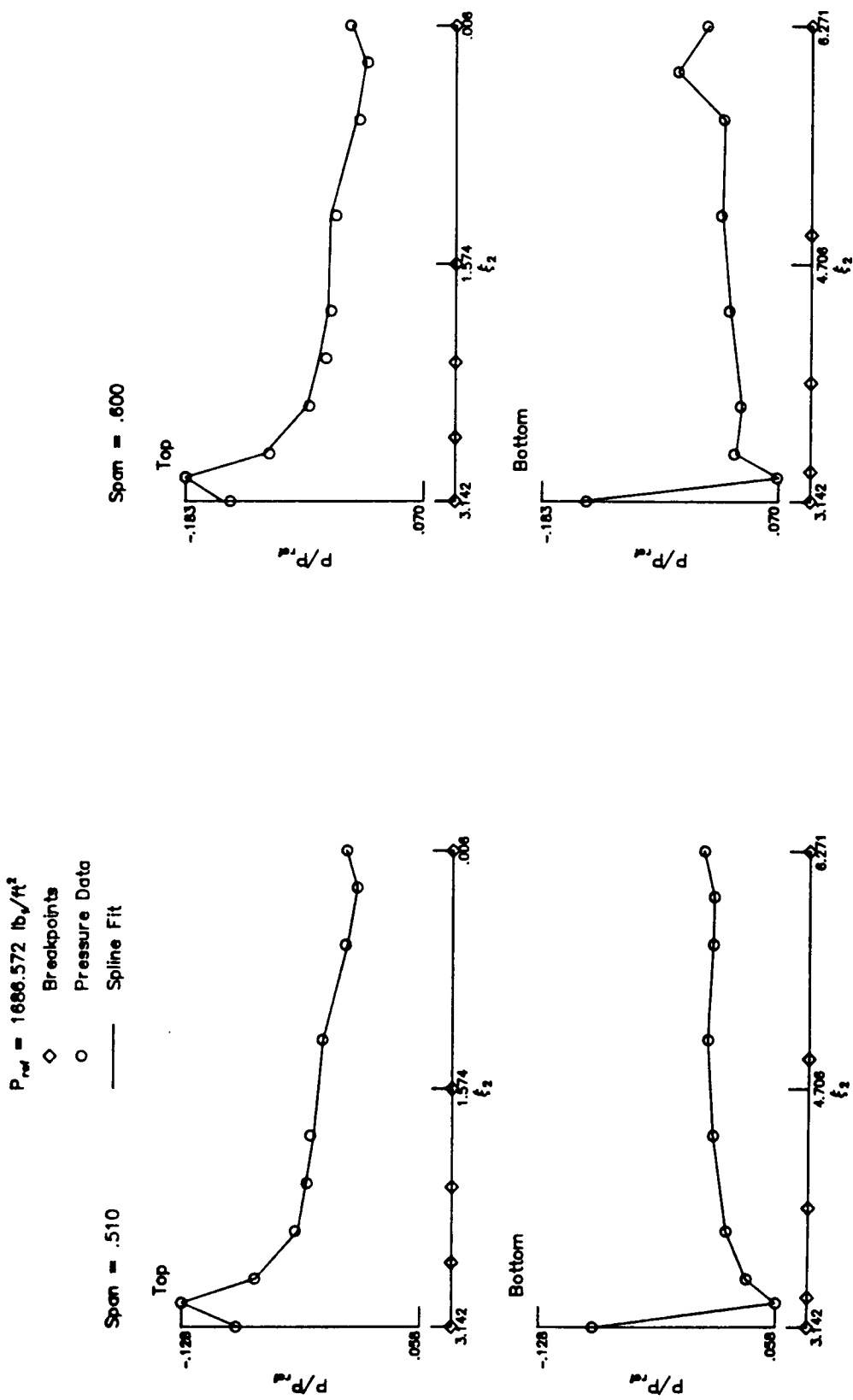


Figure 29. Span sections of the SR-2 blade comparing the unsteady loading pressure data at the center of the wake with the spline fit. Case 3.

Figure 29. Continued.



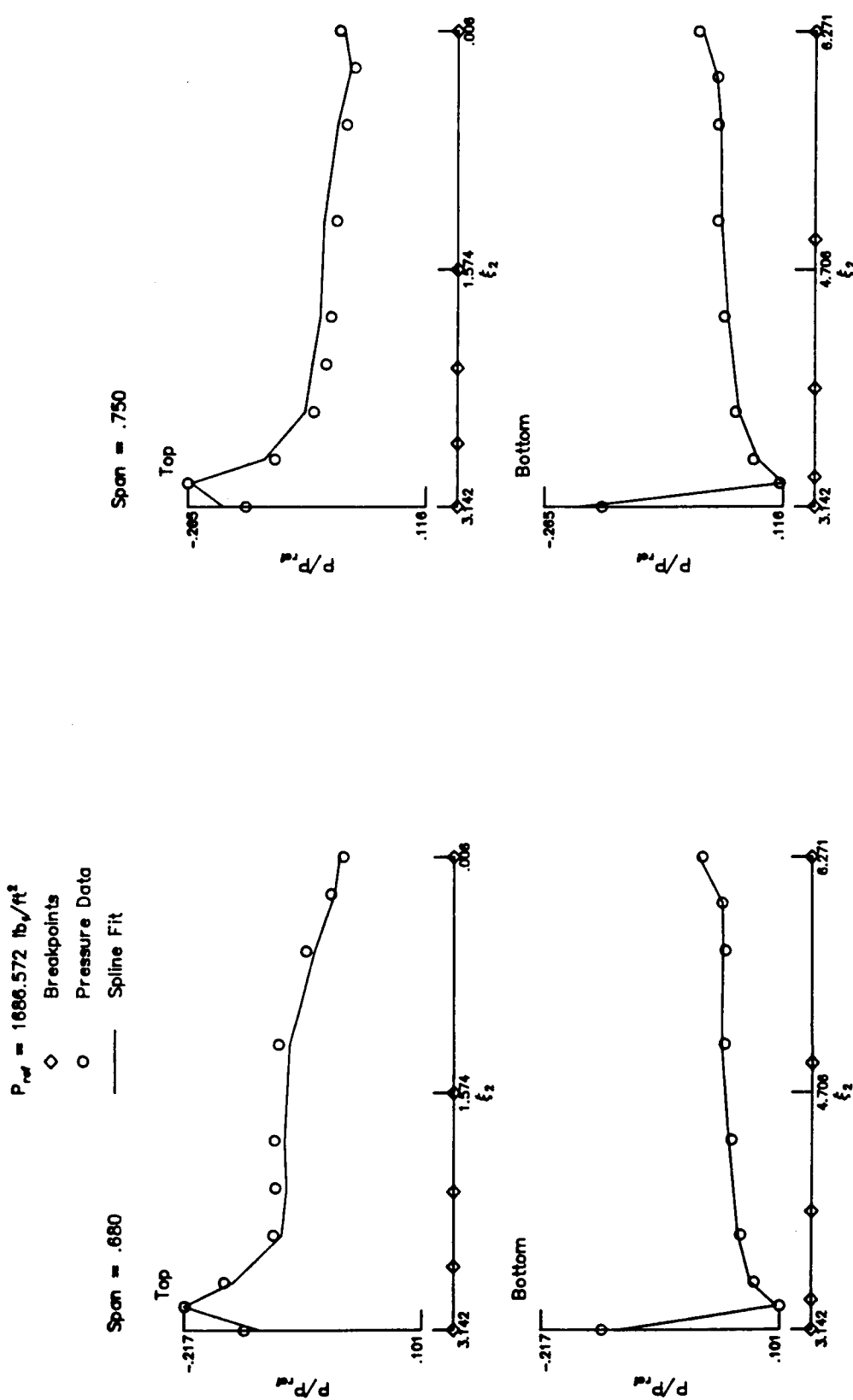
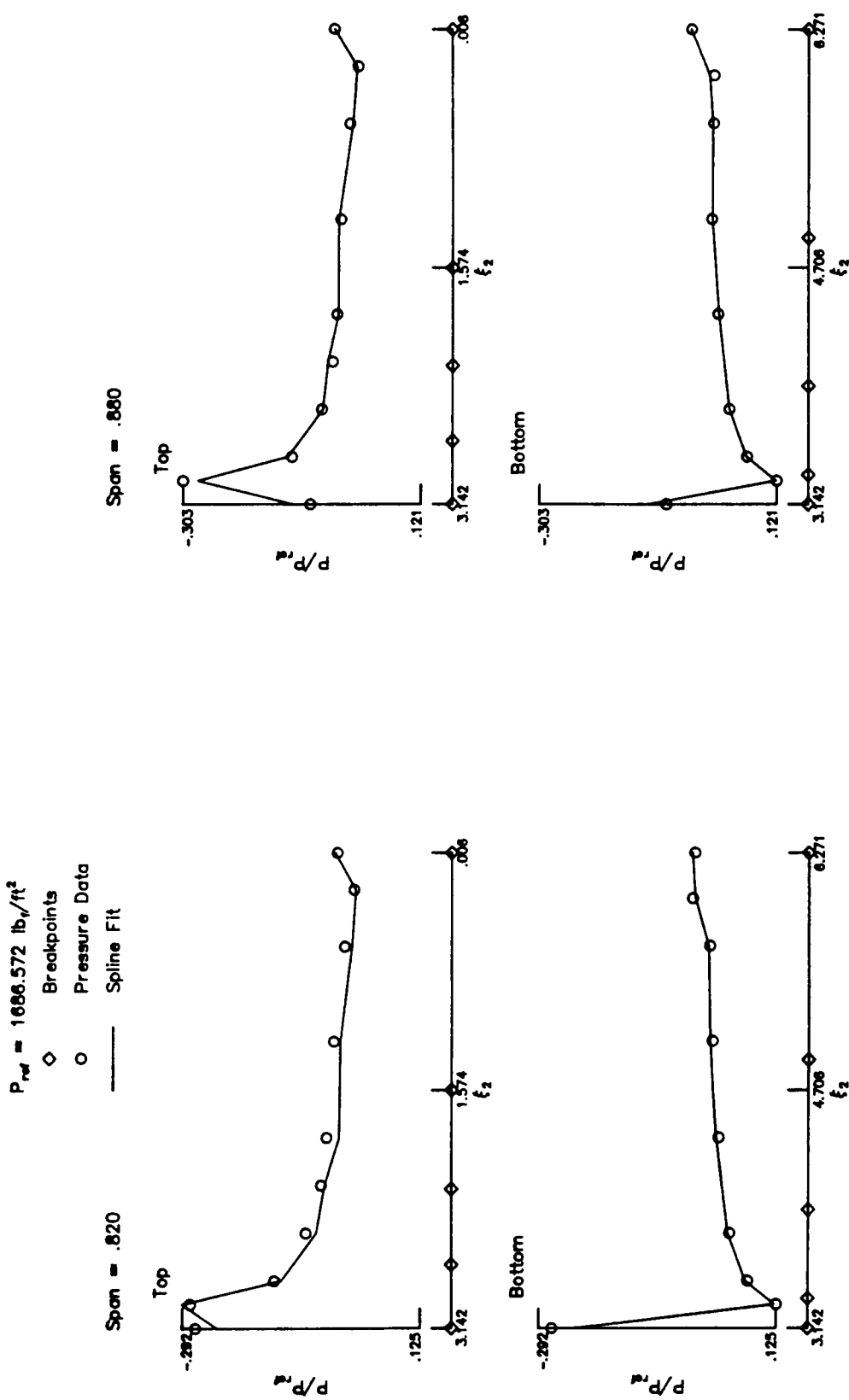


Figure 29. Continued.

Figure 29. Continued.



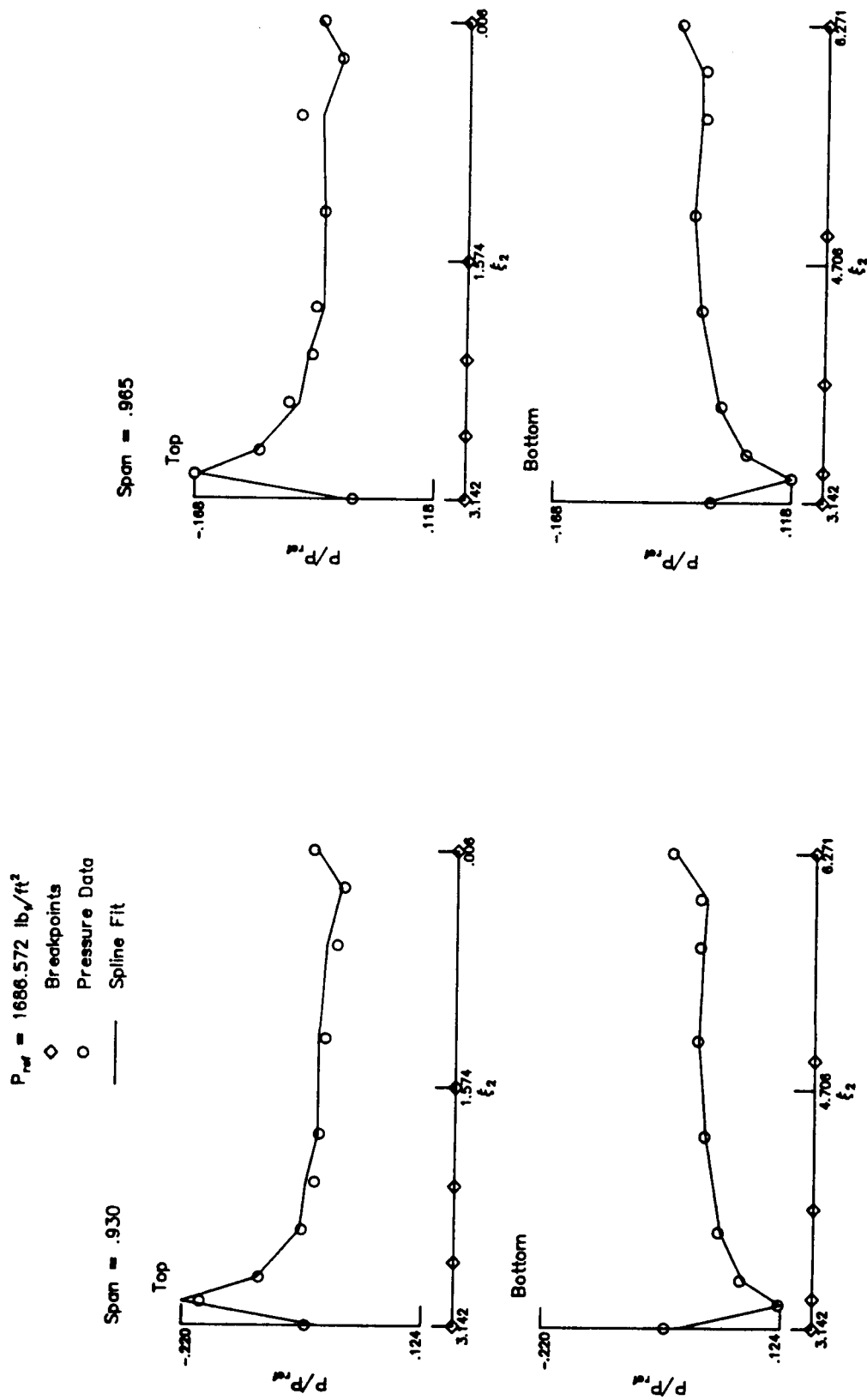


Figure 29. Continued.

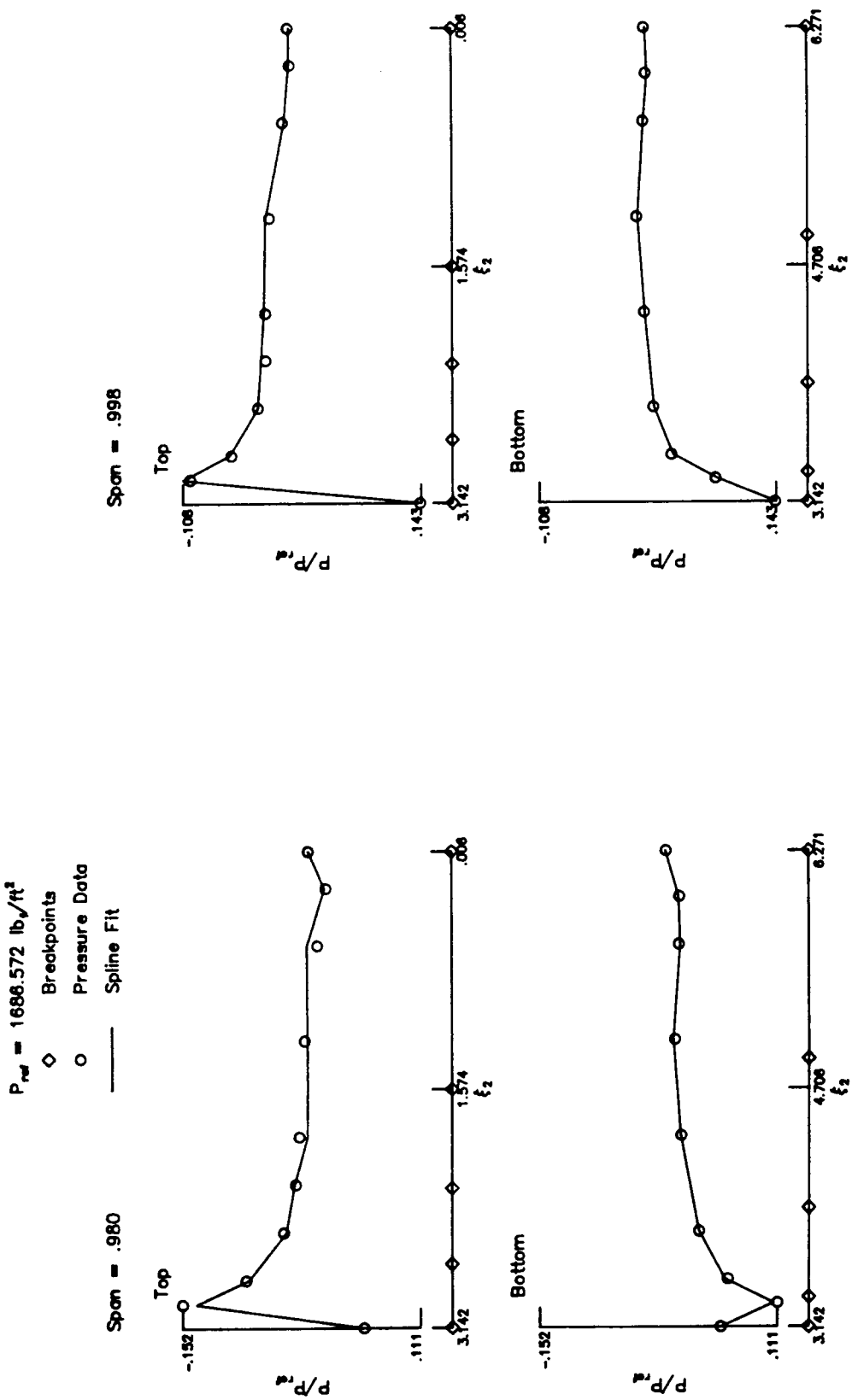


Figure 29. Continued.

$M_T = .79$ $M_\infty = .40$

FORMULATION 3
SPN/TDN

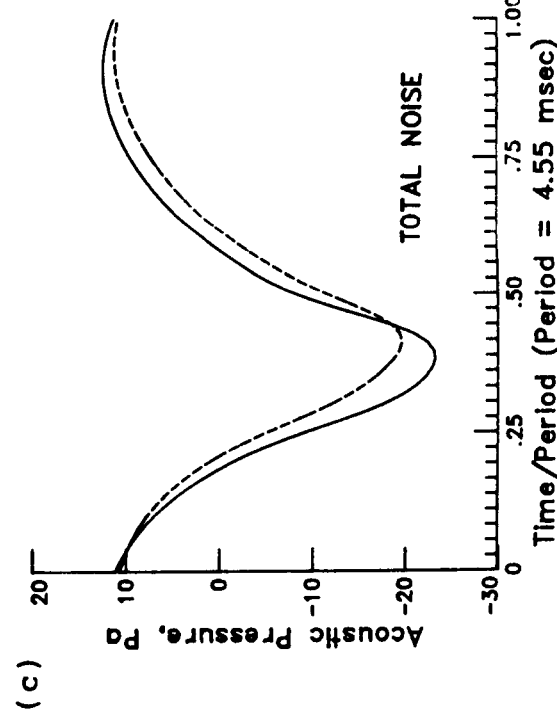
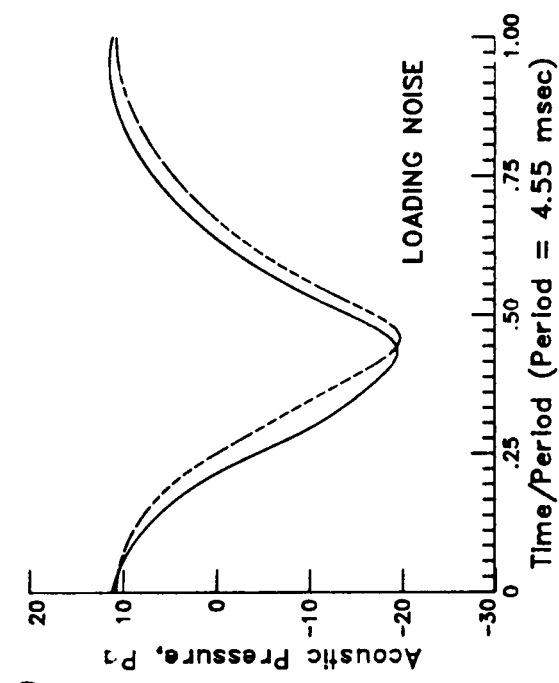
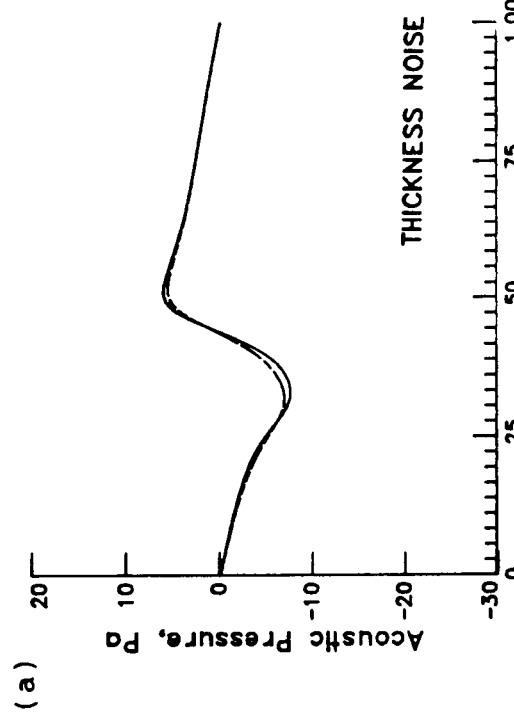


Figure 30. Comparison between Formulation 3 and SPN of the resultant acoustic pressure for the subsonic conditions of Case 1.
(a) Thickness noise. (b) Loading noise.
(c) Total noise.

$M_T = .79$ $M_\infty = .40$

○ FORMULATION 3
□ SPN/TPN

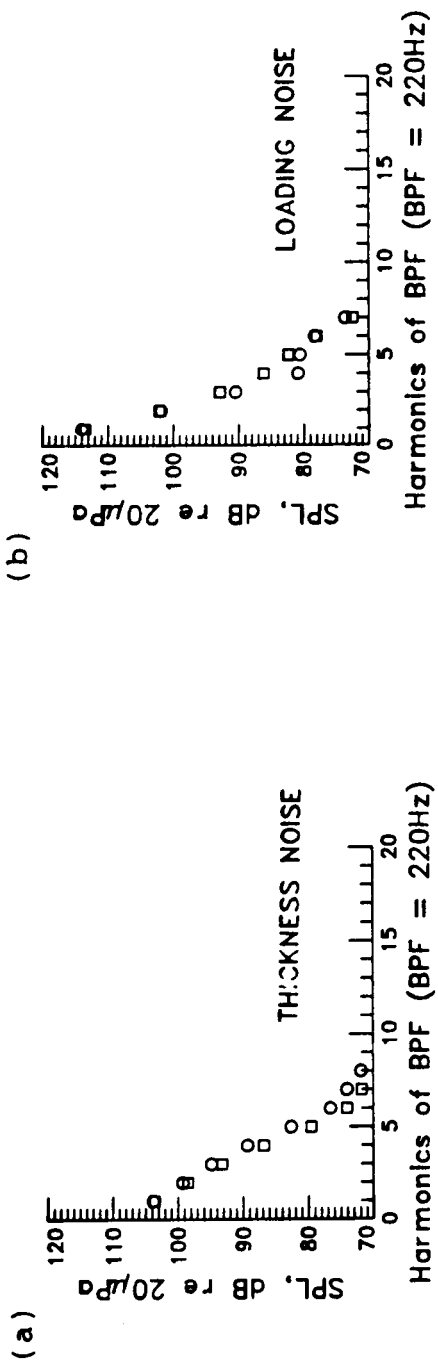


Figure 31. Comparison between Formulation 3 and SPN of the resultant noise spectra for the subsonic conditions of Case 1.
 (a) Thickness noise. (b) Loading noise.
 (c) Total noise.

$M_r = .79$ $M_\infty = .72$

FORMULATION 3
SPN /TPN

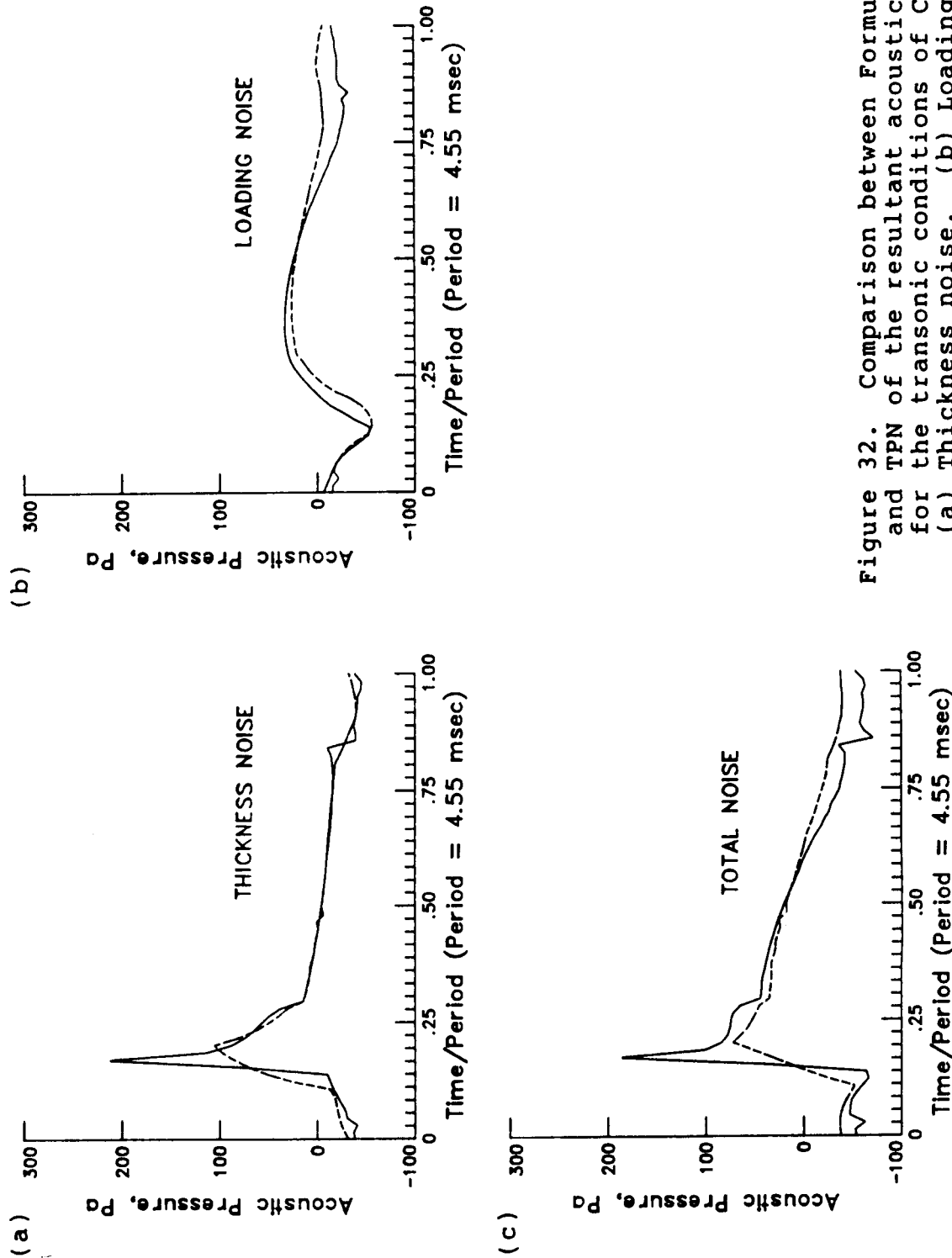


Figure 32. Comparison between Formulation 3 and TPN of the resultant acoustic pressure for the transonic conditions of Case 2.
(a) Thickness noise. (b) Loading noise.
(c) Total noise.

$$M_1 = .79 \quad M_\infty = .72$$

○ FORMULATION 3
□ SPN/TPN

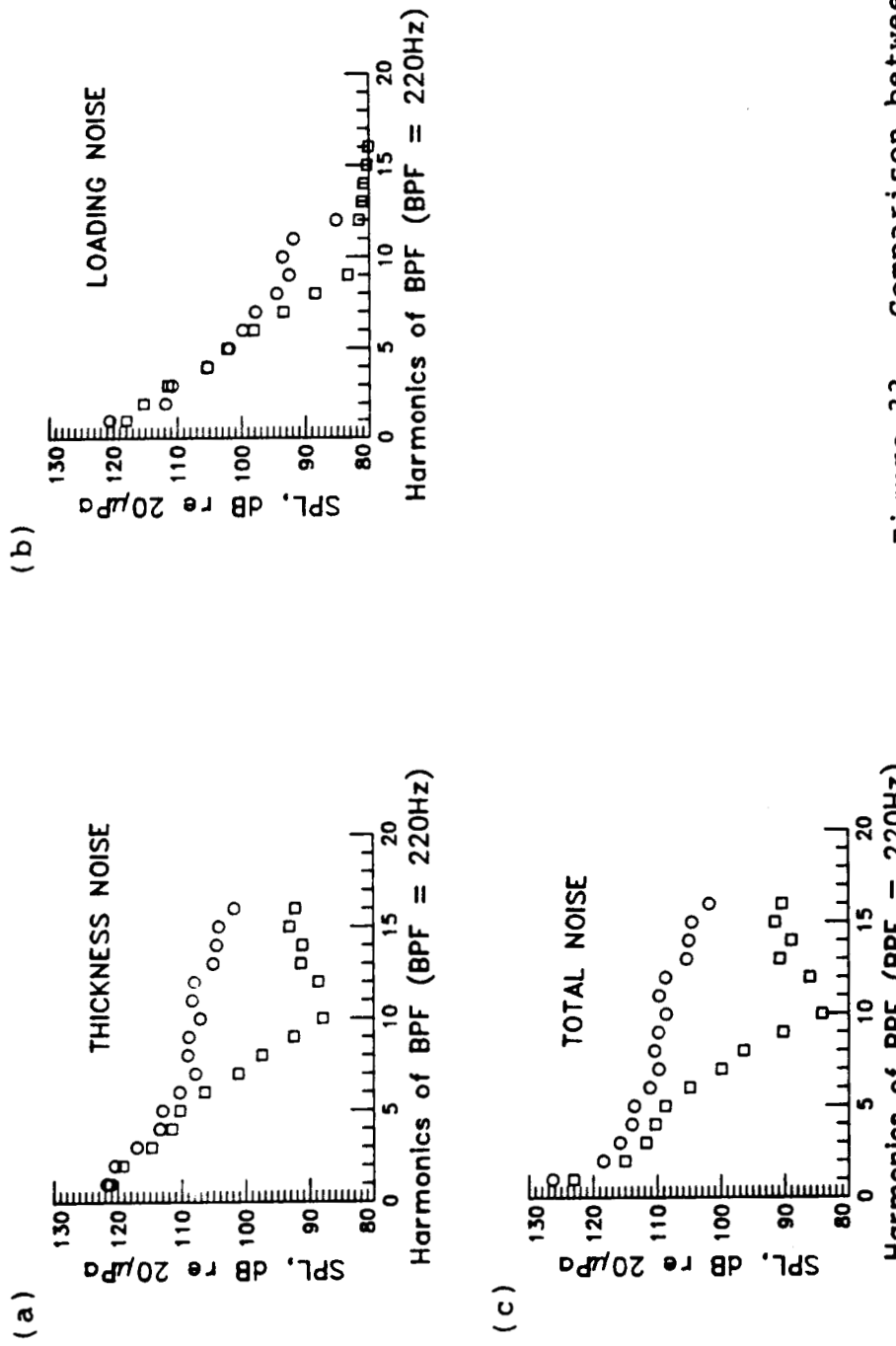


Figure 33. Comparison between Formulation 3 and TPN of the resultant noise spectra for the transonic conditions of Case 2.
 (a) Thickness noise. (b) Loading noise.
 (c) Total noise.

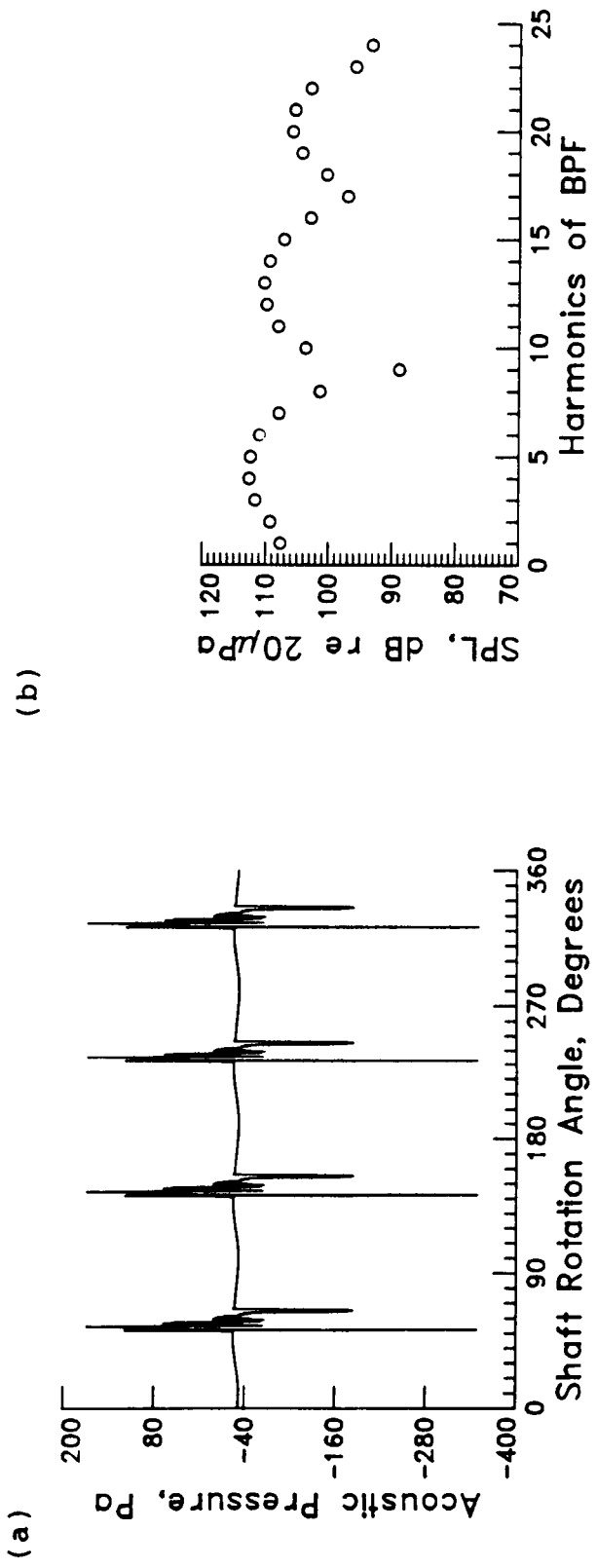


Figure 34. Subsonic results of the unsteady conditions of Case 3.
 (a) Total acoustic pressure signature.
 (b) Total noise spectrum.

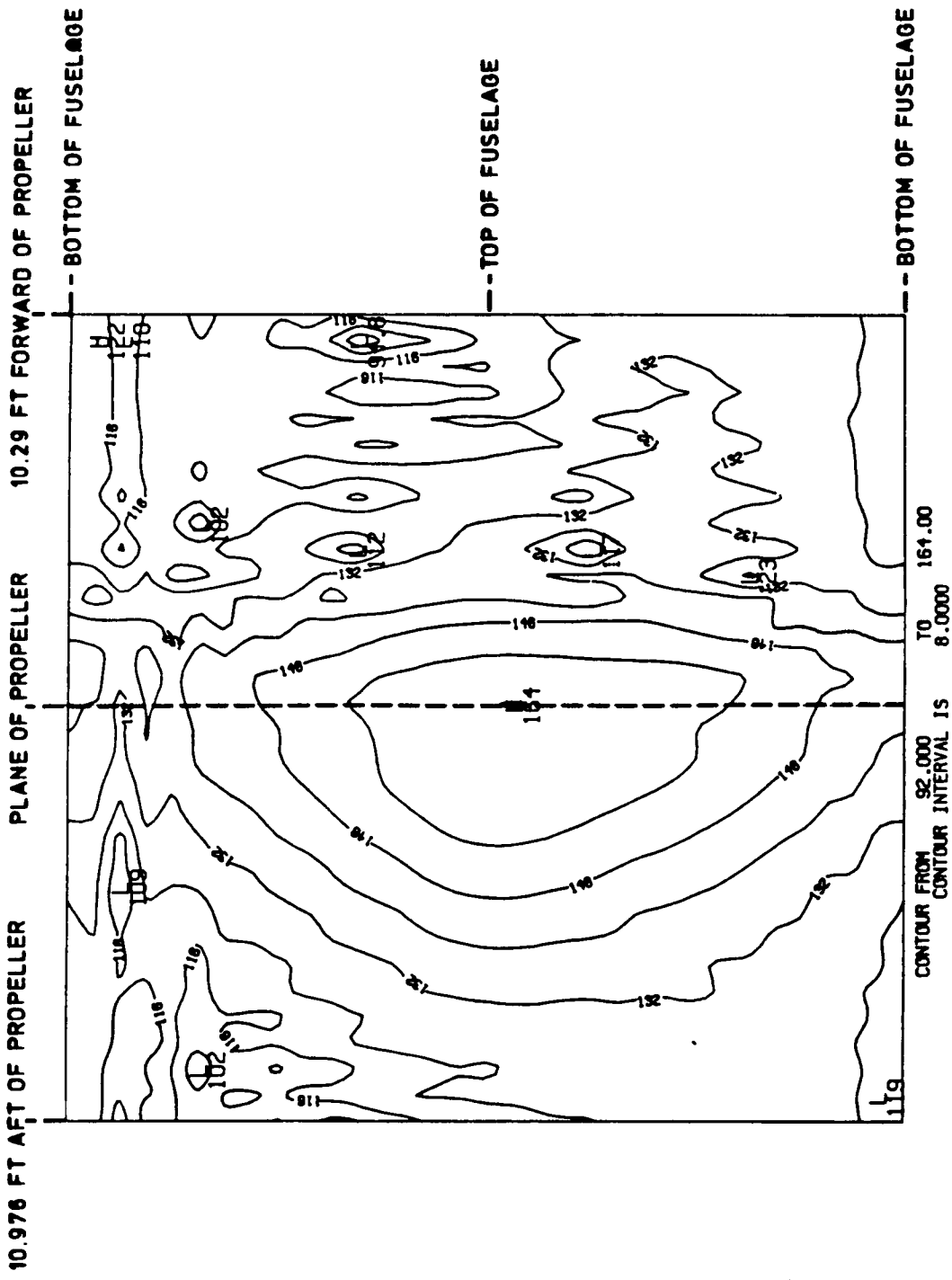


Figure 35. Sound pressure levels about a fuselage. Formulation 3 results.
Case 4.

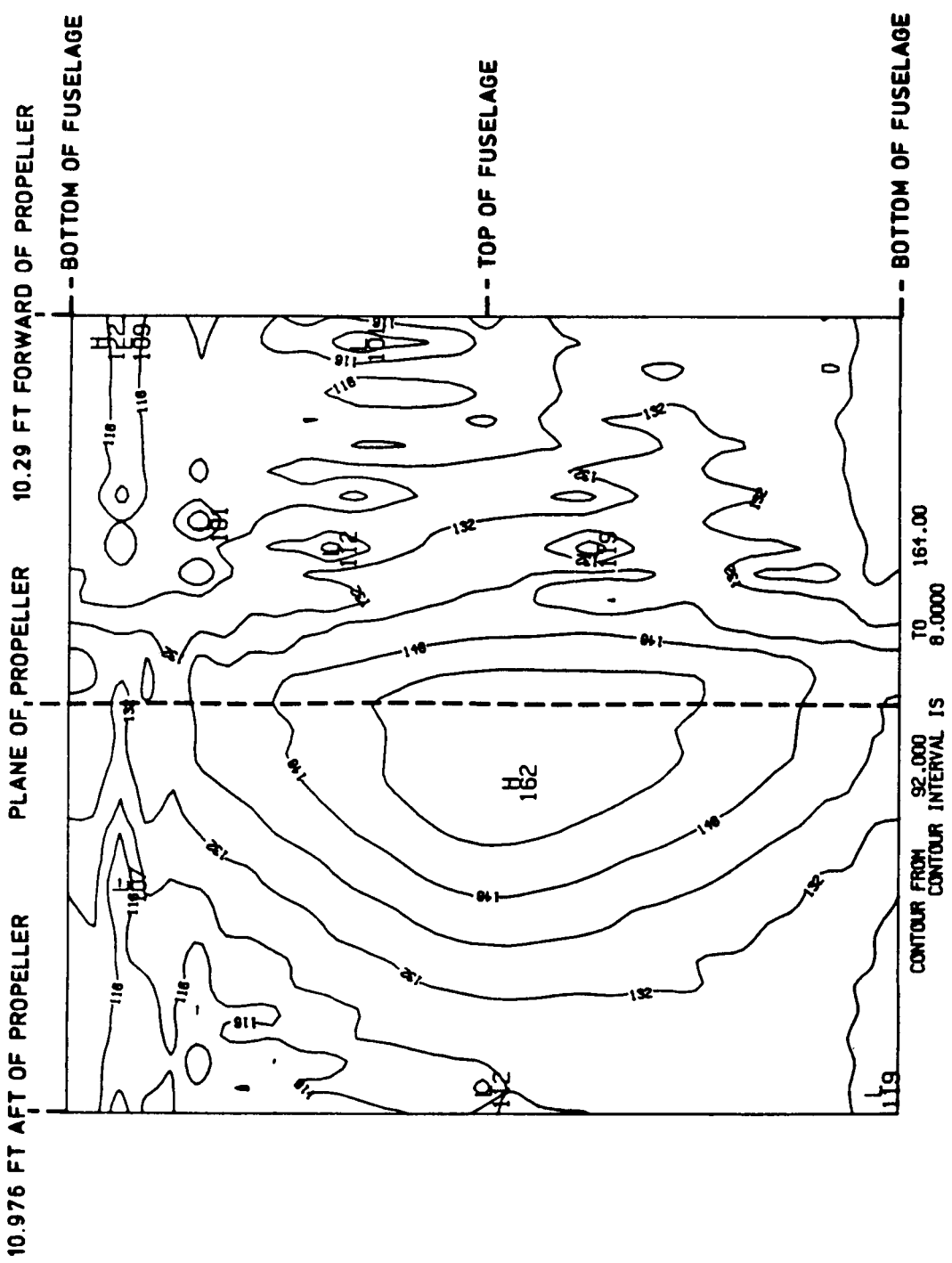


Figure 36. Sound pressure levels about a fuselage. TPN results. Case 4.

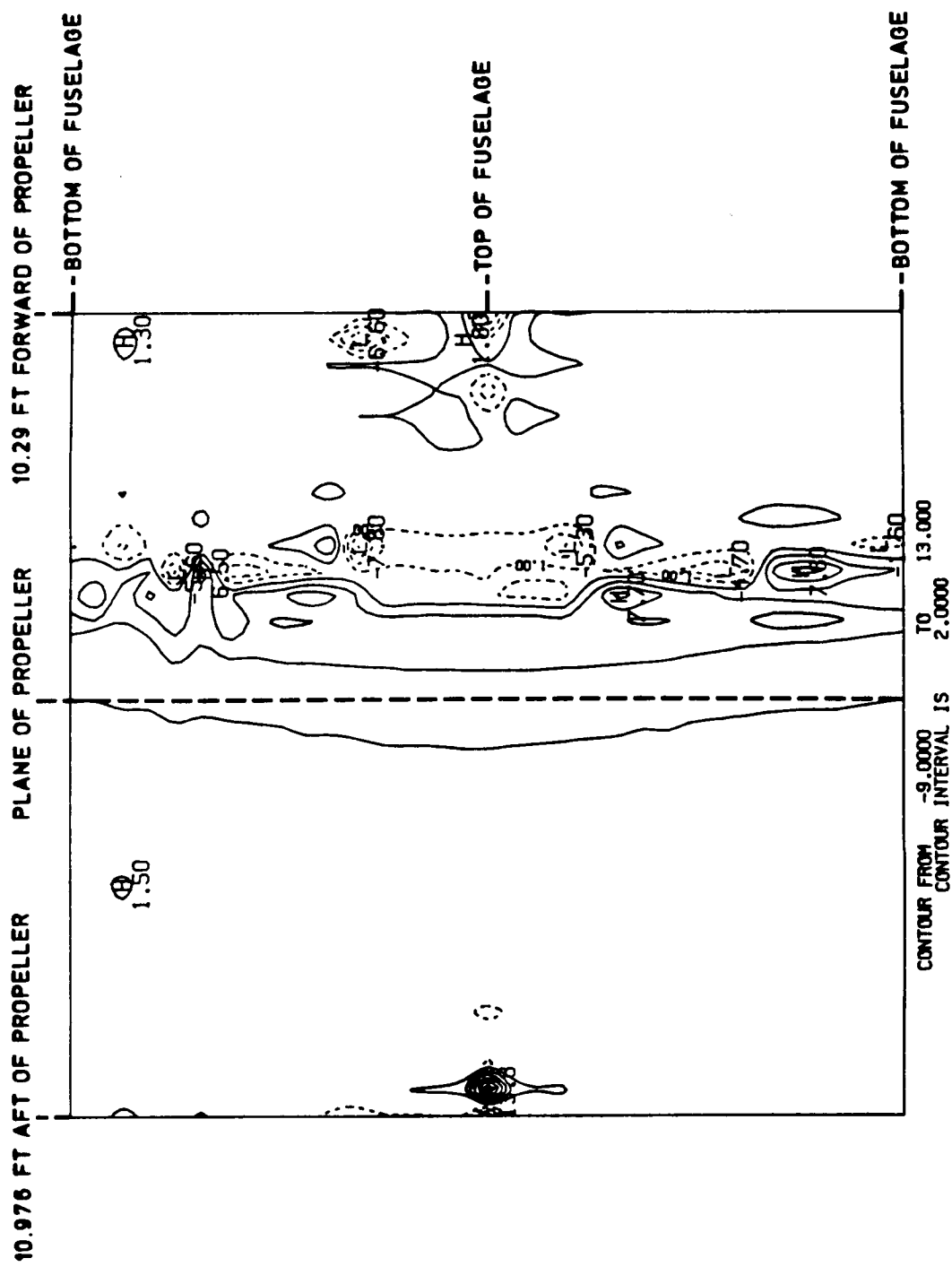


Figure 37. Contour of Formulation 3 results (figure 35) minus TPN results (figure 36). Case 4.

SUBROUTINE FTASUB 74/860 NPT=1,ROUND=A/ S/ M/-D,-75 FTN 5.1+642
 DO=-LONG/-DT,ARG= COMMNN/-FIXED,CS= USER/-FIXED,DR=-TR/-SA/-SL/-ER/-ID/-PM0/-ST,-AL,PL=5000
 FTNS,I,L=LL,R=0.

```

1      SUBROUTINE FTASUB (
2        XC1, XC2,
3        DETA, DETA1, DETA2, DFTAI, DETA12, DETA22, C1, C3,
4        M )
5
6      C      PARAMETER ( NX1DM=10, NDTDM=50 )
7
8      C      DIMENSION ETA(3), DETAI(3), DETAI2(3), DETAI1(3), DETAI12(3),
9        DETA22(3)
10     C
11     C      DIMENSION XI2T(31), XI1(NX1DM),
12       EIT(NX1DM,31), E3T(NX1DM,31), FIR(NX1DM,31), F3B(NX1DM,31),
13       XTR(NDTDM,1), YTR(NDTDM,1), YBR(NDTDM,1), YBR(NDTDM,1),
14       COFE1T(10,1), COFE3T(10,1), COFE1A(10,1), COFE3A(10,1),
15       FBCE1T(8,10), FBCE3T(8,10), FBCE1B(8,10), FBCE3B(8,10),
16       TAUT(50), TAUB(50), TAIY(2), WY(60),
17       BRKX(20), BRKXT(20), BRKXB(20), BRKY(2), BRKY(20), BRKYR(20),
18       TXT(30), TYT(30), TXB(30), TYB(30), WORK(200)
19
20     C      COMMON /SWITCH/ ISWCH,JSWCH,KSWCH,KTOP,INCASE,KNU,SGN
21     C      COMMON /PHYCON/ BTIP,VF,OMEGA,CO,RHNO,EPISILON,
22       XI1TRN,RINNER,BREF,DREF,RREF,M9,PRFF,
23       * PFACT,BPF,XI1GRID(50),XI2SUB(50),
24       * XI2SUP(50),XI1MIN,XI1MAX,XI2MIN,XI2MAX,
25       * XI6(10),X2G(10),X1S(50),X2S(50),STEADY,IEGL4,
26       * THEtar
27
28     C      LOGICAL STEADY
29
30     C      DATA WY / 60*1. /, WY / 60*1. /
31     C      IF ( M.GT.0 ) GO TO 80
32     C      IF ( M.GT.0 ) STOP
33       NXI2S = 30
34       FN = FLOAT(NXI2S)
35       NXI2 = NXI2S + 1
36       PI = 4.*ATAN(1.)
37       DEGRAD = PI/180.
38       DO 10 J = 1, NYI2
39       Z = (J-1.)/FN
40       XI2T(J) = Z*PI

```

-A1-

ORIGINAL PAGE IS
 DE POOR QUALITY

SIAROUTNIE FUNPRES 74/860 NPT=1, PDIIND= A/ S/ M/-D,-DS FTN 5.1+642
 NO=-LUNG/-UT,ARG= COMMNH-FIXED,CS= USER/-FIXFD,D9=-TR/-SB/-SL/-FP/-IN/-PMO/-CT,-AL,PL=5000
 FTN5,I,L,LL,1=0.

```

1      SUBROUTINE FUNPRES (
2        XC1, XC2, TAU,
3        PRES, DP1, DP2, DPDT,
4        SIG , DS1, DS2, DSDF,
5        I   )
6
7      C      PARAMETER ( NX1DM=41, NX2DM=41, NPSDM=1, NX12T=21 )
8      C      PARAMETER ( NLDDM=NX1DM*NX2DM*NPSDM*2 )
9
10     C      DIMENSION
11       XI1(NX1DM), XI2(NX2DM), ALNADS(NLDDM), TEMP1(NX1DM,NX2DM),
12       WX(NX1DM), WY(NX2DM), WORK(200)
13     C      DIMENSION CDF3PT( 9, 9, NPSDM), CDF3PR( 9, 9, NPSDM),
14          CDF2PT( 9, 9, NPSDM), CDF2PR( 9, 9, NPSDM),
15          CDF3ST( 9, 9, NPSDM), CDF3SR( 9, 9, NPSDM),
16          CDF2ST( 9, 9, NPSDM), CDF2SR( 9, 9, NPSDM),
17          CF3DPT( 9, 9, NPSDM), CF3DPB( 9, 9, NPSDM),
18          CF2UPT( 9, 9, NPSDM), CF2DPB( 9, 9, NPSDM),
19          CF3DST( 9, 9, NPSDM), CF3DSR( 9, 9, NPSDM),
20          CF2DST( 9, 9, NPSDM), CF2DSR( 9, 9, NPSDM),
21
22     C      COMMON /SFIT/ TX(30), TY(30), XX, KY, NX, NY,
23       PSI(NPSDM), NPSI
24     COMMON /RKPTS/ BRKX(30), BRYT(30), LYP1
25     COMMON /PHYCON/ RTIP, VF, OMEGA, CO, RH0, EPSILON,
26          XI1TRN, RINNER, AREF, RREF, NB, PRFF,
27          * PFACT, BPF, XI1GRID(50), XI2SUB(50),
28          * XI2SUP(50), XI1MIN, XI1MAX, XI2MIN, XI2MAX,
29          * XI1(10), XI2(10), X1S(50), X2S(50), STEADY, IENGLH,
30          * THEtar
31          LOGICAL STEADY
32     COMMON /SWITCH/ ISWCH, JSWCH, KSWCH, KTNP, INCASE, KNU, SGN
33
34     IF ( M.GT.0 ) GO TO 230
35       PI = 4.*ATAN(1.)
36       TPI = 2.*PI
37       MM = 0
38       PEAD (10,1000)
39       READ (10,1010) NXII
40       READ (10,1020) ( XI1(K), K=1,NXII )
41
42     FUNPRES 1
43     FUNPRES 2
44     FUNPRES 3
45     FUNPRES 4
46     FUNPRES 5
47     FUNPRES 6
48     FUNPRES 7
49     FUNPRES 8
50     FUNPRES 9
51     FUNPRES 10
52     FUNPRES 11
53     FUNPRES 12
54     FUNPRES 13
55     FUNPRES 14
56     FUNPRES 15
57     FUNPRES 16
58     FUNPRES 17
59     FUNPRES 18
60     FUNPRES 19
61     FUNPRES 20
62     FUNPRES 21
63     FUNPRES 22
64     FUNPRES 23
65     FUNPRES 24
66     FUNPRES 25
67     /PHYCON/ 2
68     /PHYCON/ 3
69     /PHYCON/ 4
70     /PHYCON/ 5
71     /PHYCON/ 6
72     /PHYCON/ 7
73     /PHYCON/ 8
74     /SWITCH/ 2
75     FUNPRES 26
76     FUNPRES 29
77     FUNPRES 30
78     FUNPRES 31
79     FUNPRES 32
80     FUNPRES 33
81     FUNPRES 34
82     FUNPRES 35

```

1 SUBROUTINE XINTRP 74/ABD NPT=1,POUND=A/ S/ M/-D,-DS FTN 5.0.1+642
 2 DJ=-LUNG/-UT,ARG= COMMUN/-FIXED,DR=-TA/-S9/-SL/-EP/-ID/-PMN/-ST,-AL,PL=5000 A7/12/04. 09.16.36
 3 FTN5,I,L=LL,R=0.

4
 5 C
 6 C SUBROUTINE XINTRP(XCL,XC2,XPSI,IDL,XL,DX1L,DX2L,XH,DX1H,DX2H,WGHT,
 7 C ,COF2T,CF3T,COF2R,COF3R),
 8 C
 9 C PARAMETER (NPSDM=1)
 10 C
 11 C DIMENSION COF3T(9, 9, NPSDM), COF2T(9, 9, NPSDM),
 12 C
 13 C COMMON /SFIT/ TY(30),TYB(30),KX,KY,NX,NY,
 14 C
 15 C COMMON /PSI/ PSI(NPSDM),NPSI
 16 C COMMON /SWITCH/ ISWCH,JSWCH,KSWCH,KTOP,INCASE,KNU,SGN
 17 C
 18 C IF (M.GT.0) GO TO 5
 19 C
 20 C NPSIM1 = NPSI - 1
 21 C M = 1
 22 C
 23 C 5 CONTINUE
 24 C
 25 C DO 10 K = IPSI1, NPSIM1
 26 C IF (XPSI.GE.PSI(K) .AND. XPSI.LE.PSI(K+1)) GO TO 20
 27 C
 28 C 10 CONTINUE
 29 C
 30 C IPSI1 = 1
 31 C GO TO 5
 32 C
 33 C 20 IPSI1 = K
 34 C
 35 C 25 IPSI2 = IPSI1 + 1
 36 C IF (IPSI2.GT.NPSI) IPSI? = 1
 37 C
 38 C 26 DO 30 I = 1, NY
 39 C
 40 C 27 DN 30 J = 1, NY
 41 C
 42 C 28 COF2T(I,J) = CJF3T(I,J,IPSI1)
 43 C
 44 C 29 COF2B(I,J) = COF3B(I,J,IPSI1)
 45 C
 46 C 30 CONTINUE
 47 C
 48 C 31 IF (SGN.LT.0.) GO TO 40
 49 C
 50 C 32 XL = EVALATE(TX,TYT,KX,KY,NX,NY,COF2T,XC1,XC2,0,0)
 51 C
 52 C 33 IF (ID.EQ.0) GO TO 50
 53 C
 54 C 34 DN1L = EVALATE(TX,TYT,KX,KY,NX,NY,COF2T,XC1,XC2,1,0)
 55 C
 56 C 35 DX2L = EVALATE(TX,TYT,KX,KY,NX,NY,COF2T,XC1,XC2,0,1)
 57 C
 58 C 36 GO TO 50
 59 C
 60 C 37
 61 C 38
 62 C 39
 63 C 40
 64 C 41



Report Documentation Page

1. Report No. NASA CR-181609	2. Government Accession No.	3. Recipient's Catalog No.	
4. Title and Subtitle Comparison of Two Transonic Noise Prediction Formulations Using the Aircraft Noise Prediction Program		5. Report Date December 1987	6. Performing Organization Code
7. Author(s) Peter L. Spence		8. Performing Organization Report No.	
9. Performing Organization Name and Address Planning Research Corporation Aerospace Technologies Division Hampton, VA 23666		10. Work Unit No. 535-03-11-02	
12. Sponsoring Agency Name and Address National Aeronautics and Space Administration Langley Research Center Hampton, VA 23665-5225		11. Contract or Grant No. NAS1-18000	
15. Supplementary Notes Langley Technical Monitor: Patricia J. W. Block		13. Type of Report and Period Covered Contractor Report	
16. Abstract <p>This paper addresses recently completed work on using Farassat's Formulation 3 (ref. 1) noise prediction code with the Aircraft Noise Prediction Program (ANOPP) (ref. 2). Software was written to link aerodynamic loading generated by the Propeller Loading (PLD) module within ANOPP with Formulation 3. Included are results of comparisons between Formulation 3 with ANOPP's existing noise prediction modules, Subsonic Propeller Noise (SPN) and Transonic Propeller Noise (TPN). Four case studies were investigated.</p> <p>Results of the comparison studies show excellent agreement for the subsonic cases. Differences found in the comparisons made under transonic conditions are strictly numerical and can be explained by the way in which the time derivative is calculated in Formulation 3.</p> <p>Also included is a section on how to execute Formulation 3 with ANOPP.</p>		14. Sponsoring Agency Code	
17. Key Words (Suggested by Author(s)) Propeller noise Noise prediction Transonic Propellers		18. Distribution Statement Unclassified - Unlimited Subject Category 71	
19. Security Classif. (of this report) Unclassified	20. Security Classif. (of this page) Unclassified	21. No. of pages 86	22. Price A05